# NANOMECHANICS FROM ATOMIC RESOLUTION TO MOLECULAR RECOGNITION

H.P. Lang<sup>1,2</sup>, R.Mckendry<sup>1</sup>, C. Gerber<sup>1</sup>

<sup>1</sup>IBM Research, Zurich Research Laboratory, <sup>2</sup>Institute of Physics, University of Basel

**INTRODUCTION:** The fields of scanning probe microscopy, molecular biology and information science have existed as individual disciplines for a long time, but only recently have moved closer to each other, as the nanometer scale has gained in importance. Biochemistry and molecular biology have moved to the nanometer scale from micrometer-sized objects such as cells, whereas physics and synthetic chemistry have extended investigations from atoms and molecules to the nanometer scale. Experiments in nano-scale science generate a wealth of data that has to be analysed and evaluated by means of modern information science. This is reflected by the interdisciplinarity in nano-scale research. A major tool to investigate the nano-scale is atomic force microscopy (AFM). Non-contact mode AFM is able to image surfaces with true atomic resolution, provided the interaction between surface and oscillated cantilever tip is controlled in an appropriate range. The cantilever per se is an excellent tool to study physical, chemical, and biochemical processes on the nano-scale. Molecules adsorbing on the surface of a cantilever produce an interfacial stress that leads to a bending of the cantilever, and to a shift in the resonance frequency of the cantilever owing to mass increase. Processes that generate heat cause a bending of a biomaterial cantilever because of differing thermal expansion coefficients of the two materials.

#### **METHODS:**

### **RESULTS / DISCUSSION:**

Cantilever Sensor Arrays as Chemical Sensors.

Adsorption processes can be studied in various environments, such as gas flows, vacuum, and liquids. An array of individually functionalised cantilevers serves as a chemical multi-sensor, such as an artificial electronic nose, to characterize and recognize analytes, and to measure physical and chemical properties on the nano-scale. In a number of examples we demonstrate the application of cantilever arrays as gas sensors for solvent vapour detection, for medical applications, and as a sensor for quality control in a plasma cleaner environment.

Cantilever Sensor Arrays as Biosensors in Liquids

Biological and chemical processes in liquids can be transduced into nano-mechanical motion using a micro-fabricated silicon cantilever array. These sensors allow the rapid, quantitative and qualitative detection of non-labelled biomolecules in solution. We have used such sensors to detect sequence-specific DNA hybridisation with single base mismatch sensitivity. Single-stranded thiolfunctionalized DNA 12-mers were anchored onto gold-coated cantilevers. Hybridisation with the respective complementary strand in buffer solution produced cantilever bending. A reference cantilever functionalised with a different oligomer sequence did not bend. The surface-solution equilibrium constant, derived from concentration-dependent studies, was similar to the hybridisation efficiency in solution. We have explored the origins of the observed compressive surface stress using radiolabelled oligomers and various surface preparations. These studies suggest that the observed signal is predominantly due to steric crowding. We have also investigated the effect of 'dangling ends' upon hybridisation with complements that include a non-specific polyadenine tail at either or both ends. Hybridisation again produced a compressive surface stress, and the magnitude of the signal was dependent on the position of the tail. Currently, we are scaling up the experiment to monitor eight cantilevers in an array to detect several sequences simultaneously.

### PROTEIN BIOCHIPS AS NEW TOOLS IN PROTEOMICS

P.Wagner

Zyomyx, Inc. Hayward, California, USA

INTRODUCTION: Novel high-throughput biomolecular analysis in genomics, proteomics, drug discovery, disease diagnosis and the development and application of patient-specific medicines require highly parallel, ultra sensitive, miniaturized device technologies. While technological innovation in form of DNA micro arrays (gene chips) and other formats have adapted the analysis of genetic material to a miniaturized format, the more delicate nature and diversity of proteins in terms of function, structure, stability and abundance have precluded the development of analogous tools for proteomics. In addition, a comprehensive proteomic analysis would require measurement and characterization of protein abundance and chemical modifications as well as discovery of unknown proteins, new pathways and functional linkages. Protein biochips have started to emerge recently based on new developments and integration efforts in advanced materials, protein engineering and detection physics. Recent developments and selected examples will be presented with an emphasis on the technical challenges in surface and assay methodologies.

### MICROARRAYS FOR DETECTION OF LOW ABUNDANCE GENES & PROTEINS

M. Ehrat, A. Abel M. Pawlak

Zeptosens AG, Witterswil, Switzerland

**INTRODUCTION:** The breakthroughs in genomics in the last years - in many cases based on the massively parallel generation and analysis of biological information - has been made possible to a large extent by the development of miniaturized and multiplexed analysis systems, among them DNA microarrays. Today, protein chips will be one of the key approaches to bridge the gap between genomics and proteomics by delivering functional information on gene expression. The development and broad dissemination of new technologies therefore will be crucial to further advance in genomics based disciplines of life sciences. Moreover, analysis of genes and their products for drug discovery and development, as well as for disease diagnostics place new demands on the sensitivity, speed and reliability of new analytical systems.

Zeptosens' goal to significantly contribute to that endeavour by initiating a new era in highly multiplexed, automated and ultrasensitive bimolecular analysis on nanotechnology-based microarrays and readout systems. With the ZeptoTM-product line, Zeptosens is developing and will introduce a new revolutionary fluorescence-based detection technology for nucleic acid and protein microarrays setting new standards in microarray readout performance in terms of detection limits, quantification and automation.

Technology: Zeptosens is developing a planar waveguide (PWG) technology based microarray readout system. In planar waveguide technology only surface-confined fluorescence labels are selectively excited for emission, bulk medium is not excited. Laser light is coupled via a diffractive grating into a thin film of high-refractive-index material deposited on a transparent support. A strong evanescent field is created, which has only a limited penetration depth of about 200 nm into the adjacent medium. This spacial discrimination results in a significant increase in signal/noise ratios compared with conventional optical detection methods and permits highly selective and sensitive measurements even in the presence of free fluorophores or scattering matrix (e.g. serum).

DNA-Arrays: Mid-density microarrays utilizing oligonucleotides or cDNAs as recognition elements have significant advantages if new and unknown target sequences are to be investigated, if high flexibility is required, or if only the expression level of a few hundred of target genes is to be queried for "focused" target studies. Up to now, however, only a minute amount of the information that could be derived out of the expression level of mRNA has been harvested: Typically, cells contain about 10 pg of total RNA, out of which about 100–500 fg are being represented by mRNA. However, 95 % of this mRNA material are composed out of low abundant genes with less then 10 copies per cell which can be monitored only with high

effort in target and signal amplification. ZeptoGENE<sup>TM</sup> chips permit highly sensitive genomic analysis with no or only linear target amplification. Low abundant genes, expressed in as little as 100 cells, could be monitored. This allows sampling via needle biopsies, laser dissection, and cultivation in miniaturized systems.

Protein Microarrays: The efficient multi-parameter analysis of high sample numbers - heal-thy versus disease ones or treated versus untreated ones - remains the key to finding and monitoring pharmaceutically relevant target or marker proteins. Zeptosens microarray technology provide the ability to detect low abundant protein markers in a quantitative manner. The microarray platform was designed to provide a comprehensive solution. The concept includes the highest sensitivity, multi-colour fluorescence reader, high quality microarray chips with integrated flowthrough micro-fluidics (15 µl chamber volume) adapted to the micro-titer plate format for automated high-throughput measurements. This platform is the base for high performance multiplexed assays with improved biological information content. sensitivity of the system, enabled by surface-confined fluorescence detection on planar waveguides, is designed to cover the requirements of a wide range of multiplexed microarray applications, without being compromised by instrumental parameters. detection of down to 1 zeptomole of labelled protein (600 proteins, 3000 labels) on a single spot was demonstrated. The dynamic range of the system, determined to be a factor of 105 through variation of the capture probe density in a spot (103 proteins at the detection limit up to 108 molecules at full monolayer coverage) times the signal dynamics of 103-104 within an image, satisfies the needs for the analysis of low to high abundance protein expression levels or ligandreceptor affinity interactions from uM to fM. The waveguide-based read-out principle allows simple "mix & measure" protein assay formats. Measurement in full serum or blood is well possible, as demonstrated for multiplexed cytokine marker analysis. Assay sensitivities of down to 1-10 pg/ml of analyte in serum have been demonstrated. The ability of in situ measurement without additional washing steps is a benefit for simple assay ZeptoMARK<sup>TM</sup> protein microarrays include medium density - medium throughput antibody arrays (1000 spots per array) for target and marker finding in pharmaceutical R&D, and low density, predefined or customized microarray chips (10-50 analytes, high throughput with a multitude of identical arrays per carrier) for marker validation and monitoring in (pre-) clinical drug development.

# RECENT ADVANCEMENTS IN PROTEINCHIP® ARRAY TECHNOLOGY FOR BIOAFFINITY STUDIES

S.Weinberger

Research Proteomics, Ciphergen Biosystems, Inc. Dumbarton Circle, Fremont, CA, USA

INTRODUCTION: Surface Enhanced Laser Desorption / Ionisation Mass Spectrometry (SELDI- MS) is an advanced analytical technique providing facile protein analysis of complex biological mixtures. Commercially, SELDI-MS embodied Ciphergen's been within ProteinChip® Array technology (Fremont, CA, USA). ProteinChip Array surfaces function as solid phase extraction media that support on-probe isolation and cleanup of analytes prior to mass spectrometric investigation. Retained proteins are subsequently desorbed and ionised using matrix assisted, surface enhanced laser desorption / ionisation and detected using a time-of-flight mass spectrometer. ProteinChip Array technology has been successfully applied to the discovery and characterization of many valuable biomarkers of organic disease and cancer as well as extended to routine toxicological studies employing samples of various origin. Convenient sample preparation schemes for whole cell, biological fluids, and cellular lysates have been developed using this simplified approach.

This talk focuses upon some of the most recent SELDI technological advancements made in our laboratory. Recent progress in the realms of array development, tandem ms technology, and on-chip proteolysis will be reviewed with an emphasis upon their utility in analysing real world, complex biological samples.

### PROTEIN MICROARRAY TECHNOLOGY

### T.O.Joos

NMI Natural and Medical Sciences Institute at the University of Tuebingen, Markwiesenstr. 55, 72770 Reutlingen, Germany.

#### INTRODUCTION:

Biochip technology allows the simultaneous analysis of thousands of molecular parameters within a single experiment. Most of the current applications focus on DNA array technology for gene expression analysis or the detection of single nucleotide polymorphism<sup>1</sup>. However, any kind of ligand binding assay which relies on the product observation of an immobilized capture molecule and its binding partner from the surrounding solution can be imagined to be performed as an array experiment<sup>2</sup>. Such protein chips will provide a powerful and reliable platform for extending molecular analysis beyond the limitations of DNA chips. In our laboratory we are developing microarray based sandwich immunoassays looking at different types of immunglobulins. Autoantigen micro arrays are used to screen in parallel for the presence of auto-antibodies from minimal amounts of patient sera. Furthermore, immobilized peptides and proteins can be used to search for their corresponding cell surface receptor on living cells.

METHODS: A GMS417 Arrayer (Affymetrix, USA) was used for the fabrication of the arrays. The capture molecules were diluted in stabilizing buffer containing 20% glycerol in PBS and 5 Silylated BSA. slides (TeleChem International, Inc., USA) or Poly-L-Lysine coated slides (Sigma Aldrich; FRG) were used as solid supports. Prior to spotting bromophenol blue was added to the stabilized antigen solutions to a final concentration of 0.1%. This enabled us to control the microspot application and the integrity of each array. Capture molecules on the slides were rehydrated in PBS for 5 min, incubated with blocking buffer (1.5% bovine serum albumin, BSA, 5% low fat dry milk in PBS) for 30-60 min and incubated with 20 ul target diluted in blocking buffer + 0.1% Tween20). Unbound target was washed away. Detection of bound target was performed with either a Cy5 conjugated secondary antibody or for the sandwich immunoassas with a biotinylated secondary antibody followed by a final Cy5 streptavidin incuabtion. Images of the microarrays were taken with a Affymetrix GMS 418 Scanner.

**RESULTS:** Our micorarray based sandwich assays allows us to determine in parallel IgG, IgA and IgM from minimal amount of sera.

For autoantibody detection involved in Type 1 or insulin-dependent diabetes mellitus (IDDM) GAD65, IA-2, insulin and control proteins were screened simultaneously the sera of individuals. Autoantibodies present in just a few  $\mu$ l of serum can be detected via a micro-ELISA by fluorescence measurements.

Cell based microarray have been developed that can be used to screen for peptides that improve specific cell adhesion. Laminin peptide sequences with different spacers were covalently bound to the arrays. On these coated solid supports, tectum cells (chicken) were cultivated for 24 hours. The cells adhering to the single spots were made visible using a DAPI dye. Cells were found only on those surfaces coated with the adhesion mediating peptide. The evaluation of the average spot intensity offers an easy and efficient method to elucidate varying cell adhesion on different surfaces quickly and reproducibly.

**DISCUSSION & CONCLUSIONS:** Microarray Technology allows the simultaneous analysis of a multitude of parameters with a single experiment. Miniaturization and parallelization succeed in increased speed, higher precision and decreased reagent consumption, thereby lowering costs considerably in diagnostics.

**REFERENCES:** <sup>1</sup>Phimister, B., ed. *The chipping forecast.* supplement ed. **21**. 1999, Nature Genetics, <sup>2</sup>Ekins et al., 1989 J. Bioluminescence and Chemiluminescence **4**, 59-78,

ACKNOWLEDGEMENTS: Experiments were done by MF Templin, M. Schrenk, P. Traub, C. Voehringer and Dieter Stoll. This work is supported by U.S. Grant No. DAMD 17-01-1-0009 "New Advanced Technology to Improve Prediction and Prevention of Type I Diabetes"

# HIGH CONTENT SCREENING AND THE CELLCHIP™ SYSTEM: LIVING CELLS AS BEACONS FOR DRUGS AND TOXINS

R. Kapur

Cellomics, Inc., 635 William Pitt Way, Pittsburgh, PA 15238

INTRODUCTION: The new face of drug discovery is focused on the living cell with its myriad ionic, metabolic, macromolecular, and organellar networks as the ultimate target of drug activity. Cellomics® has developed 'High Content Screening' (HCS) technology1,2,3 for the automation of information-rich cell based assays using an integrated platform comprised of imaging instrumentation, fluorescent reagents, engineered cells, and bioinformatics tools. HCS is defined as multiplexed functional screening based on fluorescence imaging of multiple targets in the context of intact cells. This novel approach measures temporal and spatial distributions and activities of targets and cellular constituents in and between cells. An HCS multiparameter yields 20-200 assav target-related measurements on up to four different cell targets, each of which is identified on a separate fluorescent channel. Drug or toxin effects on complex molecular events such as signal transduction pathways can be measured, in addition to effects on cell functions ranging from apoptosis to cell-cell communication. The unique advantages of HCS are High-content screens extract high quality information on a cell-by-cell basis rather than providing an average population response measurement. Furthermore, individual cells of interest are distinguishable within a mixed cell population. HCS eliminates potential sources of variability including those associated with pipetting error, transfection efficiency, and cell preparation. Interactions between drug candidates, or toxins, and multiple cellular targets, as well as downstream events, can be monitored in a single HCS assay via multicolour fluorescence. content screens can be performed using fixed or live cell formats to yield the temporal-spatial dynamic information necessary to determine the role of selected targets in cell functions and the specificity of drug compounds or toxins. The evolution of HCS into a higher throughput and miniaturized platform will be realized with the CellChip<sup>TM</sup> System4 under development.

**METHODS:** By harnessing the power of fluorescence imaging, bioinformatics, robotics, and advances in cell biology we have developed the High Content Screening (HCS) method. At the core of HCS is the multiparameter image analysis of numerous whole cells in parallel which provides extreme flexibility, speed and capacity to quantify complex biology

The ArrayScan® II, optimised for fixed endpoint assays enables HCS on living cells. The ArrayScan II System's unique optical path is optimised for performing rapid automated scans through the bottom of clear-bottom microplates. The system automatically focuses on a field of cells and acquires images at each selected colour channel. The ArrayScan software identifies and measures individual features and structures within each cell in a field of cells, so that hundreds of cells are analysed in parallel. The software then tabulates and presents the results in user-defined formats. All of the raw data-including images of individual cells-are archived and available for inspection and analysis. The ArrayScan II software provides for multicolour

imaging, automated cell-based image analysis, and data management for archiving, analysis and creation of reports. An intuitive, graphical user interface guides you through image acquisition, image analysis, data review and data reporting.

RESULTS: High Content Screening enables a quantitative analysis of multiple intracellular pathways affected by interaction with drugs or toxins. Intracellular cytoplasm to nuclear translocation of transcription factors, receptor internalisation, discrimination of apoptotic cells from necrotic cells, and functional measure of drug or toxin induced cellular toxicity are some of the measured HCS parameters for functional assessment of change in cellular physiology induced by drugs or toxins. High Content Screening, applied to lead optimisation, predictive toxicology, and new target validation can ultimately reduce the "idea to clinic" cycle time while increasing the probability of therapeutic success of leads.

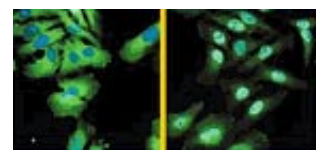


Figure 1. Images of immunofluorescent stained HeLa cells before and after activation of NFkB by IL-1í. Nuclei (blue) are labelled

with Hoechst dye. Cells were stimulated with 25 ng/mL IL-1i for 20 min. LEFT: NFκB labelling in unstimulated cells (green). RIGHT: NFκB labelling in stimulated cells (green).

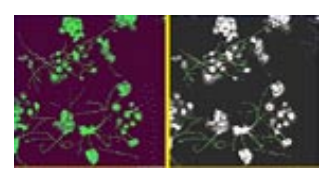


Figure 2. Application of the Neurite Outgrowth imaging algorithm on a field of PC-12 cells acquired with a 10X objective lens on the

ArrayScan II System. The left image displays a composite of the nuclear and neuronal raw images acquired by the ArrayScan II System. Cell nuclei (blue) are labelled with Hoechst Dye. The neurons and their neurites (green) are identified by immunofluorescence. The panel on the right shows the neuronal image in greyscale, with the neurites identified by the algorithm overlaid with a green trace.

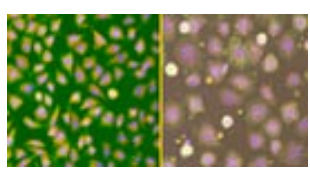


Figure 3. L929 cells treated with 2.5 µM paclitaxel for 30 hours (right), and untreated (left). F-actin (Ax488-ph) appears in green, nuclear

staining (Hoechst) appears in blue, and mitochondria (MitoTracker® Red) appear in red. Images taken from the ArrayScan II System.

**REFERENCES:** <sup>1</sup>KA Giuliano, DL Taylor, Trends in Biotechnology, 16:135 (1998). <sup>2</sup>KA Giuliano, RL DeBiasio, TR Dunlay, A Gough, JM Volosky, J Zock, GN Pavlakis, DL Taylor, J. Biomolecular Screening, 2:249 (1997). <sup>3</sup>DL Taylor, ES Woo, KA Giuliano, Curr Opin Biotechnol 12:75 (2001). <sup>4</sup>R Kapur, KA Giuliano, M Campana, T Adams, K Olson, D Jung, M Mrksich, C Vasudevan, DL Taylor, Biomedical Microdevices, 2:99 (1999)

# TAILORED SUBSTRATES FOR STUDYING AND CONTROLLING CELL ADHESION

### M. Mrksich

Department of Chemistry and the Institute for Biophysical Dynamics, The University of Chicago, USA

INTRODUCTION: Most cells are adherent and must attach to and spread on an extracellular protein matrix in order to survive, proliferate and carry out normal functions. The complex structure of this protein matrix often hinders mechanistic studies of cell adhesion, necessitating the development and use of model substrates. This presentation will give an overview of the use of self-assembled monolayers of alkanethiolates on gold as model substrates for studying and controlling the interactions of mammalian cells with non-natural materials.

The approach emphasizes a molecular level design and preparation of monolayers that exhibit specific ligand-receptor interactions with cell-surface proteins. This surface chemistry approach begins with monolayers terminated in short oligomers of the ethylene glycol group, because these films are inert to the non-specific adsorption of protein. The immobilization of ligands to these inert films gives substrates to which proteins can selectively bind, but which otherwise rule out non-specific interactions of proteins. These model substrates which permit complete control over the ligandinteractions receptor between cells substrates—are valuable for mechanistic studies of cell adhesion and migration and for related applications in biotechnology.

#### **METHODS:**

**RESULTS & DISCUSSION:** Self-Assembled Monolayers as Model Substrates for Cell Adhesion.

The attachment of cells is mediated by the binding of integrin receptors to peptides contained in the extracellular matrix. The short tripeptide Arg-Gly-Asp is a common ligand for integrin receptors and has been used frequently to promote cell adhesion to materials. Monolayers that presented this peptide, at 1% density among tri(ethylene glycol)-terminated alkanethiolates supported the efficient attachment and spreading of 3T3 Swiss fibroblast cells. Immunostaining showed that cells had

mature focal adhesion complexes and actin stress filaments. Control experiments showed that cells did not attach to substrates presenting a scrambled peptide and that cell attachment could be inhibited by a soluble peptide, both demonstrating the specificity of cell-substrate interactions. This strategy has been applied to the design of monolayers used for studies of cell adhesion to several other peptide and carbohydrate ligands.

Dynamic Substrates for Studies of Cell Adhesion.

This strategy for engineering surfaces for selective interactions with cells has been extended to the design of dynamic substrates that can alter the presentation of ligands. These substrates, which can modulate ligand activity in real-time, offer a opportunity for studying the cellular responses to changes in the composition and pattern of ligands on the underlying substrate. These active substrates are based on electroactive monolayers that present redox-active groups which can be switched by applying electrical potentials to the underlying gold. A first example uses substrates that can be switched to turn on ligands. This property stems from the Diels-Alder reaction of ligand-diene conjugates with a benzoquinone group of the monolayer. The dynamic property is based on the electrochemical reduction of quinone to a hydroquinone, which is not reactive with This strategy has been used to switch regions of the substrate from an inert state to a state that permits the adhesion and migration of cells. It has also been used in a method to pattern the attachment of multiple cell types to a common substrate. A second example uses substrates that can selectively release immobilized ligands from the monolayer. Taken together, these examples establish that self-assembled monolayers of alkanethiolates on gold are an excellent model system for controlling the adhesion of cells and will find wide use both in fundamental studies for biology and in applied targets for biotechnology.

# CELL ADHESION ON MICRO- AND NANOPATTERNED PROTEIN-COATED SUBSTRATES: CONNECTING THE DOTS

M. Bastmeyer

Department of Biology, <u>University of Konstanz</u>, Germany

**INTRODUCTION:** Cell adhesion involves the interaction of cells with the extracellular matrix (ECM). It is mediated by integrins and is essential for the integrity and function of multicellular organisms. The initial phase of cell/matrix interaction is characterized by the binding of integrin receptors to ECM molecules and the assembly of receptors at the contact sites<sup>1</sup>. This leads to the induction of intracellular signalling cascades that cause the aggregation of specific molecules linking the actin cytoskeleton via integrins to the ECM<sup>2</sup>. Focal adhesions are therefore also the sites at which contractile forces produced inside the cell are exerted onto the substrate and, consequently, their distribution dictates the size and shape of the cell<sup>3</sup>. The types of ECM that cells encounter in vivo range from the homogeneous meshwork of basement membranes to the fibrillar scaffold of connective tissue or healing wounds. A cell is therefore confronted either with a nano-patterned surface or with ECM fibrils spaced in the um range. To understand how cell behaviour is dictated by the architecture of the ECM, we exposed cells to a patterned substrate of ECM molecules obtained by the micro contact printing technique ( $\mu$ CP). By controlling the size of square ECM dots and the distance between them, we created nano-patterns resembling either basement membranes or connective tissue. Adherent cells were plated on these patterns, and the spreading and migration of the cells were analysed.

**METHODS:** We used micro contact printing  $^4$  to create patterned substrates of ECM molecules (fibronectin, vitronectin, laminin) consisting of squared dots (3  $\mu$ m, 1  $\mu$ m, 800 nm, 500 nm, 300 nm) separated by non adhesive regions of variable distances (2  $\mu$ m-30  $\mu$ m). Cells were cultivated on the patterned substrates for 1 h, fixed and fluorescently labelled for actin, focal adhesion associated molecules and markers for intracellular signalling and analysed.

**RESULTS:** We first determined the capacity of cells to spread on ECM dots with increasing distance from each other. As long as the spacing of dots was less than 2  $\mu$ m, cells spread as they would on a homogeneous substrate. With increasing distance between fibronectin dots (5-20)

 $\mu m),$  cells adapted their shape to the dot pattern and grew with straight edges from dot to dot. In these cells, the actin cytoskeleton formed stress fibres between adjacent dots. When the distance between dots exceeded 25  $\mu m,$  cell spreading was limited and the cells became triangular, ellipsoid or round. At 30  $\mu m,$  cells adhered to one dot and did not spread.

The minimum size of an ECM dot required for cell spreading was determined using fibronectin patterns with dot sizes from 0.1 to 1  $\mu m^2$  and a constant spacing of 5  $\mu m$  (centre to centre). Cells readily spread on dots which were 0.25  $\mu m^2$  or larger. In these cells, the actin cytoskeleton formed normal stress fibres connecting the dots. A dot surface of 0.1  $\mu m^2$  still allowed cell adhesion but the cells no longer spread. This indicates that cells can properly adhere to and spread on patterned ECM-coated areas equal to or larger than 0.25  $\mu m^2$  spaced at 5  $\mu m$ .

We next studied the molecular composition of focal adhesions formed on patterned substrates and by immunostaining that \( \beta 3-\) integrin, phosphotyrosine, focal adhesion kinase (FAK), paxillin, talin, and vinculin were localised to fibronectin- or vitronectin-coated dots, suggesting that classical focal contacts were formed. The accumulation of these molecules at the dots occurred rapidly and was already visible 10 min after plating. They even accumulated over dots of 0.1 µm<sup>2</sup>, showing that the size of focal contacts is determined by the microenvironment and can be much smaller than previously described in the literature. Clustering of focal adhesion molecules occurred only when cells were grown on ECM molecules. When plated on patterned substrates prepared with polylysine, cells were able to adhere but actin stress fibres were not formed and accumulation of focal adhesion molecules did not occur.

**DISCUSSION & CONCLUSIONS:**  $\mu$ CP in combination with cell culture is a powerful technique to study basic principles of cell adhesion and migration. We show, that the limits for cell adhesion are a maximal distance of 25  $\mu$ m between adhesive surfaces and a minimal size of 0.25  $\mu$ m<sup>2</sup> of an adhesive dot. Knowing these limits will

allow a better understanding of in vivo cell behaviour in situations such as embryogenesis, wound healing and leukocyte migration and it will be essential for the design of implants with artificial surfaces allowing optimal interaction with cells in a tissue.

We are currently using transformed cell lines expressing GFP-fluorescent proteins (integrins, tubulin, actin) to investigate the dynamics of focal adhesion formation on patterned substrates in living cells.

REFERENCES: <sup>1</sup>Burridge,K. & Chrzanowska - Wodnicka,M. Focal adhesions, contractility, and signaling. *Annu Rev Cell Dev Biol* **12**, 463-518 (1996). <sup>2</sup>Yamada,K.M. & Geiger,B. Molecular interactions in cell adhesion complexes. *Curr Opin Cell Biol* **9**, 76-85 (1997). <sup>3</sup>Ingber,D.E. Tensegrity: the architectural basis of cellular mechanotransduction. *Annu Rev Physiol* **59**, 575-599 (1997). <sup>4</sup>Mrksich,M. & Whitesides,G.M. Using self-assembled monolayers to understand the interactions of man-made surfaces with proteins and cells. *Annu Rev Biophys Biomol Struct* **25**, 55-78 (1996).

ACKNOWLEDGEMENTS: Experiments were done by D. Lehnert with technical assistance of U. Binkle. We thank C. David (PSI, Villigen) for preparing the wafer, V. Eck (University Heidelberg) for the ethyleneglycol-terminated alkanethiols and C. Schäfle (University Konstanz) for help during initial printing problems. GFP-transfected cells were provided by B. Wehrle-Haller and B. Imhof (CMU, Genf) This work is supported by the DFG (SFB 513).

### BIOMECHANICS OF CELL-MATERIAL ADHESION

#### A.Yamamoto

Biomaterials Research Team, Materials Engineering Laboratory, National Institute for Materials Science, Japan

INTRODUCTION: Cell adhesion to material generally been evaluated by surface has morphological observation of the cells adhering to the material surface using an optical and electron microscope, which is subjective, and not a quantitative method. Many researchers have tried to measure the adhesive strength between a cell and material surface to quantify the cell-material adhesion. A few methods have been developed to evaluate the strength of cell-material adhesion. One of them is determining the ratio of cells still adhering to the material surface after applying detaching force to a population of cells. centrifuge is used to apply tensile detaching force to the cells, whereas a viscometer and a parallel flow chamber is used to cause a shear force to detach the cells by the flow of a physiological solution. In these methods, however, the force which a cell actually receives is non-uniform along the cell surface or between cells, and its magnitude is unknown. Therefore, this method evaluates the strength of cell-material adhesion qualitatively. Another method is micromanipulation, which is able to measure directly the force necessary to detach a cell from material surface. micromanipulator with glass micropipette is used to pull out a single cell from material surface in normal direction. However, this method can only measure the detachment force of the cell which weakly attach to the material surface because it should have a spherical shape to be pulled by the micropipette. We developed a new system to measure the shear force necessary to detach a cell adhering and spreading onto the material surface in cell culture medium, observing the detachment process by an optical microscope[1]. In the present paper, the adhesive properties of murine fibroblasts to tissue culture polystyrene and extracellular matrix (ECM)-coated polystyrene dishes were examined[2]. The observation of the detachment process by interference reflexion microscopy (IRM) will also be discussed.

**METHODS:** A principle of the measurement of the adhesive shear force is shown in Figure 1. A cell adhering to the bottom of the dish on a XY-stage is moved to the tip attached to a cantilever. When the tip touches to the cell, a lateral load is applied to the cell. The cantilever is deflected corresponding to the load applied to the cell, and

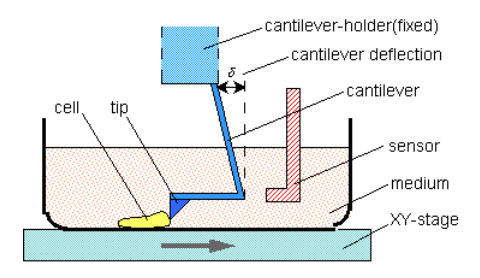


Figure 1. Principle of the measurement of cell adhesive shear force.

the deflection is recorded as a function of the displacement of the XY-stage. The cell adhesive shear force F is defined as the critical force to detach the cell from the material surface, and given by equation:  $F = k \delta$ , where k is the spring constant of the cantilever and  $\delta$  is the maximum cantilever deflection. The cell adhesive shear strength S is defined as the cell adhesive shear force per a unit apparent cell adhesive area A, which was analysed on the optical-microscopic i m a g e o f t h e c e l l.

RESULTS & DISCUSSIONS: Figure 1 shows the cell adhesive shear strength of L929 to ECM-coated and uncoated dishes after 24h-incubation. Among these surfaces, cells cultured on collagen (type I) have the highest cell adhesive shear strength, followed by those on fibronectin. This fact indicates that cells adhere strongly to ECM-coated surfaces than uncoated polystyrene surface. It was generally observed that coating the surfaces of glass and polystyrene by ECM increases the

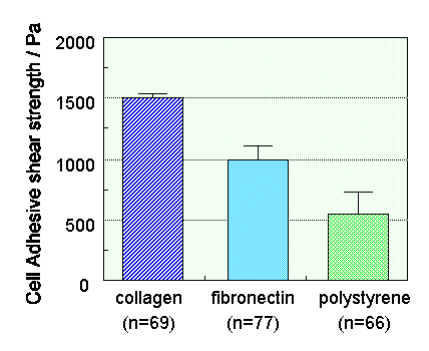


Figure 2. Cell adhesive properties of L929 on fibronectin-coated, collagen(type I)-coated, and uncoated polystyrene dish.

number and the morphology of the cells adhering to these surfaces. These fact suggest that morphological and qualitative evaluation of cell adhesion onto ECM-coated and uncoated surfaces relates to the strength of adhesion between the cell and these surfaces.

A cell adheres to a substrate surface not the whole area facing to the substrate surface but with some parts of it, forming adhesion plaques. Adhesion plaque is the cluster of adhesive molecules such as transmembrane integrins binding to ECMs adsorbed onto the substrate surface. The integrins are connected to the cytoskeletal structures by attachment proteins such as talin, vinculin, and αactinin. Cell-substrate adhesion is constructed by a series of bindings; the binding between a cytoskeletal protein and an integrin, the binding between the integrin and an ECM, and the binding between the ECM and the substrate surface. The differences in cell adhesive shear force are caused by the following factors; 1) the difference in the number of the complete set of serial bindings between the cell and the surface (an "entire" binding) per a cell or per a unit cell adhesive area, and 2) the difference in the strength of each "entire" binding.

Figure 3 shows the schematic explanation of the differences in cell adhesion to ECM-coated and uncoated dishes. In normal cell culture condition, cell adhesion onto glass or polystyrene is mediated not by fibronectin but by vitronectin(a).

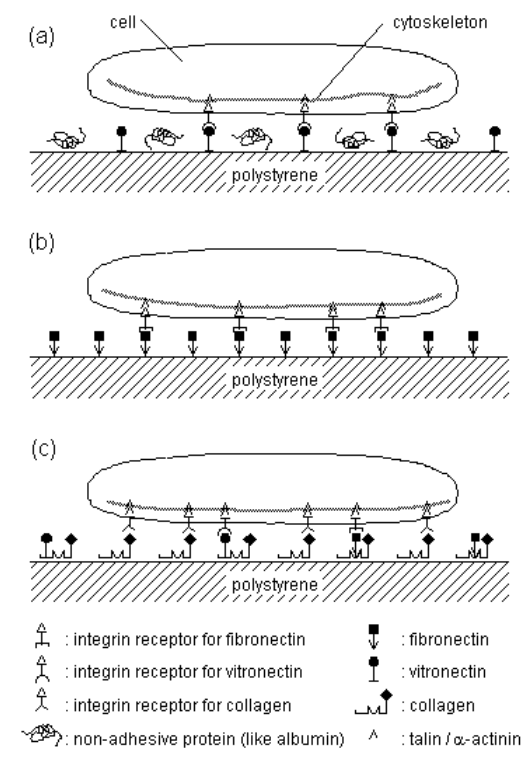


Figure 3. Schematic explanation of cell adhesion to polystyrene with cell adhesion molecules

When the polystyrene surface is coated with fibronectin, only a serial binding including fibronectin is formed (b). Comparing to the polystyrene uncoated surface, cells can easily form the "entire" bindings since the binding between the polystyrene surface and fibronectin is already done. In the case of collagen-coated dish, the binding between polystyrene and collagen is also done. Furthermore, collagen could bind directly to the cell and indirectly through fibronectin and vitronectin (c), which is an advantage for making the larger number of "entire" bindings comparing to fibronectin-coated and uncoated dishes.

The strength of the "entire" binding is decided by the strength of the weakest "fragmentary" binding in the "entire" binding. It is observed that an "entire" binding of the cell-cell or cell-substrate adhesion is frequently fractured at the binding between the transmembrane receptor and the cytoskeletal protein, resulting in the extraction of the receptors from the plasma membrane[3]. Transmembrane integrins are found on the substrate surface after the cell moved away spontaneously[4]. Furthermore, the force necessary to extract an transmembrane receptor from plasma membrane was measured as 10-20 pN[5], which is the same order of the magnitude as the force required to break another "fragmentary" binding such as the binding between a transmembrane receptor and its ligand[6]. These fact suggests that the "entire" binding of cellsubstrate adhesion can be fractured at any "fragmentary" binding and that the strength of cell-substrate adhesion mainly depends on the "entire" bindings formed. of the number According to IRM observation of cell detachment process by this system, a part of cell surface proteins were remained on the substrate surface after cell detachment, suggesting that the extraction of transmembrane receptors is occurred. In future, the fracture point of the "entire" binding of cell-material adhesion should be confirmed by fluorescent microscopy to elucidate the mechanism of cell detachment from material surface.

**REFERENCES:** <sup>1</sup>A. Yamamoto, et al (1998) *Biomater*. **19**:871-879. <sup>2</sup>A. Yamamoto, et al (2000) *J. Biomed. Mater. Res.* **50**:114-124. <sup>3</sup>E. Evans, D. Berk, and A. Leung (1991) *Biophys J* **59**:838-848. <sup>4</sup>C.M.Rengen and A.F. Horwitz (1992) *J Cell Biol* **119**:1347-1359. 5L. Chu, L.A. Tempelman, C. Miller et al (1994) *AIChE J* **40**:692-703. <sup>6</sup>S.C. Kuo, D.A. Lauffenburger (1993) *Biophys J* **65**:2191-2200.

# SELECTIVE MOLECULAR ASSEMBLY PATTERNING - A NEW APPROACH TO MICRO- AND NANOCHEMICAL PATTERNING OF SURFACES FOR BIOLOGICAL APPLICATIONS

R. Michel<sup>1</sup>, J. W. Lussi<sup>2</sup>, G. Csucs<sup>3</sup>, A. Goessl<sup>2</sup>, I. Reviakine<sup>1</sup>, J. A. Hubbell<sup>2</sup>, G. Danuser<sup>3</sup>, M. Textor<sup>1</sup>, N. D. Spencer<sup>1</sup>

<sup>1</sup> <u>Laboratory for Surface Science and Technology</u>, <sup>2</sup> <u>Institute for Biomedical Engineering</u>, <sup>3</sup> <u>Bio Micro Metrics Group</u>, Swiss Federal Institute of Technology, Zurich, Switzerland.

**INTRODUCTION:** The repertoire of receptors and signalling markers expressed on the surface of cells in vivo is nothing else than a complex topochemical pattern, the function of which is to elicit response from other cells. Our ability to investigate and manipulate the interaction between cells and extra-cellular environment (extra-cellular matrix or an implant) depends crucially on the availability of suitably patterned surfaces. Patterned surfaces have already been shown to affect growth, differentiation, and death of cells<sup>1,2</sup>. Here, we present a novel techniques—Selective Molecular Assembly Patterning (SMAP)—for creating various chemical patterns by means of selective self-assembly on oxide surfaces.

METHODS: Standard photolithography was used to create patterns of titanium oxide within a matrix of silicon oxide. Using the fact that ordered SAMs of alkane phosphates form on the TiO2, but not on the SiO<sub>2</sub>, surfaces, by self-assembly from aqueous solutions, the TiO<sub>2</sub> structures were rendered hydrophobic and hence protein-adsorbing. Poly-Llysine-g-poly(ethylene glycol) (PLL-g-PEG)<sup>3,4</sup> was used to render the exposed SiO<sub>2</sub> protein-resistant, thus creating a contrast with respect to protein adsorption. X-ray photoelectron spectroscopy and imaging time-of-flight secondary ion mass spectrometry were used to characterize the surfaces in vacuum, while fluorescence microscopy was used for studies in aqueous media.

**RESULTS:** Ouantitative XPS as well as qualitative ToF-SIMS results proved that dodecylphosphate adsorbed on the TiO2 surface forming a self-assembled monolayer<sup>5</sup>, leaving SiO<sub>2</sub> bare. Subsequent modification with PLL-g-PEG resulted in protein-adhesive patches (TiO<sub>2</sub>/DDP) in a matrix resistant to protein adsorption (SiO<sub>2</sub>/PLL-g-PEG), as shown in Figure 1A. Human foreskin fibroblasts (HFF), incubated with such substrates in serum, exhibited preference towards attaching to the proteinadhesive (hydrophobic) areas (Figure 1B), where they form focal contacts. The non-adhesive areas remained cell-resistant for up to two weeks.

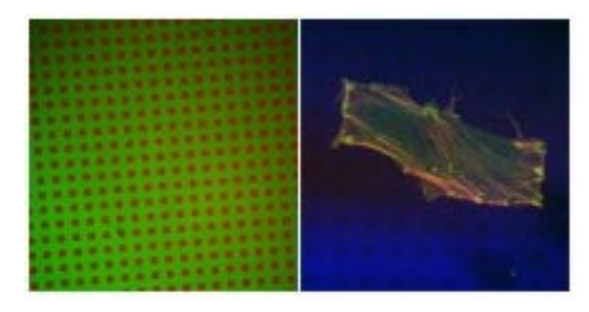


Fig. 1: A. Left: Rhodamine labelled streptavidin adsorbed to 5x5 µm TiO2/DDP patches (red) surrounded by fluorescein labeled PLL-g-PEG (green) matrix. B. Right: HFF, incubated for 20h in serum on a patterned surface, fixed, and stained for actin (red) and vinculin (green).

DISCUSSION & CONCLUSIONS: Protein adsorption studies conclusively established that the resulting surfaces present protein adhesive (the TiO<sub>2</sub>/alkane phosphate SAM region) and non-adhesive (the PLL-g-PEG-coated SiO<sub>2</sub>) areas. Human foreskin fibroblasts were shown to selectively attach to the protein-adhesive areas. Current research is focusing on creating patterns in the sub-micrometer range and evaluating the response of a variety of cell types to pattern geometry and chemistry. The high quality, reproducibility, simplicity, and versatility of SMAP make it a promising technique for both scientific and industrial applications in the context of biomaterial and biosensor surface technology.

**REFERENCES:** <sup>1</sup> Wheeler *et al.*(1999) *J Biomech Eng* **121**:73-78. <sup>2</sup>Chen *et al.* (1997) *Science* **276**: 1425-1428. <sup>3</sup>Elbert and Hubbell (1998), *Chem Biol* **5**:177-83. <sup>4</sup>Kenausis *et al.* (2000) *J Phys Chem B* **104**:3298-3309. <sup>5</sup>Textor *et al.* (2000) *Langmuir* **16**:3257-3271.

**ACKNOWLEDGEMENTS:** We thank Dr. J. Vörös for enticing discussions. This work is financially supported by the TOP NANO 21 Program of the ETH-Council.

# DYNAMICS OF PROTEIN MOVEMENTS ON THE CELL SURFACE; ROLE IN ATTACHMENT AND EFFECTS OF SURFACE DIPOLES & ELECTROSTATIC POTENTIALS

<sup>1</sup>Paul O'Shea & Josep Cladera

<sup>1</sup>Cell Biophysics Group, School of Biomedical Sciences, University of Nottingham England UK

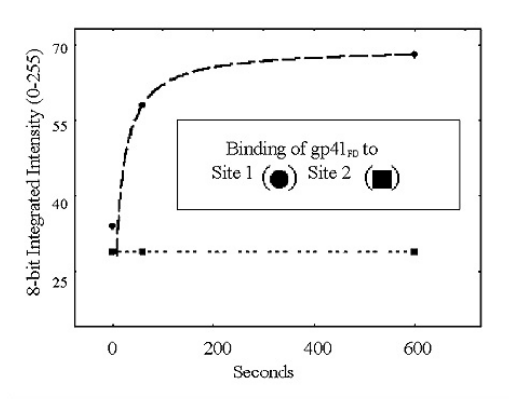
INTRODUCTION: The behaviour of proteins located upon and within the plasma membranes of living cells has long been recognised to underlie the many types of interaction of such cells. In terms of communication with various substrata, this involves responses from signalling systems as well as those simply involved in physical adherence. The movements of plasma membrane proteins also seem likely to be involved in such interactions. In our laboratory we have made efforts to study the physical nature of the membrane surface with a view to determining how this affects and is affected by membrane components. In particular, we have developed techniques to measure the surface electrostatic properties of the cell surface as well as the influence molecular dipoles have on many types of inter-molecular interactions with membranes (1-5). These factors also have a significant bearing on how cells interact with artificial surfaces and may be used for the rational design of 'bioactive' surfaces.

The current presentation will outline this technology and indicate how it may be applied to studies of relevant cell properties involved in communication with biocompatible surfaces. This will be illustrated with examples of intermolecular interactions with membranes, protein movements and controlled cellular adhesion. Studies are routinely undertaken with populations of cells for kinetic measurements of molecular interactions and for single cell imaging for studies of localised interactions on the cell surface.

**METHODS:** The sensing technologies involve labelling the plasma membranes of living cells with fluorescent indicators sensitive to the surface electrostatic potential and the membrane dipole potential (see <sup>1-5</sup>). For populations of cells, studies are undertaken with any standard benchtop fluorimeter. For studies of more localised interactions on the cell surface, ultra-high resolution imaging facilities have been developed utilising the same sensor technologies.

**RESULTS AND DISCUSSION:** A body of knowledge has been built up of the role that the surface electrostatic potential and membrane dipole potential plays in the molecular interactions

of membranes. Fig 1 illustrates some of these techniques showing that the interactions of a surface-active peptide (involved in HIV infection) is highly localised about the cell surface. Similar-such studies have been performed with other kinds of protein such as fibronectin (paper in preparation). An outline of the factors that control these membrane properties will be given.



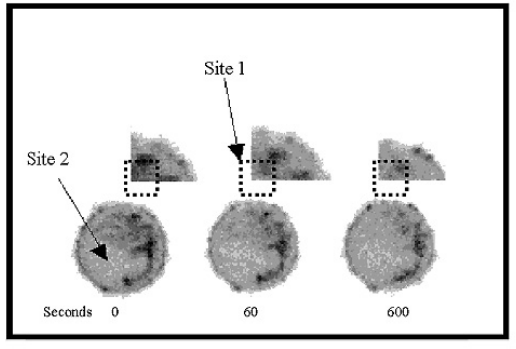


Fig 1 – localised binding of HIV peptide with T cells. See ref.  $^4$ 

**REFERENCES**: <sup>1</sup> Cladera, J. & O'Shea, P. (2001) Generic techniques for fluorescence measurements of protein-ligand interactions; real-time kinetics & spatial imaging. pp. 169-200. In *Protein-Ligand Interactions*. Harding & Chowdery (eds.) Oxford University Press. UK.

- <sup>2</sup> Wall, J., Ayoub, F. & O'Shea, P. (1995) *J. Cell. Sci.* **108**, 2673-2682
- <sup>3</sup> Cladera, J. & O'Shea, P. (1998) *Biophys. J.* **74**, 2434-2442.
- <sup>4</sup> Cladera, J., Martin, I. and O'Shea, P. (2001). *EMBO J.* **20**, 19-26.
- <sup>5</sup> Asawakarn, T., Cladera, J. & O'Shea, P. (2001). Effects of the Membrane Dipole Potential on membranes etc.. *J.Biol.Chem* In press Nov 2001.

# SURFACE ENGINEERING OF MATERIALS FOR BIOMIMETIC IMPLANTS AND CELL-BASED SENSORS

K.E. Healy

University of California, Berkeley, Depts. of <u>Bioengineering</u>, Materials Science and Engineering Berkeley, CA 94720-1762, USA

**INTRODUCTION:** A central theme in the design of materials that actively regulate the response of either mammalian cells or tissue formation is that they do so through a combination of biomolecular recognition processes and device microarchitecture. In my research group we have designed and synthesized model biomimetic materials that can be used to test hypotheses regarding cell-materials interactions. control cell behaviour chemically either through specific ligand-receptor interactions or by modifying the projected area of cells to limit growth and promote differentiation. These surfaces may find use in applications such as combinatorial analyses, novel culture systems, the modification of implant surfaces, DNA chips, and cell-based biosensors. In this work we have elicited these materials to begin to understand the details in the cascade of events involving cell cytoskeletal organization, morphology, intracellular signalling, nuclear shape, nuclear matrix organization, promoter geometry, and gene expression. We report the first method for both precisely controlling cell and nuclear shape, and measuring in situ mRNA expression and collagen I expression in an effort to help elaborate these mechanisms.

METHODS: We have developed methods that incorporate photolithography, organosilane chemistry, photoinitiated polymerisation, and peptide chemistry to create surfaces that control the spatial distribution, projected area, and nuclear shape of mammalian cells. For example, we synthesized novel interpenetrating polymer networks (IPNs) based on polyacrylamide [p(AAm)] and poly(ethylene glycol) [PEG] that form thin coatings (~ 20nm) on both metal oxides TiO2) and polymers SiO2, polystyrene). We have determined that these IPNs prevent protein adsorption and cell adhesion and therefore represent an excellent surface to control the spatial distribution of either biological macromolecules, cells, or viruses. surfaces were fabricated using a photolithographic process resulting in islands of cell binding N-(2aminoethyl) - 3 - aminopropyl - trimethoxysilane (EDS) separated by a non-adhesive IPN

[poly(acrylamide-co-ethylene glycol); p(AAm-co-EG)] as described previously.1 The surfaces contained over 3800 adhesive islands/cm2, allowing for isolation of single cells with projected areas ranging from 100 □ m2 to 10,000 □ m2. Surfaces were characterized using ToF-SIMS with imaging capabilities. Additionally, protein adsorption from serum was analysed using immunostaining and confocal microscopy.

Bone cells were isolated from rat calvaria (6-12 days old) and exposed to the surfaces. Cytoskeletal organization was examined, using Factin staining, to determine the influences of confining cell projected area on stress fibre formation. Determination of single cell protein expression on these surfaces required a reverse transcriptase in situ polymerase chain reaction (RT in situ PCR) be performed. Therefore, protein expression at the mRNA level could be observed within single cells with 56 different projected areas (>12,000 cells) on one surface. In particular, osteocalcin expression was examined within primary bone-derived cells exposed to these chemically patterned surfaces. Collagen I synthesis was determined intracellularly via indirect immunofluorescence microscopy.

**RESULTS:** ToF-SIMS with imaging capabilities verified that the photolithographic preparation of the surface resulted in spatially-resolved chemistries. Preferential adsorption of Vn to the EDS regions directed the distribution and projected area of mammalian cells.2

Cell attachment, distribution, and spreading was dictated by the EDS chemistry, resulting in single cell attachment to regions <2000 □m2. Larger EDS regions supported multiple cell attachment and/or cell proliferation. F-actin staining indicated that stress fibre formation was influenced by the shape of the adhesive EDS region. The shapes of the nuclei of primary osteogenic cells were also controlled on microfabricated substrata. Gene expression and protein synthesis were altered by simply changing the shape of nucleus, dictated by the island size, without the use of chemical intermediates or changing the surface density of adsorbed

extracellular matrix proteins. Collagen I synthesis correlated directly with cell shape and nuclear shape index (NSI), where intermediate values of nuclear distension (6 < NSI < 8) promoted maximum synthesis. Osteocalcin mRNA, a bone-specific differentiation marker, was observed intracellularly using RT in situ PCR at 4 days in cells constrained by the pattern and not detected in unconstrained cells of similar projected area, but different NSI (Fig. 1). These data support the concept of "architectural" transcription factors that promote gene expression based on optimal stress within the nuclear matrix transduced by the cytoskeleton.

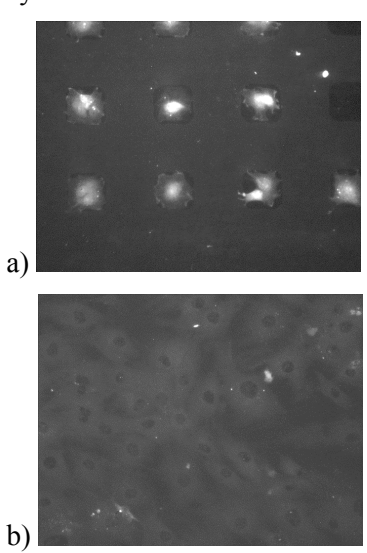


Figure 1: RT in situ PCR for osteocalcin on a.) EDS/P(AAm-co-EG) and b.) homogeneous EDS surfaces. Light regions indicate presence of osteocalcin mRNA.

DISCUSSION & CONCLUSIONS: Our data supports the concept of gene expression and protein synthesis based on optimal distortion of the nucleus, possibly altering transcription factor affinity for DNA, transport to the nucleus, or nuclear matrix organization. The combination of microfabricated surfaces, RT in situ PCR, and NSI measurement is an excellent system to study how transcription factors, the nuclear matrix, and the cytoskeleton interact to control gene expression and may be useful for studying a wide variety of other cell shape/gene expression relationships

**REFERENCES:** <sup>1</sup> Thomas, C.H., et al., JBME, 121:40, 1999. <sup>2</sup>Thomas, C.H., et al., JBMR, 37:81, 1997.

**ACKNOWLEDGEMENTS:** This research was supported by N.I.H and the Whitaker Foundation.

# FUNCTIONALIZED SURFACES THAT LIMIT NON-SPECIFIC PROTEIN BINDING FOR BIOASSAY AND ARRAY PLATFORMS

D.W. Grainger

Department of Chemistry, Colorado State University, Fort Collins, CO 80523-1872 USA

**INTRODUCTION:** Long-desired improvements to immunodiagnostic, protein micro array, and various biosensor device platforms require careful material/biomolecule control of synthetic interactions at surfaces. Frequently, current assay and array designs require tethering a biomolecule or signal transduction element to a surface in a manner that optimises surface density for signal production while maintaining bioactivity. Simultaneously, non-specific inhibition of biological adsorption is desired in order to minimize background noise. Optimal surface chemistry for bioanalytical applications thus provides a means for immobilizing specific biomolecules while minimizing non-specific binding, often including control over spatial patterning and repeat assay/surface renewal. This presentation will describe two different newly developed polymeric coatings formulated to provide these features and their properties under bioassay conditions. Two graft copolymers, a copolysiloxane and a terpolysiloxane, have been synthesized by grafting with dialkyl disulfide chains and methoxy-terminated poly(ethylene glycol) (PEG) chains. The terpolysiloxane also has grafted PEG sidechains terminated with the reactive ester, N-hydroxysuccinimide (NHS). These copolymers have been attached to gold surface plasmon resonance (SPR) assay surfaces, analysed using surface analysis and assessed for protein binding in both specific and non-specific modes in the SPR biosensing configuration.

A new commercial bioassay polymer coating, OptiChem<sup>TM</sup>,\* was also tested for non-specific and specific binding on a variety of polymer, glass and metal substrates. This crosslinked organic polymer thin film surface, while proprietary, is derivatized with controlled amounts of either biotin or reactive vinyl sulfone ligands capable of bioimmobilization at high densities. Analysis using colorimetric and particle-based detection schemes both demonstrate the combination of high specific antibody and oligo-DNA capture in sandwich assay format, with low non-specific protein uptake from serum.

**RESULTS & DISCUSSION:** Both grafted polysiloxanes spontaneously form monolayers on gold surfaces with estimated thicknesses of 23Å and 31Å, respectively. Combined analysis with

angle-dependent X-ray photoelectron spectroscopy (XPS) and static time-of-flight secondary ion mass (ToF-SIMS) spectrometry support attachment of dialkyl disulfide sidechains to the gold surface, while also concentrating the grafted PEG chains at the outer surface. **ToF-SIMS** provided evidence for NHS group surface exposure as well. Single protein adsorption onto both polymer monolayers examined with SPR was below the method's detection limit (~1 ng/cm2). Under chemical coupling conditions, the NHSgrafted terpolymer monolayer immobilized significant amounts of antibody, reflecting NHS reactivity.

The OptiChem<sup>TM</sup> polymer surface is coatable from solvent, crosslinking into stable transparent <100nm-thick films independent of substrate chemistry. Streptavidin, antibody and serum protein adsorption is minimal (<5 ng/cm2) on "inert" (no ligand) OptiChemTM controls coated on thermoplastic, metal or metal oxide supports. Specific streptavidin binding on biotinylated OptiChemTM surfaces can be varied with biotin load, and actively promotes further biotinylated antibody binding in the typical sandwich format. Biotinylated DNA probes also bind at high density.

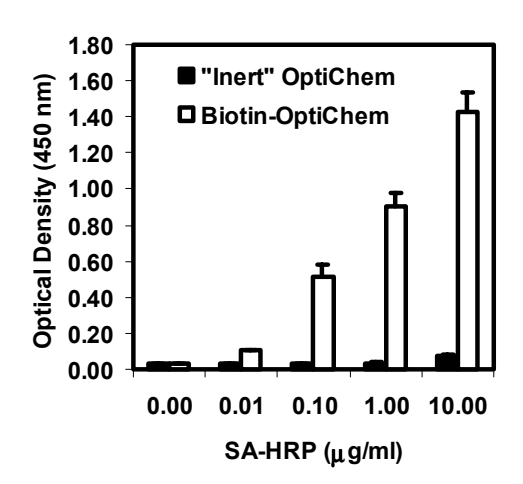


Figure: Colorimetric assay of streptavidin-HRP binding to biotinylated and inert OptiChemTM coatings on tissue culture polystyrene substrates. (n = 6, error bars +/- standard deviation in the set).

\*OptiChem<sup>TM</sup> surfaces are owned and licensed by Accelr8 Technology Corp. (www.accelr8.com)

## MOLECULAR DIVERSITY OF ACTIN-INTEGRIN ADHESION COMPLEXES

B.Geiger<sup>1</sup>, E.Zimmerman<sup>2</sup>, E.Zamir<sup>1</sup>, Z.Kam<sup>1</sup>, A.Bershadsky<sup>1</sup> L.Addadi<sup>2</sup>

Departments of Molecular Cell Biology<sup>1</sup> and Structural Biology<sup>2</sup>, <u>Weizmann Institute of Science</u>, Rehovot 76100, ISRAEL

**INTRODUCTION:** Cell adhesion is a multistep process, initiated by surface recognition and attachment, and continuing with cell spreading, formation of focal adhesions (FA) and the activation of adhesion-mediated signalling. A conceptual temporal and spatial gap exists between the first encounter of a cell with an adhesive substrate and the advanced stages of FA formation. While ample information is available on focal adhesions structure and function, the mechanism of the first interaction events and the nature of the molecules mediating them are largely unknown. We have identified cell surface-associated hyaluronan as a major mediator and modulator of the first steps of adhesion of A6 and other cells to conventional tissue culture substrates, as well as to the surfaces of calcium-(R,R)-tartrate tetrahydrate crystals. Treatment of A6 cells with hyaluronidase suppresses their rapid interactions with these adhesive substrates, and incubation of either the hyaluronidase-treated cells or the substrate with hyaluronan restores cell adhesion. In contrast, excess hyaluronan on both the cells and the substrate strongly inhibits adhesion. We thus propose that cell surface-associated hyaluronan regulates cell-matrix adhesion at the very first encounter with the substrate. It may promote it through the establishment of exquisitely stereospecific chemical interactions, or inhibit it by virtue of steric exclusion and/or electrostatic repulsion.

Following incubation on appropriate extracellular matrix (ECM) these initial adhesion are replaced by integrin-mediated adhesions, in the form of focal complexes and FA. The latter adhesion sites were extensively characterized at the molecular level and shown to contain numerous anchor and cytoskeletal proteins (over 50 by now). Studies of these proteins, both biochemically and in situ has provided valuable information on the complexity of these adhesion sites and the molecular interactions which take place in them. These studies also raised intriguing questions concerning the structural and functional differences which may exist between the various forms of actinintegrin adhesion complexes (including FA, focal complexes, fibronexus, ECM adhesions, fibrillar adhesions and podosomes). Our studies indicate that these sites are highly heterogeneous at the molecular level. They are also highly dynamic, continuously exchanging components with the cytoplasmic soluble pool, and translocating along the ventral cell membrane. This translocation plays an important role in the assembly and reorganization of the ECM, and is regulated by the actomyosin contractile machinery of the cells, by the Src/FAK signalling system, as well as by the physical properties (e.g. stiffness or pliability) of the extracellular matrix

## CONTROL OF CELL RECOGNITION AND ATTACHMENT OF HEPATOCYTES BY GLYCOPOLYMERS

T.AKAIKE<sup>1,2</sup>

<sup>1</sup> Graduate School of Bioscience and Biotechnology, Tokyo Institute of Technology <sup>2</sup> Graduate School of Medicine, Shinshu University

INTRODUCTION: Tissue engineering and regenerative medicine are now very attractive field of biomaterials. New polymers design for cell recognition and attachment is growing important. We paid attention to asialoglycoprotein receptor (ASGP-R) which appears in hepatocyte surface and E-cadherin that mediates the intercellular adhesion between hepatocytes, with the aim of the molecular design of new extracellular matrices (ECM) alternatives for cell and tissue engineering. On the former topics, the amphipathic polymer, PVLA, was designed by the combination of βgalactose into the styrene monomer and the functional expressions of hepatocytes that are phagocytosis, adhesion, drug metabolism (P-450) and bile acid secretion, etc., were examined by the adjustment of the coating condition of PVLA polymeric micelle. On the latter, the fusion molecule (E-cad-Fc) chimeric between extracellular domain of E-cadherin and fragment crystallisable region (Fc) of antibody molecule by the genetic-engineering designed technique. The model system of attachment of hepatocyte onto polystyrene substrate coated with E-cad-Fc molecule which mimics the formation of cell-cell adhesion mediated by E-cadherin molecules between hepatocytes was established. Using this model system, we aimed at the intercellular elucidation of adhesion in comparison with hepatocyte-adhesions to PVLA and collagen.

### **RESULTS & DISCUSSION:**

Control of drug metabolic activity in hepatocytes on collagen and PVLA.

Aminopyrine N-demethylase (AMND) activity which is one of the drug metabolic activity of the hepatocyte showed the oscillational change with the cultivation time on the collagen-coated dish. This period of oscillation is synchronized with bile acid quantity in culture medium. And synchronization phenomenon between AMND activity and bile acid quantity was also observed on PVLA-coated dish (coating conc.:1 $\Box$ g/ml). However, the period of oscillation on PVLA has slowed down than the oscillation period on

collagen and was partially perturbed. This time, the expression of mRNA of various proteins in hepatocyte is greatly different. That is, it synchronized to the oscillatory phenomenon of AMND activity and bile acid concentration, and the heat shock protein has appeared on collagen, and transcriptional regulatory factors appeared on PVLA.

Biomimetics of Cell-Cell Adhesion mediated by E-cadherins:

In order to clarify the cell adhesion mechanism through E-cadherins, the analysis in the model system was made . For the surface coated with the chimeric protein (E-cad-Fc), the hepatocyte remarkably adhered to the surface and cell adhesion was inhibited by addition of anti-E-Generally, the hepatocyte cadherin antibody. keeps the differentiated capacity by forming spheroid, and the DNA synthetic ability of spheroid lowers in comparison with the spreading form of hepatocytes. When cultured on E-cad-Fc, low DNA synthetic ability was also observed. In addition, the expression of tryptophan oxygenase, which is a special differentiative marker of hepatocyte, was maintained as same as spheroid. From these facts, the possibility of inducing the differentiation of hepatocyte by the cell adhesion through the E-cadherin was indicated. Chimeric protein (EGF-Fc) was also designed as new EMC analogues and examined in the viewpoint of cell adhesion and signal transduction

# TOTAL INTERNAL REFLECTION FLUORESCENCE (TIRF) MICROSCOPY: APPLICATIONS TO CELL BIOLOGY

### D.Axelrod

University of Michigan, Ann Arbor, USA

INTRODUCTION: Total internal reflection fluorescence (TIRF) microscopy (also called "evanescent wave microscopy") provides a means to selectively excite fluorophores in an aqueous or cellular environment very near a solid surface (within £ 100 nm) without exciting fluorescence from regions farther from the surface. Fluorescence excitation by this thin zone of electromagnetic energy (called an "evanescent field") results in images with very low background fluorescence, virtually out-of-focus no fluorescence, and minimal exposure of cells to light at any other planes in the sample. The unique features of TIRF have enabled numerous applications in biochemistry and cell biology.

TIRF can be set up in a variety of configurations. All involve only simple add-on modifications of standard upright or inverted fluorescence microscopes and all are easily switchable with other forms of illumination. Some of the configurations involve deployment of an extra prism to direct the excitation light toward the sample plane at an angle exceeding the critical angle for total internal reflection. Other configurations use a very high aperture objective (NA>1.4) now commercially available. Although laser illumination is most convenient, TIRF can also be set up with a conventional arc lamp source.

Three particular applications to quantitative observation of the dynamics of the cell surface are discussed. The first employs the exponential decay of the evanescent field intensity with distance from the surface to characterize the nanometer-scale motions of GFP-marked secretary granules relative to the plasma membrane in both unstimulated and stimulated bovine chromaffin cells. The second takes advantage of the unique polarization properties of the evanescent field to observe dynamic changes in the micromorphology of the diI-labeled plasma membrane macrophages (e.g., at putative endocytotic sites). The third combines TIRF with fluorescence recovery after photobleaching to measure the spatially-resolved association/dissociation kinetic rates of labelled actin at the submembrane of living smooth muscle cells.

# FIBROBLAST MECHANICS IN A MODEL EXTRACELLULAR MATRIX - AN APPLICATION OF OPTICAL SECTIONING MICROSCOPY

S. Vanni<sup>1</sup>, B.C. Lagerholm<sup>1</sup>, C.A. Otey<sup>2</sup>, D. Velegol<sup>3</sup>, D.L. Taylor<sup>1</sup>, F. Lanni<sup>1</sup>

<sup>1</sup>Center for Light Microscope Imaging & Biotechnology, and Department of Biological Sciences, Carnegie Mellon University, Pittsburgh PA 15213 USA. <sup>2</sup>University of North Carolina, Chapel Hill NC 27599 USA. <sup>3</sup>Penn State University, College Park PA 16802 USA

INTRODUCTION: The cytoskeleton in a nonmuscle cell is dynamic and versatile, and drives many essential processes ranging from cell division to wound healing. Through our work, we hope to understand how and where cells such as fibroblasts build and regulate the cytoskeletal machinery needed to carry out well-defined motile tasks. In essence, we aim to get, for non-muscle cells, the type of information routinely available to the muscle physiologist - detailed mechanics in addition to cytoskeletal kinematics. As a basis for this project, we need quantitative information on the spatial pattern and magnitude of the forces (tractions) applied by a cell to its surrounding matrix and neighbours, and a means for matching those patterns identifiable cytoskeletal structures. pioneering work of Harris [1] in growth of cells on transparent elastic substrata provides a means for estimating complex tractions through microscopy and digital image processing [2]. We have extended this approach to cells in collagen matrices, and we have automated the mechanics analysis.

METHODS: In our experiments, mouse 3T3 fibroblasts expressing GFP-alpha-actinin or YFPactin are grown in a three-dimensional (3D) model extracellular matrix (ECM) composed of type I collagen hydrogel with specific isometric constraints and free-boundaries. Collagen is the primary constituent of connective tissue ECM and thus approximates a native environment for this cell type. The entire specimen is made small enough (5mm square x 0.3mm thickness) so that a large fraction of its volume is accessible to view with high-NA optics. By use of a perusable, thermostatted environmental chamber, the specimen can be maintained on the microscope for periods up to seven days. Our Automated Interactive Microscope (AIM) supports time-lapse, repetitive serial-focus operation, and switching between transmitted-light (Nomarski DIC) and fluorescence imaging modes. In the fluorescence illuminator light path, we utilize a grating imager [3] for optical sectioning. In a typical experiment, 10-60 fields are logged over which image sets are captured on a schedule. The AIM log and schedule can be complex, for example with differing frequency in DIC and fluorescence, and it can be modified interactively to eliminate or add fields as the specimen develops. In most cases, serial-focus data are acquired on each visit to each field. The AIM software creates a hierarchical data

structure which can be tiled, or indexed by time, focus plane, or imaging mode for review and processing.

In DIC collagen fibrils are visible as a 3D network, so the model ECM can serve as an "in-situ strain gauge" readable through high-resolution time-lapse microscopy without extrinsic marker particles. The microscope is used in two ways: to image by fluorescence the distribution of key cytoskeletal proteins in individual cells, and by DIC the displacements in the ECM caused by the mechanical action of each cell. For most cells, which are embedded in the collagen matrix, the quasi-static displacement field,  $\underline{U}(x,y,z,t)$ , extends in all directions within the surrounding volume. Although our serial-focus DIC data in principle allows us to track displacements in 3D, we currently use a 2D plane-strain approximation to analyse image sets in which the cell major axis coincides with a plane of focus. The configuration of the model system produces a high percentage of cells that meet this condition. A series of 2D vector displacement fields,  $\{Ux(x,y),Uy(x,y)\}$ , is generated by use of our Deformation Quantification and Analysis software (DQA), which runs on a PC-based server. DQA utilizes windowed cross correlation to compare selected images from a time-lapse sequence. Using basic elasticity theory, DQA derives the 2D density increment, d(x,y), and the plane-strain tensor field:  $e_{ii}(x,y) = (\partial U_i/\partial x_i + \partial U_i/\partial x_i)/2$ 

Both *d* and [eij] are independent of material properties. Furthermore, from microrheometric measurements in cell-free gels [4], we know that the matrix is elastic under small deformations with a shear modulus averaging 50 Pa in the 2 mg/ml range. If a material constitutive relation is incorporated, the stress tensor field can be computed from the strain for estimating tractions. DQA software may be used on-line at dqa.web.cmu.edu.

RESULTS AND DISCUSSION: Over a period of several days in culture, 3T3 fibroblasts migrate long distances, proliferate, and contract the collagen gel to form a dense matrix resembling connective tissue. Deformations caused by the action of relatively isolated cells can produce anisotropy in the collagen which may affect other cells through contact guidance over 100-1000um distances. Sparse cells appear to organize into clusters or chains that

produce large-scale (non-elastic) condensation of the collagen. Single cells extend and retract long processes (pseudopods and filopods) and small lamellipods over 1- to 15-minute periods. In serum-deprived cultures, this activity produces little change in the model ECM. However, in growth medium (10% serum), cellular action leads to prominent elastic deformation of the collagen coupled to cell shape changes and locomotion. In fluorescence optical sections, GFP-alpha-actinin shows a highly non-uniform distribution throughout the cell (Fig.1), with major concentration in pseudopods and filopods. Deformation is quantified in corresponding

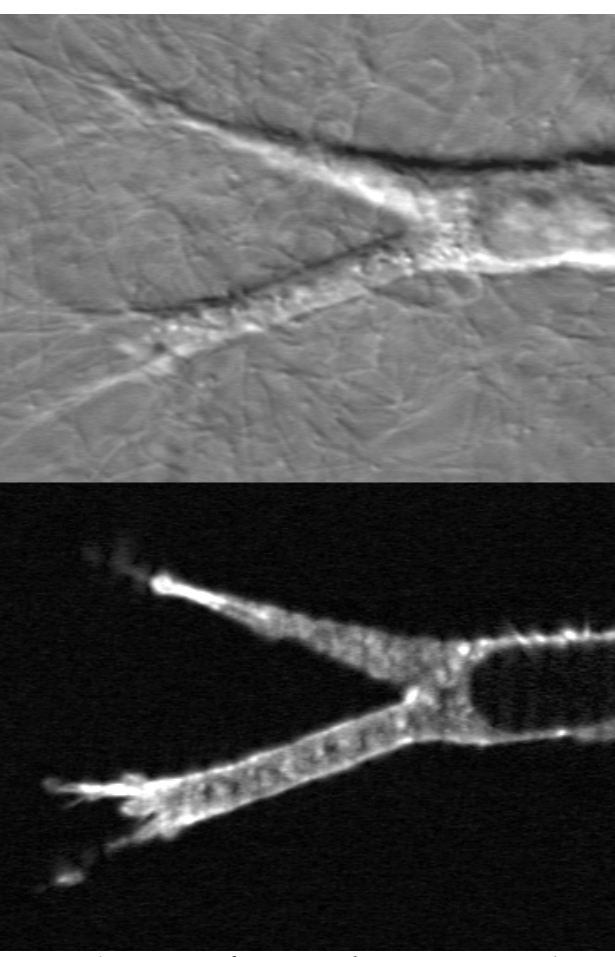


Figure 1. Images from time-lapse sequence. (upper panel) DIC image showing 3T3 fibroblast in collagen matrix. (lower panel) Corresponding fluorescence optical section showing GFP-alpha-Actinin. Field-of-view = 120um.

image maps of collagen density increment and of strain (Fig.2). Further data analysis will test the hypothesis that alpha-actinin is concentrated in the actin cytoskeleton at locations under the greatest tensile stress. In addition to the analysis of single-cell mechanics, it is possible to quantify large-scale deformation in tiled image sets. This opens the way to analysis of fibroblast behaviour in reshaping tissue in terms of single-cell effects, direct effects on neighbours, and collective action mediated by long-range effects on material properties.

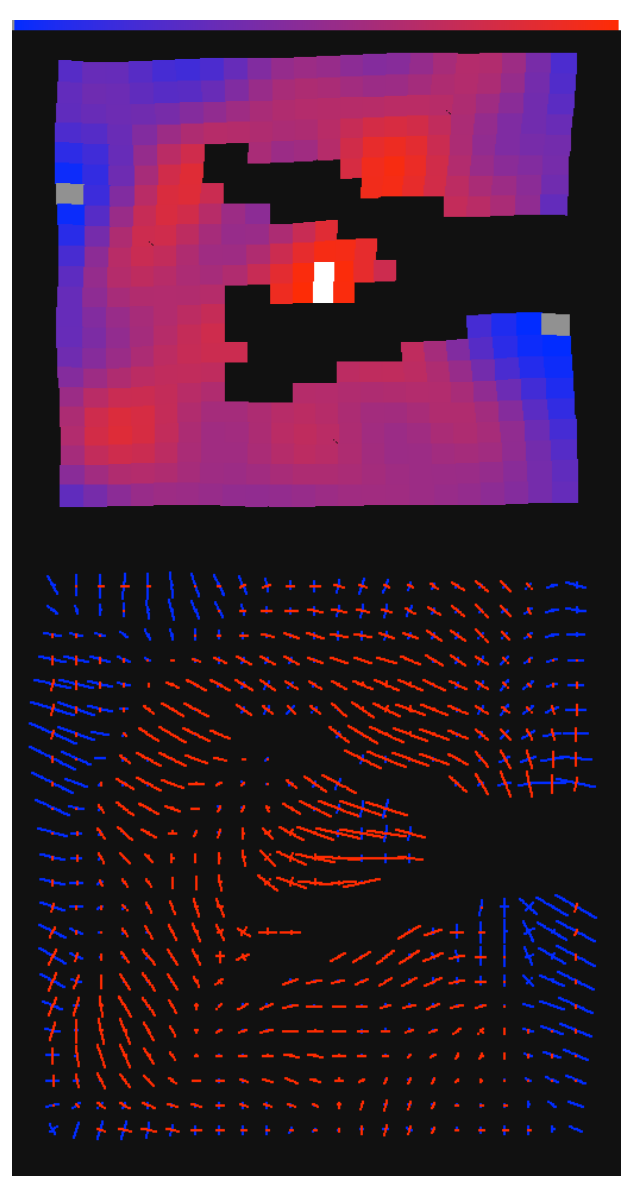


Figure 2. Mechanics analysis. (upper panel) 2D density increment (red = density increase, blue = density decrease, white = peak increase, gray = peak decrease). (lower panel) 2D principal strain field (red = material compression, blue = material extension).

REFERENCES: [1] A.K. Harris, P. Wild and D. Stopak (1980) Science 208: 177-179; [2] K. Burton, J.H. Park and D.L. Taylor (1999) Mol. Biol. Cell 10: 3745-3768; [3] M.A.A. Neil, R. Juskaitis and T. Wilson (1997) Opt. Lett. 22: 1905-7; F. Lanni and T. Wilson (2000) in *Imaging Neurons-A Laboratory Manual*, Cold Spring Harbor Laboratory Press; [4] D. Velegol and F. Lanni (2001) Biophys. J. 81: 1786-1792.

ACKNOWLEDGMENT: We thank Dr. Sunil Saigal (CMU) for advice on mechanics analysis, and David Pane, Michael Mantarro, and William Galbraith for AIM software development. This research was supported by grants NIH AR-32461, NSF STC MCB-8920118, and NSF DBI-9987393.

# INTEGRIN DENSITY IN FOCAL ADHESION SITES: A MEASURE FOR INTRACELLULAR TENSION AND RIGIDITY OF ADHESIVE SURFACES

B. Wehrle-Haller, C. Ballestrem, B.A.Imhof

Department of Pathology, Centre Médical Universitaire, University of Geneva, Switzerland

INTRODUCTION: Adhesion, spreading and migration of cells on extracellular matrix (ECM) are complex processes that play fundamental roles in development, wound healing and immune response. Heterodimeric transmembrane receptors of the integrin family provide the mechanical link between the extracellular environment and the actin cytoskeleton required for adhesion and migration. Prior to adhesion, integrins diffuse freely in the cell membrane. Upon recognition of ECM ligands, integrins aggregate laterally and get anchored at their cytoplasmic side within a scaffold of cytoskeletal proteins [1]. This protein complex forms an adhesion site in which mechanical forces required for cell motility are exchanged between the actin cytoskeleton and the extracellular environment [2]. It is our aim to understand the architecture and behaviour of integrins within adhesion sites in response to biological surfaces and how this architecture is modulated by changes in intracellular contractile forces during cell spreading and migration.

**METHODS:** We developed a new tool to directly study integrin behaviour in living cells. Green fluorescent protein (GFP) was fused to the cytoplasmic domain of the mouse \( \beta \)-integrin subunit (GFP-\u00ed3 integrin). Transfected GFP-\u00ed3 integrin was expressed on the cell surface and formed fully functional integrin heterodimers with the endogenously expressed aV integrin subunit [3]. We plated stably GFP-\(\beta\)3 integrin expressing cells on ECM coated glass coverslips and studied adhesion site dynamics by time lapse microscopy. Relative fluorescence intensity of integrin adhesion sites was measured using a CCD-camera piloted by the Openlab software. Modification of intracellular contractile forces was accomplished by transfecting cells with dominant active or dominant negative members of the Rho family of small GTPases (Rac1, CDC42, RhoA) or by pharmacological activation or inhibition of the acto-myosin contractile system.

**RESULTS:** Dynamic analysis of adhesion sites in migrating cells revealed the existence of two functionally different types of  $\alpha V \beta 3$  integrin containing adhesion sites. At the cell front, protruding lamellipodia exhibited many stationary, low-density integrin adhesion sites. While the cell

moved forward, low-density integrin adhesion sites transformed into high-density  $\alpha V\beta 3$  integrin containing adhesion sites, which began to slide when located to retracting parts of the cell rear. Integrin densities could vary up to 3-fold between these two types of contacts. Low-density integrin adhesion sites formed after relaxation of intracellular tension or stimulation by dominant active forms of Rac1 and Cdc42. In contrast, high-density integrin adhesion sites formed in a RhoA induced acto-myosin dependent manner.

**DISCUSSION & CONCLUSIONS:** The integrity of focal adhesion sites is maintained by a scaffold of actin filaments, that is cross-linked by bivalent actin-binding proteins. Integrins are physically linked to this framework by adaptor proteins such as talin. Due to the cytoplasmic anchorage of integrins within this actin lattice, we postulate that the integrin density is a direct reflection of the degree of acto-myosin contraction within an adhesion site. During cell migration, exploring organelles like lamellipodia or filopodia always form low-density integrin contacts that are subsequently transformed into high-density contacts by an acto-myosin dependent process. We propose, based on the ability of integrins to directly link the ECM to the actin cytoskeleton, that intracellular contraction of low-density integrin contacts is a way to probe the nanorigidity of the encountered ECM surfaces and determine the maximal intracellular force that can be applied to such contacts. By linking different adhesion sites through the actin cytoskeleton, a cell may be able to integrate information of substrate rigidity, and modify its spreading and migratory behaviour accordingly resulting in durotaxis [4].

**REFERENCES:** <sup>1</sup>M. Hynes, R.O. (1992) *Cell* **69**, 11-25. <sup>2</sup>I.R. Balaban, N.Q. et al (2001) *Nat Cell Biol* **3**, 466-72. <sup>3</sup>Ballestrem, C. et al (2001) (submitted). <sup>4</sup>Lo, C.-M. et al (2000) *Biophys. J.* **79**, 144-152.

**ACKNOWLEDGEMENTS:** We would like to thank Marie-Claude Jacquier for excellent technical assistance and Patrick Ross for the mouse cDNA of  $\beta 3$  integrin.

### QUANTITATIVE FLUORESCENT SPECKLE MICROSCOPY OF LAMELLIPODIAL ACTIN MESHWORK ACTIVITY

G.Danuser<sup>1</sup>, A.Ponti<sup>1</sup>, C.Waterman-Storer<sup>2</sup>

<sup>1</sup>Swiss Federal Institute of Technology, Zurich, <sup>2</sup> The Scripps Research Institute, La Jolla, CA, USA

**INTRODUCTION:** Cell morphological activity is dictated by a constant, dynamic rearrangement of the actin cytoskeleton. Recently, we have discovered a direct interdependence between the geometries of lamellar actin retrograde flow and leading edge [1]. This finding led to the hypothesis that the actin meshwork acts as a mechanical transducer, translating spatial flow variations promptly into morphogenetic responses. One of the key factors controlling the flow geometry are and extra-cellular cross-links cvtosolic transmembrane proteins (integrins) which establish a molecular coupling between the cytoskeleton and adhesive surface proteins. Thus, we may speculate that the distribution of surface proteins has an immediate impact on the actin dynamics, which, in turn, affects cell shape formation and motility. To test this line of arguments we have started to implement techniques that allow us to quantify actin dynamics as a function of adhesive and nonadhesive patterns. Here, we report first results in applying fluorescent speckle microscopy (FSM) as a means to measure actin assembly, translocation, and turnover in living cells.

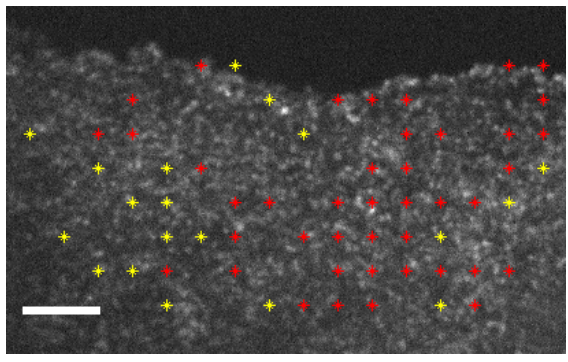
METHODS: FSM is a new technique for visualizing cytoskeleton activity [2]. In time-lapse FSM, movement of the speckles represents polymer translocation, while changes in speckle intensity and number density represent polymer assembly and turnover. However, the speckle signal is extremely complex and the density of image events is overwhelming for a human observer. The full power of FSM can only be exploited with specialized image analysis. Thus, our first effort is to implement software that enables us to extract the sought mechanical and chemical characteristics of f-actin from speckle image sequences.

**RESULTS**: To develop this program we have imaged actin speckles in two classes of living newt lung epithelial cells:

- 1.) Contact-inhibited cells within epithelial sheets do not exhibit obvious actin translocation. Thus, they are ideally suited for life-time analysis of spatially stationary actin speckles.
- 2.) In contrast, migrating cells at the periphery of the sheets exhibit actin flow from the leading edge towards the cell body. This provides us with a

system for developing tools that measure speckle field translocation.

Time lapse sequences were acquired for up to 3 hours at a frame-rate of 2-30 s with a cooled CCD camera (ORCA II) on a Nikon inverted microscope with 100X / 1.4NA optics. First results indicate that our FSM implementation indeed is capable of providing quantitative spatial information about cytoskeleton assembly, dissociation (Fig. 1) and translocation from inside



living cells (Fig. 2).

Fig. 1: Map indicating sites of polymerization (red) and depolymerization (yellow) in the lamellum of a contact-inhibited epithelial cell. Scale bar:  $2.5 \mu m$ .

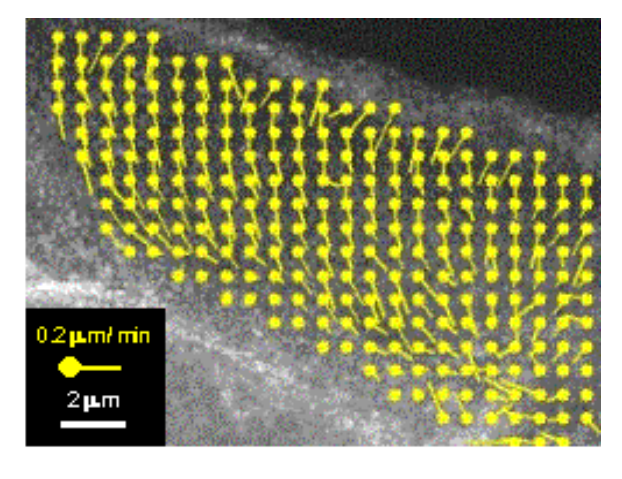


Fig. 2: Map of f-actin retrograde flow in a cell at the border of an epithelial sheet.

**REFERENCES:** <sup>1</sup>G. Danuser, and R. Oldenbourg (2000) *Biophys. J.* **79**:191-201. <sup>2</sup>C.M. Waterman-Storer, et al. (1998). *Current Biol.* **8**:1227-1230.

### DNA-CARRYING POLYMERS AND POLYMERIC NANOPARTICLES M.Maeda<sup>1, 2</sup>

<sup>1</sup> Department of Applied Chemistry, Kyushu University, Fukuoka 812-8581, Japan <sup>2</sup> Bioengineering Laboratory, The Physical and Chemical Research (RIKEN), Wako 351-0198, Japan

**INTRODUCTION:** Gene diagnosis shows tremendous promise for medical, pharmaceutical, forensic, and other applications. Recognition of DNA sequence and chain length is the basis of A number of methods for gene diagnosis. recognition of DNA sequence have been proposed DNA hybridisation, such on oligonucleotide micro array (DNA chip). However, it is rather difficult to detect the single nucleotide polymorphisms (SNPs) by those methods, because there is only a small difference between their melting temperatures (Tm). In other words, it is difficult to find appropriate discrimination conditions.

In this paper, I will discuss about DNA which conjugate can recognize oligodeoxynucleotide (ODN) fragments with one base specificity. The conjugate is used in its aqueous solution or transparent dispersion. Such a system is very much different from conventional solid materials on which biological components including enzymes, antibodies, and receptors are immobilized. In addition to soluble bioconjugates, dispersed colloidal nanoparticles are promising for biological and medical diagnosis.

We have synthesized ODN-poly(N-isopropylacrylamide) (polyNIPAAm) conjugate, and found that it formed colloidal nanoparticle by heating over the phase transition temperature of polyNIPAAm. Moreover, the nanoparticles aggregated in the presence of the complementary DNA, while dispersed in the presence of the noncomplementary DNA.

**METHODS:** The ODN  $(dT_{12})$  modified with amino group at 5' ends (amino-dT<sub>12</sub>) was reacted with N-menthacryloyloxysuccinimide (39 mmol) to give vinyl-dT<sub>12</sub>, which was then copolymerised with NIPAAm with the aid of redox initiator system from ammonium persulfate and N,N,N',N'tetramethylethylenediamine. The resulting mixture was purified with dialysis and gel filtration to yield the ODN-polyNIPAAm conjugate. The molecular weight (Mw) of the conjugate was determined by static light scattering The solution of ODN-polyNIPAAm conjugate was incubated at 40°C for 30 min to form a stable nanoparticle. As target DNAs, we used a complementary ODN (dA<sub>12</sub>), a point-mutant ODN ((dA<sub>6</sub>)dT(dA<sub>5</sub>)) and four kinds of different length ODN  $(dA_{16}, dA_{18})$  and  $dA_{24}$ . assembling behaviour of the nanoparticles after adding the target DNA was monitored by UV spectrometer.

RESULTS AND DISCUSSION: The apparent behaviour of phase transition of ODN-polyNIPAAm conjugate was different from that of polyNIPAAm, which has lower critical solution temperature (LCST) at around 32°C to change its conformation between coil and globule. Figure 1 shows that the transmittance of the polyNIPAAm solution decreased rapidly above LCST. This is due to the change of polyNIPAAm from hydrophilic coil to hydrophobic globule. On the other hand, the transmittance of the DNA conjugate solution scarcely decrease even above

40°C. This is probably due to the formation of nanoparticles, which disperse in an aqueous In fact, the averaged radius of the nanoparticles was estimated to be 25 nm at 40°C by dynamic light scattering measurement using cumulants method. Mw of nanoparticle was determined to be 8.6×10<sup>6</sup> by SLS. In average, one particle is calculated to consist of ca.30 conjugate molecules. In contrast, an obvious decrease of transmittance was observed at 38 °C for the conjugate solution containing the complementary ODN (dA<sub>12</sub>) due to the aggregation of the However, no decrease was nanoparticles. observed in the case of a point-mutated ODN  $((dA_6)dT(dA_5))$ , the result being just similar to the solution containing the DNA conjugate only. The single nucleotide change of the target ODN (dA to dT) can be detected clearly by using the DNAlinked nanoparticles.

The rate of aggregation of the ODNpolyNIPAAm after adding the equimolar complementary ODN (dA<sub>12</sub>) was examined (Fig. A rapid decrease of transmittance was observed in the conjugate solution containing the complementary ODN (dA<sub>12</sub>) at 40 °C. nanoparticles aggregated within 5 min, showing usefulness for a rapid gene diagnosis. On the other hand, no decrease was observed at 60 °C; the nanoparticles kept dispersed. Since the melting temperature (Tm) of the duplex between native ODN  $(dT_{12})$  and ODN  $(dA_{12})$  was 51 °C as determined by UV measurement under the identical conditions, the duplex should almost dissociated at 60°C. These results indicate that the nanoparticles aggregate in response to the DNA hybridisation. When the same experiment was conducted at 30 °C, the transmittance did not change, indicating that aggregation takes place only when the nanoparticles are present.

Figure 3 shows the response of the  $dA_{18}$ nanoparticles to  $dA_{16}$ Surprisingly, the nanoparticles did not aggregate with the addition of these ODNs, which are longer than  $dA_{12}$  but still complementary to  $dT_{12}$  on the This strongly suggests that the nanoparticles. aggregation was not brought about by crosslinking mechanism between (dAn) oligomers (n>12) and (dT<sub>12</sub>)-linked nanoparticles. In other words, it is suggested that the DNA chain length of target DNA can be detected clearly by using the DNAlinked nanoparticles.

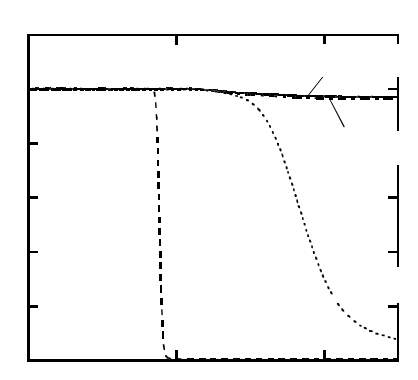


Fig. 1 Temperature-dependence of the transmittance at 500 nm of the polyNIPAAm or conjugate solution (0.05wt%) with or without target DNA ( $dA_{12}$  or ( $dA_6$ ) $dT(dA_5$ )) equimolar to that on the nanoparticle.

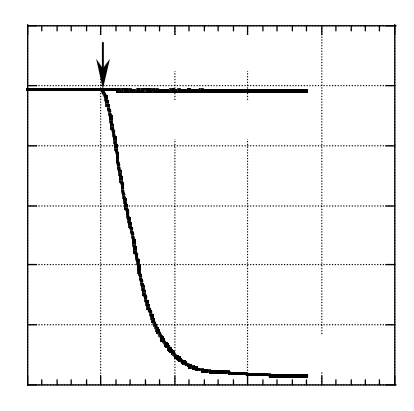


Fig. 2 Time course of the transmittance at 500 nm of the conjugate solution (0.05 wt%) after the addition of target ODN ( $dA_{12}$ ) (14.0  $\mu$ M) at 30°C, 40°C or 60°C.

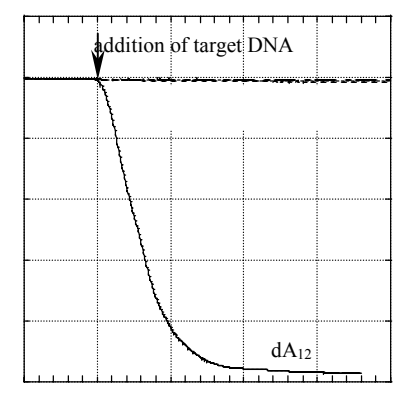


Fig. 3 Time course of the transmittance at 500 nm of the conjugate solution (0.05 wt%) after the addition of target ODN ( $dA_{12}$ ,  $dA_{16}$ ,  $dA_{18}$  and  $dA_{24}$ ) (14.0  $\mu$ M) at 40°C.

**REFERENCES:** T. Mori, D. Umeno, M. Maeda (2001) *Biotech. Bioeng.*, **72**: 261-268.

# PHOTOLUMINESCENCE OF NANO-STRUCTURED PARTICLES: SYNTHESIS AND PROPERTIES

### H.Weller

Institut für Physikalische Chemie der Universität Hamburg Bundesstr. 45, D-20146 Hamburg

INTRODUCTION: The wet-chemical of semiconductor preparation nanoparticles enables an easy access to quantized matter in gram scale. Synthetic routes have been developed for high quality samples of a wide variety of semiconductors (as well as metals and ceramics) with narrow size distributions and high crystallinity. Due to the quantum size effect, the colour of the particles and their fluorescence can be shifted through the entire visible and near infrared spectral region by varying the size of the particles. The line-width of the luminescence is much narrower than that of organic fluorescence dyes making them interesting candidates for multiplex labelling of biological material.

Since comparable numbers of molecules are located at the surface of nanoparticles and in their crystalline core the electronic structure and, thus, the luminescence properties of the particles is also strongly determined by surface chemistry. State-of-the-art synthesis allows, however, an almost perfect electronic termination of the surface leading to fluorescence quantum efficiencies of up to  $\sim$ 70 % at room temperature and a photo-stability which exceeds that of the best organic fluorescence dyes by orders of magnitudes.

Another advantage of the large surface fraction is the possibility to covalently link the particles via bi-functional ligand molecules to proteins and other biomolecules.

The talk will give an overview of the synthesis and properties of today-available luminescent nanoparticles.

# PRECLINICAL AND CLINICAL EXPERIENCES WITH MAGNETIC DRUG TARGETING – DIAGNOSIS AND THERAPY – POSSIBILITIES AND LIMITATIONS

U.O.Häfeli

The Cleveland Clinic Foundation, 9500 Euclid Ave T28, Cleveland, OH 44195, U.S.A.

INTRODUCTION: A major challenge in cancer therapy is the delivery of antineoplastic agents to remote, difficult to reach anatomic sites. Specific targeting enhances the delivery efficiency and at the same time reduces the toxicity. In magnetic targeting, a drug or therapeutic radioisotope is bound to a magnetic compound, injected into a patient's blood and then stopped with a powerful magnetic field in the target area. It is thus possible to replace high concentrations of freely circulating drug with much lower drug concentrations (Fig. 1). This decreases side effects and whole body toxicity substantially, and at the same time increases localized drug levels several fold [1-3].

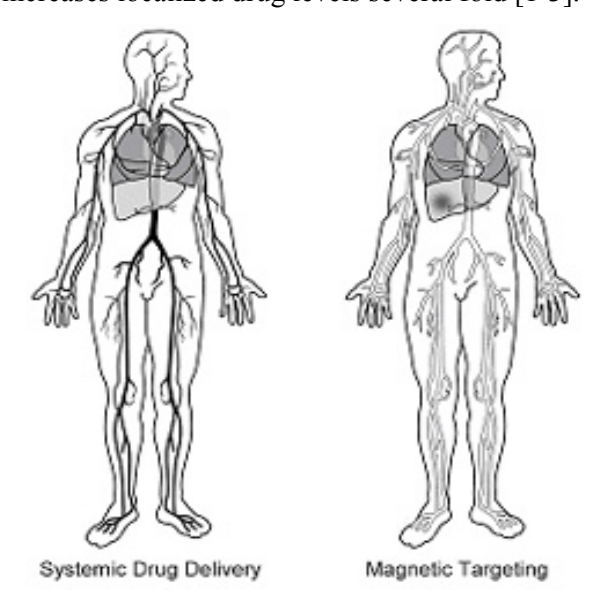


Fig. 1. Concept of magnetic drug targeting.

**METHODS:** Preclinical targeting tests and experimental treatment trials have been performed in cell culture, in mice growing EL-4 lymphomas and in rats with 9L-glioblastomas. Biodistribution and toxicity evaluations were performed in a swine model. A clinical trial is ongoing with doxorubicin loaded magnetic microspheres for the treatment of unresectable liver tumours.

**RESULTS:** Our animal studies confirmed that magnetic microspheres can be magnetically concentrated in different areas of the liver. Fig. 2A shows that the liver is homogeneously filled with magnetic microspheres sized 1-5  $\mu$ m with no magnet present. Positioning a permanent rare earth magnet above the liver during and for 15 minutes

after injection leads to accumulation of more than 90% of the microspheres in the target area (Fig. 2B). Double injections, for example for the treatment of two distinct metastases, are also possible, as shown in Fig. 2C.

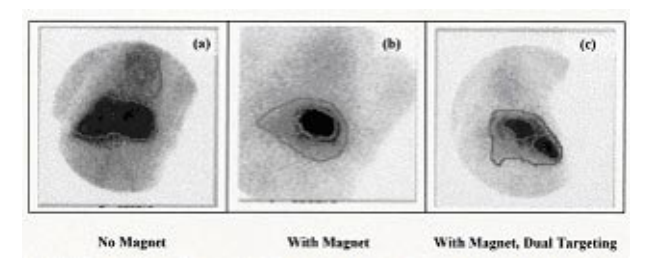


Fig. 2: Targeting of radio-labelled magnetic microspheres to specific liver sections.

DISCUSSION & CONCLUSIONS: Our experiments confirmed the promises of magnetic targeting such as low toxicity, few side effects and high target organ uptake. The microspheres seemed to stay in the target area even after removing the magnetic field. Histological studies showed that the magnetic carriers extravasate. They are "pulled" through the capillary walls of the target organ and remain in the target tissue for long times. This effect can be exploited by making magnetic microspheres, which slowly release a (chemotherapeutic) drug, or encapsulate a therapeutic radioisotope for local tumor therapy.

Areas of further research are magnetic microsphere synthesis (more responsive, homogeneous size, biocompatibility, target cell affinity), magnet optimisation (shape and strength) for more precise targeting control, imaging method development during magnetic targeting, and extension of magnetic targeting to other organs than the liver.

**REFERENCES:** <sup>1</sup>K. J. Widder, A. E. Senyei, and D. F. Ranney (1979) Adv. Pharmacol. Chemother. **16**:213-271. <sup>2</sup>P.K. Gupta, C. T. Hung (1989) Life Sciences **44**:175-186. <sup>3</sup>U. Häfeli, W. Schütt, J. Teller, M. Zborowski (1997) *Scientific and clinical applications of magnetic carriers*, Plenum.

**ACKNOWLEDGEMENTS:** We are grateful to FeRx Inc., San Diego, CA and the NIH (SBIR grant #1R43 CA88597-01).

# SUPERPARAMAGNETIC NANO-PARTICLE PREPARATION FOR MEDICAL APPLICATION

H.Hofmann, A.Petri, M.Chastellain, M.Hofmann

Swiss Federal Institute of Technology Lausanne, <u>Laboratory for Powder Technology (LTP)</u>, Lausanne, Switzerland

INTRODUCTION: Today nanotechnology has developed to a stage, which makes it possible to produce, characterize and specially tailor the functional properties of nanoparticles for clinical applications and diagnostics. Such an approach would considerably improve the efficiency of drug delivery to the specific area of need in a human body, and most importantly minimize the negative side and after effects of dosage, localization and focus medical treatment. The use of magnetic nanoparticles can contribute to a precise delivery of drugs to the exact area (e.g. of inflammation, cancer etc.) by application of external magnetic fields.

On the other hand separations with magnetic polymer particles of nano- size are becoming increasingly important in all fields of science as well as in engineering and environmental technologies. The simple and fast separation method is mostly predetermined for automated separation processes (e.g. DNA separation, cell separation etc.) which can facilitate many operations. Highly functional magnetic particles are required for this technology to allow an application in as many fields

Therefore new more effective techniques to generate these nanosized magnetic particles are requested, which should be non-toxic and These biocompatible. particles with consequent large active surface will be prepared in a specially designed segmented flow tubular reactor (SFTR) developed at LTP. Advanced techniques will applied to tailor the particles to have higher magnetic saturation, a semi-spherical needle-like morphology, and to superparamagnetic. The overall objectives of the research at LTP is to produce these nanoparticles (mostly g-Fe2O3 or g-Fe3O4 single domains of about 5-10 nm in diameter) as free particles or attached on a surface for targeted applications, e.g. cell engineering, cell biology and tissue repair. Among the special fields of applications are:

- 1. Free particles for potential clinical application like Drug delivery
- 2. Free particles for diagnostics
- Quantitative histological imaging

- Cell separation
- DNA sequencing
- Blood purification
- 3. As a tool for cell-biology research
- 4. To separate and purify cell populations

In all cases only superparamagnetic particles are of interest because they do not retain any magnetism after removing the magnetic field. The effectiveness of the particles depends upon

- high magnetic susceptibility for an effective magnetic enrichment
- size of particles, which should be monosized in the range of 9 15 nm to be superparamagnetic
- prevention of agglomeration of particles
- long range stability, i.e. high circulation time in the blood, if used in-vivo
- low sedimentation
- the polymer shell and the biological functionalization of this

The application of the particles in-vivo or ex-vivo needs special surface modification of magnetic particles, which has to be not only non-toxic and biocompatible but also stable reticuloendothelial system (RES). As phagocytosis depends strongly on the surface charge (hydrophobic/hydrophilic) surface the modification is an important factor in the processing of magnetic nanoparticles, otherwise they undergo phagocytosis by the Kupffer cells. Another approach is to develop magnetic nanoparticles with different surface charges and zeta potentials at their surfaces, but only limited results exist regarding the combination of the demand of very small particles for a long circulation time in the blood and high magnetic susceptibility.

Until now, especially in cell separation the potential of the magnetic separation technology remains limited due to the low binding capacity and insufficient surface area of the available materials. Together with appropriate functionality, enabling attachment of biological ligands

numerous new applications and emerging new technologies in biotechnology and medicine would be envisioned (e.g. purification of recombinant proteins in preparative quantities, which is not technological feasible at present)

Although well-dispersed magnetic nanoparticles can be obtained by ball-milling,[7,8] a serious limitation on this techniques, beside the high-energy requirements, is the unavoidable contamination of the product, which necessitates the development of more economical and reliable technology to fabricate magnetic particles by well controlled chemical methods.

Iron oxide (Fe3O4), the dominant magnetic material for the foreseen application, can be synthesized through the co-precipitation of Fe(II) and Fe(III) aqueous salts solution by addition of a base. The control of size, shape, and composition of Fe3O4 or g-Fe2O3 nanoparticles depends on the type of salt (chlorides, nitrates, perchlorates, etc.), the Fe(II) and Fe(III) ratio, and the pH and ionic strength of the media. Organized assemblies or complex structures have been used as reactors to obtain ultrafine magnetic iron oxide particles. Stable aqueous magnetic suspensions can be fabricated using various saturated and unsaturated fatty acids as primary and secondary surfactants. In practice, however, little control can actually be exercised over the size and size distribution of the micro-structures, and moreover, only small quantities of iron oxide can be obtained owing to the constraints of low reagent concentrations necessitated by this synthetic procedure.

Aim of the Work: The aim of this work is to synthesize and characterise improved ferrofluids for cell separation and drug delivery. The sizecontrolled precipitation of iron oxide particles and the coating step are the two main parts of the project. The nanoparticles are synthesized by coprecipitation of iron-based salts in different media. The use of various compounds such as dextran, polyvinyl alcohol (PVA), sodiumdodecylsulphate (SDS) and silica allows to obtain stable colloids. The particles composition and morphology are characterized using TEM, XRD and FTIR. SQUID magnetometery is used to investigate the magnetic characteristics of the particles but this technique is discussed more in detail in the presentation D5.

**RESULTS:** TEM pictures show ellipsoidal particles. A first statistical analysis based on hundred particles per sample lead to an average size of less than 10nm with an ellipse aspect ratio of about 1.2. XRD patterns show a wide

amorphous background due to the presence of polymer, nevertheless typical peaks, which can be attributed to nanocrystalline magnetite (Fe3O4) or maghemite (g-Fe2O3) are also present. The size calculated from these data using the Scherrer formula confirms the TEM results. FTIR spectrometry led to the conclusion of a defect magnetite structure with a lattice parameter in between the one of bulk maghemite and magnetite.

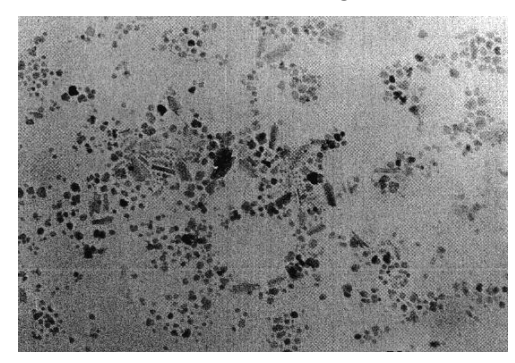


Fig. 1: Bright field TEM image of iron oxide particles stabilised with SDS. The sample consists of stable colloids at physiological pH, diluted and dried on a copper grid. The agglomerated structure is thought to be mainly due to the drying step

**ACKNOWLEDGEMENTS:** This project is supported by EU - under the project MAGNANOMED - Magnetic Nanoparticles for Medical and Biological Diagnostics and Devices.

# DISPOSABLE AFFINITY MICROCHIPS WITH ELECTROCHEMICAL AND NANOSPRAY DETECTION

Ph. Michel, C. Vollet, F. Reymond, J. Rossier

DiagnoSwiss SA, Rte de l'Ile au bois 2, c/o Cimo S.A., CH-1870 Monthey, Switzerland

**INTRODUCTION:** In modern (bio)chemical analysis, the need for contamination free platforms offers great commercial potential to plastic μ-systems. This is reinforced by simplified manufacturing procedures (compared to glass μ-chips) that enable mass production of low cost disposable devices. In addition to the variety of polymers that can be chosen to adsorb biological materials, polymer μ-chips are particularly well suited for high performance analysis and medical diagnosis, since they allow reduced analysis time, low reagent consumption, as well as parallelism and multi-analyte testing.

We present here Enzyme Linked Immunosorbent Assays (ELISA) with electrochemical detection in industrial  $\mu$ -chips manufactured by plasma etching of polyimide foils. This method is further used here to produce disposable nano-electrospray interfaces for applications in proteomics.

**FABRICATION:** Mass production of  $\mu$ -chips is performed by plasma etching, a method developed for printed circuit boards [1]. A polyimide foil coated with a copper mask is exposed at low temperature to a plasma of oxygen. The plastic is thus etched to produce (e.g. 40  $\mu$ m deep x 100  $\mu$ m wide)  $\mu$ -channels and/or openings, and the copper is then removed in such a manner that only contact pads remain at the bottom of the  $\mu$ -channels.

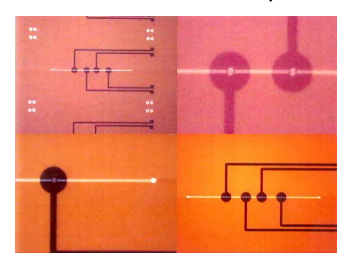


Figure 1: Top views of  $\mu$ -channels with integrated gold electrodes

Gold is then electroplated on these copper tracks, thereby leading to electrodes that are thus integrated during the fabrication process (see Fig. 1). The  $\mu$ -chips are finally sealed by lamination of a second polymer layer.

### **EXAMPLES OF APPLICATIONS: ELISA** with electrochemical detection

Micro-chips are well suited for the development of fast immunoassays. It is demonstrated here that very short incubation time (<5 min) can be used

due to the small diffusion distance between the bulk solution and the surface ( $<20~\mu m$ ) [2]. The use of electrochemical detection is advantageous because it is proportional to the concentration of redox molecules even in these small volumes (<60~nL) [3]. The performances of the chips are illustrated here by presenting a highly sensitive immunoassay for the measurement of alkaline phosphatase with a detection limit of 5 x  $10^{-21}~mol$ .

### Plastic $\mu$ -chips as disposable mass spectrometry (MS) interfaces for protein analyses

Plasma etching has also been used to fabricate hydrophilic  $\mu$ -channels with an open end surrounded by an hydrophobic surface in order to produce nano-electrospay tips. As presented in Fig. 2, the soft generation of the nano-spray of proteins is demonstrated here by the MS detection of myoglobine (applied voltage: 1.4 kV; spray solution: 4  $\mu$ M myoglobine in 50 % methanol, 49 % water, 1 % actetic acid). In this system, no additional flow is needed to generate the spray, the alignment to the MS entrance is simplified, low flow rate can be used and multiplexing is easy.

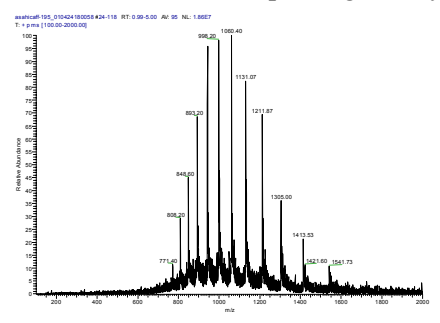


Fig. 2: Mass spectrum of a 4  $\mu$ M myoglobine sample sprayed with plasma etched micro-chips (acquisition time: 3 min; flow rate: 50nL/min)

**CONCLUSIONS:** Plasma etched  $\mu$ -chips are industrial platforms suitable for sensitive medical tests and high-throughput MS analysis. This robust method is also very attractive to produce lab-on-a-chip, affinity platforms and disposable biosensors.

**REFERENCES:** <sup>1</sup> see: www.dyconex.com. <sup>2</sup> Rossier et al (2000) *Langmuir* **16**: 8489. <sup>3</sup> Rossier et al (1999) *Anal. Chem.* **71**: 4294.

(Abstract also presented at the 3rd HPLPuS meeting in Amsterdam in October 2001)

# NEW INSTRUMENT BASED ON EVANESCENT WAVE FOR AFFINITY SENSING

<u>G. Voirin</u><sup>1</sup>, R.E. Kunz<sup>1</sup>, H. Chai-Gao<sup>1</sup>, K. Cottier<sup>1</sup>, F. Crevoisier<sup>1</sup>, E. Bernard<sup>1</sup>, R. Ischer<sup>1</sup>, M. Wiki<sup>2</sup>

<sup>1</sup>CSEM, Neuchatel, Switzerland. <sup>2</sup>Unaxis, Balzers, Liechtenstein

**INTRODUCTION:** A new instrument was developed for surface reaction monitoring. It is based on waveguide grating and wavelength modulation<sup>1</sup>. The wavelength at which the resonant coupling occurs depends on the waveguide grating characteristics. The changes in the resonance wavelength represent variations that occur in evanescent wave of the waveguide (refractive index, layer deposition, material phase change or swelling).

METHODS: The instrument breadboard is composed of a tuneable semiconductor laser, a waveguide grating chip with two waveguide grating pads per measurement channel, one pad with a 360 nm period grating and about 150 nm thick waveguide (incoupling) and one pad with same grating period but with a 300 nm thick waveguide (outcoupling), the waveguide layer is made of a Ta<sub>2</sub>O<sub>5</sub> on glass substrate (Schott AF45). The chip is mounted in a cell for pipetting liquid (a cell with two different chambers is also available). A fibre ribbon is used to collect the outcoupled light and to propagate it to the detectors. The electronic system controls the laser temperature. modulates the laser current (in order to modulate the laser wavelength), amplifies the detector signal. The PC makes data acquisition calculates the resonance position, and display it. The system was tested in three cases: refractive index change, recognition photo-bonded molecular using material and antibody, molecular recognition with physisorbed biotinilated neutravidin molecules.

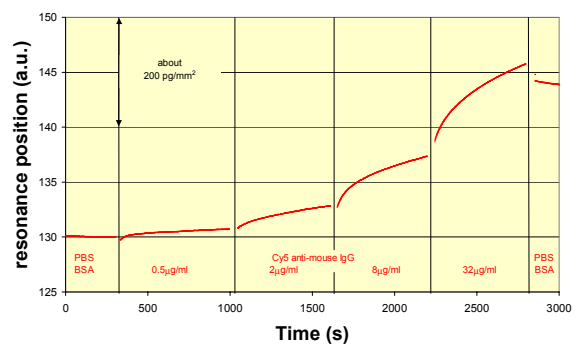


Fig. 1: Recognition of photo-bonded mouse IgG with an antimouse antibody.

**RESULTS:** Refractive index changes are made using mixtures of water and glycerol (0 to 2%). Solutions with different concentration of glycerol applied on the chip. Standard deviation on effective refractive index measurement as low as 3 10<sup>-8</sup> are obtained. For molecular recognition with antibody, mouse IgG was photo-bonded with OptoDex<sup>®</sup> on the waveguide surface and an antimouse antibody solution at different concentration were applied to see the immunoreaction (see Fig. 1).

The third experiment was made using the double chamber cell, in one chamber BSA was physisorbed and in the other neutravidin, then Biotin-5N-FITC at  $10 \mu g/ml$  was put in both chambers and the binding of biotin on neutravidin only is observed (Fig. 2).

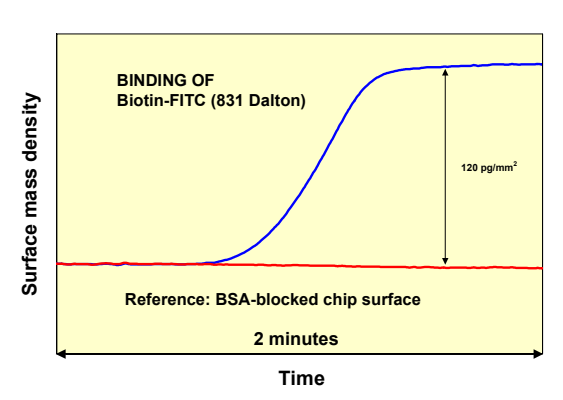


Fig. 2: Binding of biotin-FITC on physisorbed neutravidin

**DISCUSSION & CONCLUSIONS:** The measurements show that very high sensitivity (3 10<sup>-8</sup> refractive index variation) can be reached. This proves the potential of the new concept combining wavelength modulation and glass waveguide grating. The system is well adapted for the study of affinity binding of large (antibody) and small (less than 1000 Dalton) molecules.

**REFERENCES:** <sup>1</sup> M. Wiki and R.E. Kunz, "Wavelength-interrogated optical sensors for biochemical applications," Opt. Lett. Vol. 25/7, 463-465 (April 1, 2000)

**ACKNOWLEDGEMENTS:** Part of this work was funded by CTI (Commission for Technology and Innovation)

### PROTEIN AND CELL ADSORPTION KINETICS

C. Galli, M. Collaud Coen, U. Greber<sup>2</sup>, T. Greber<sup>3</sup>, L. Schlapbach

<u>Solid State Physics</u>, Université de Fribourg, Chemin du musée 3, CH-1700 Fribourg, Switzerland University of Zürich, Institute of Zoology<sup>2</sup>, Physics Institute<sup>3</sup>, Winterthurerstrasse 190, CH-8057 Zurich, CH

INTRODUCTION: The adsorption kinetic of proteins or cells and their viscoelastic properties during their interaction with a surface as function of different environments or different surface states are determinant for biocompatibility and biosensors applications. In this view we built a new Quartz Crystal Microbalance (QCM), which measures simultaneously the frequency shift and the Dissipation factor (D). We combine these measurements with different microscopy methods (optical, AFM), in order to better characterise the adsorbed material.

**METHODS:** We used 3 different proteins: the globular Protein A, that is well-known in immunology, and their antibodies, the rabbit immunoglobulin IgG. Secondly we chose a filamentous protein, the Fibronectin. We also adsorbed the A549 human lung carcinoma cells. The Quartz Crystal Microbalance (QCM) enables us to detect the deposition of some nanograms per cm<sup>2</sup> by measuring the resonant frequency of the crystal, which decreases linearly with increasing adsorbed mass ( $\Delta m \sim \Delta f$ ). The dissipation factor, which is the inverse of the Q factor, can be obtained by fitting the exponential decrease of the amplitude after the stopping of the crystal excitation. The quartz crystals have gold electrodes that we have also coated with Ti.

The QCM allows to follow the **RESULTS:** adsorbed mass as a function of time, as well as the energy dissipated in the system, which gives information about the adhesion, water content or thickness of the adsorbed film. Fig. 1 presents the frequency shift  $\Delta f$  vs. time and the dissipation factor D vs.  $\Delta f$  for different concentrations of Fibronectin on Ti. On the upper graph, it can be seen that the time to reach a saturation state is proportional to the protein concentration. Furthermore at least 2 different kinetics occur during the protein adsorption. concentrations, it is visible that a rapid adsorption occurs, followed by a slower process. This phenomenon is also observable in the D vs.  $\Delta f$ graph. The measurements can at least be fitted by 2 lines of different slopes, which means that the viscoelastic properties of the fibronectin film change during the adsorption process.

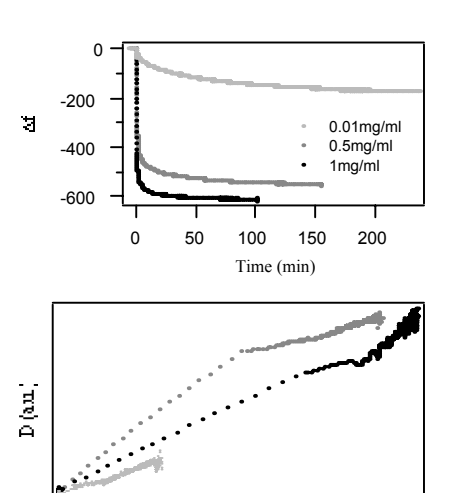


Fig. 1:Adsorption of Fibronectin on Ti at different concentrations.

2f (Hz)

-400

-600

-200

**DISCUSSION & CONCLUSIONS:** The QCM is a powerful technique which permits to follow in time the adsorbed mass and the viscoelastic changes of the adsorbed film, as well as to evaluate the arrangement, packing or crystallisation degree or to determine the cell growth in different environments.

In this example, 3 different adsorption processes take place. A tentative explanation is that at low concentration, the filaments adsorb slowly to the surface, forming a non-complete thin film. At the concentration of 0.5mg/ml, the firstly adsorbed filaments must have a high content of entrapped water because the energy dissipation is the highest, in contrast to the frequency shift. Afterwards the filaments are rearranged so that the film becomes more rigid. Finally at high concentration packed filaments adsorb on the surface to form a film containing less entrapped water. At the end, the dissipated energy increases, probably due to the increases of contact area of the upper adsorbed filaments with water.

**ACKNOWLEDGEMENTS:** We gratefully acknowledge the financial support provided by the Dr. H.C. Robert Mathys Foundation (RMS) and the Swiss National Foundation (Top Nano21).

# MICROPATTERNING OF LIPID BILAYERS AND ITS APPLICATION TO

THE BASIC STUDIES OF INTERFACIAL AGGREGATION PHENOMENA

K. Morigaki

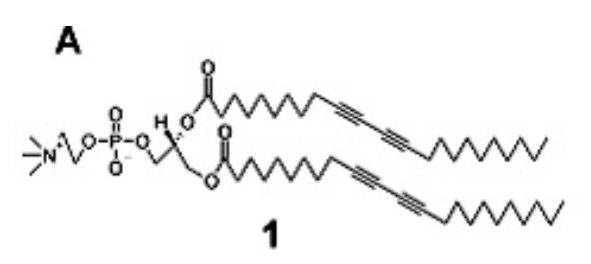
A. Offenhäusser

W. Knoll

and P. Walde

Max-Planck-Institut für Polymerforschung, Ackermannweg 10, 55128 Mainz, Germany <sup>2</sup>Institute of Polymers, ETH-Zentrum, Zürich, Switzerland

Solid-supported lipid bilayers have been studied as a simple model of the biological membrane (1). The supported planar bilayer membranes are fluid and can also incorporate membrane proteins, providing possibilities to prepare biosensors based on electrical and optical detection. Patterning of lipid bilayers on the solid surface has attracted considerable interest in recent years (2). It should enable spatially controlled integration of biological components into the artificial membrane system. In this contribution we present a novel approach for creating patterned lipid bilayers on solid supports. The patterning makes use of lithographic polymerisation of a diacetylene-based phosphatidylcholine (1) that polymerises with its neighboring lipids photochemically (Fig. 1).



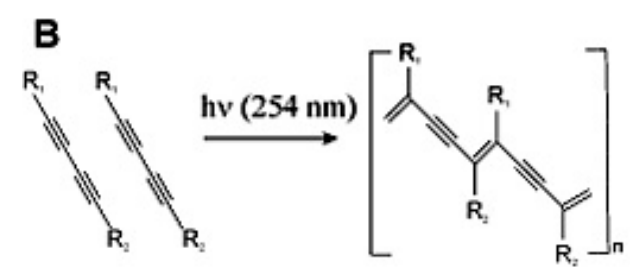
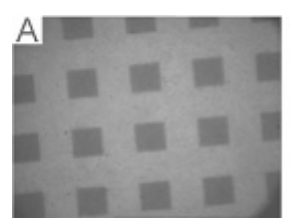


Fig. 1 The chemical structure of the diacetylene phospholipid 1 and its polymerisation scheme.

The formation of a highly conjugated polymer backbone induces strong absorption fluorescence in UV/ VIS range and we observe the polymerised bilayers fluorescence by the microscope (Fig. 2). Two-dimensional (2D) polymeric network makes the irradiated bilayer insoluble in organic solvents. By removing the monomeric lipids with an organic solvent, one can create a 2D master structure for the incorporation of biologically relevant lipid bilayer membranes. We have fused small unilamellar vesicles of egg yolk phosphatidylcholine doped with 1 % of the

fluorescent lipid, N-(7-nitrobenz-2-oxa-1,3-diazol-4-yl)-1,2-dihexadecanoyl-sn-glycero-3-phoshoethanolamine (NBD-PE). The newly incorporated bilayers retain their fluidity, whereas the polymerised lipid bilayer functions as an effective barrier for the lateral diffusion of lipids (3).



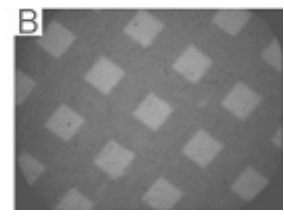


Fig. 2 Fluorescence micrograph of polymerised bilayers. (A) Polymerised bilayer domains are brightly fluorescent because of the conjugated backbone. The dark squares are monomeric bilayers. (B) After removal of the monomeric bilayers, new lipid bilayers were incorporated into the corrals. The corrals are more brightly fluorescent due to the fluorescence marker (NBD-PE).

The micropatterned lipid bilayer membranes should provide new avenues to create complex and mechanically robust biomimetic interfaces. Furthermore, polymerised bilayers could be potentially useful for the basic studies of interfacial amphiphile aggregation phenomena by confining the materials within a defined area. We are currently investigating aggregation behaviours of lipids and surfactants on micropatterned and non-patterned surfaces.

### **References:**

- 1. E. Sackmann (1996) Science (Washington) 271:
- 2. J. T. Groves, N. Ulman, S. G. Boxer (1997) Science (Washington) 275: 651-653.
- 3. K. Morigaki, T. Baumgart, A. Offenhäusser, W. Knoll (2001) Angew. Chem. Int. Ed. Eng. 40: 172-174.

### SURFACE DOCKING SITES FOR MACROMOLECULES: INTERFACE ARCHITECTURE BASED ON PLL-G-PEG/PEGBIOTIN-(STREPT)AVIDIN

N. P. Huang, J. Vörös, S. M. De Paul, I. Reviakine, M. Textor, N. D. Spencer

Laboratory for Surface Science and Technology, Department of Materials,

Swiss Federal Institute of Technology, ETH-Zürich, CH-8092 Zürich, Switzerland

INTRODUCTION: Surface docking sites (nanoscale islands) are desirable for the specific adhesion of macromolecules, such as proteins and oligonucleotides, onto surfaces. Ideally, the surrounding areas of such docking sites should be non-adhesive so that the adsorbed macromolecules are prevented from denaturing after adsorption. We have mixed poly(L-lysine)-g-poly(ethylene glycol) (PLL-g-PEG) and a variant of PLL-g-PEG in which some of the PEG chains are biotinylated (PLL-g-PEG/PEGbiotin) to form a novel polymeric interface, in order to tailor chip surfaces in terms of non-specific and specific analytesurface interactions. We expect that such a platform could serve as a powerful tool for the investigation of molecular recognition effects.

**METHODS:** PLL-*g*-PEG derivatives were synthesized from poly(L-lysine) hydrobromide (mol wt  $\sim$ 20 kDa), N-hydroxysuccinimidyl ester of methoxy-poly(ethylene glycol) propionic acid (mol wt  $\sim$ 2 kDa) and α-biotin- $\omega$ -N-hydroxysuccinimidyl ester of poly(ethylene glycol)-carbonate (mol wt  $\sim$ 3.4 kDa) [1].

**Optical** Waveguide Lightmode Spectroscopy (OWLS) technique [2] was used for the in situ monitoring of macromolecule interface adsorption. including polymeric formation based on mixtures of PLL-g-PEG and PLL-g-PEG/PEGbiotin in various ratios and sequential immobilization of streptavidin and biotinylated goat-anti-rabbit immunoglobulin (\alpha RIgG-biotin) to sense the target molecule, rabbit immunoglobulin (RIgG). The OWLS technique is highly sensitive (i.e. ~1ng/cm<sup>2</sup>) to adsorption up to a distance of 200 nm above the surface of the waveguide.

The distribution of surface docking sites was investigated by forming mixed polymeric layers, adding streptavidin and finally using biotinylated liposomes (as markers) for Atomic Force Microscopy measurements.

**RESULTS:** By means of optical waveguide lightmode spectroscopy (OWLS), streptavidin is shown to bind specifically to the biotinfunctionalised PEG, while the resistance of the remaining PEG chains to protein adsorption yields a high specific-binding-to-non-specific-binding ratio, especially when using a buffer with

physiological ionic strength. Subsequent binding of biotinylated goat-anti-rabbit immunoglobulin (\alpha RIgG-biotin) to streptavidin as a capture molecule allows the system to be used as an immunoassay for the target molecule, rabbit immunoglobulin (RIgG). Changing the ratios of PLL-g-PEG and PLL-g-PEG/PEGbiotin in the mixture changes the distribution of docking (biotin) sites on the interface and, thus, allows optimisation of the sensing response (see Fig.1). AFM images of the distribution of docking sites streptavidin and reflected by biotinylated liposomes also show a reasonable correlation among streptavidin, biotinylated liposomes and the surface biotin concentration.

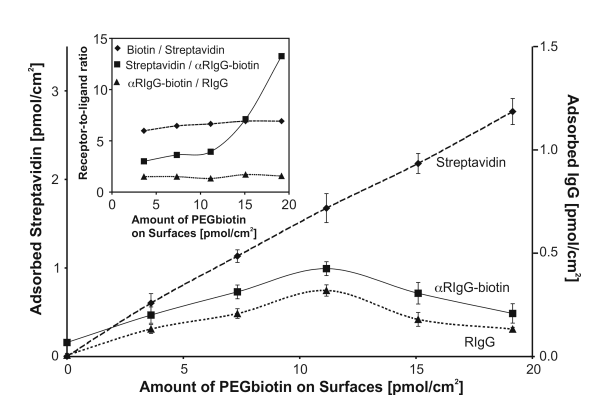


Fig.1 Results from OWLS measurements on the sequential adsorption of streptavidin,  $\alpha$ RIgG-biotin and RIgG on mixed polymeric interfaces. The surface concentration of adsorbed streptavidin is plotted on the left axis, whereas the concentration of adsorbed IgG is indicated on the right. The inset shows the receptor-to-ligand ratio for each step of the bioaffinity assay.

polymeric interfaces tailored by PLL-g-PEG and PLL-g-PEG/PEGbiotin are shown to be highly resistant to nonspecific adsorption from serum while still allowing for the specific surface binding of the linkage protein, streptavidin. The amount of immobilized streptavidin is shown to be closely related to the surface biotin concentration. The subsequent adsorption behaviour of αRIgG-biotin and RIgG, however, depends in a more complex

manner on each individual surface modification step and orientational and steric repulsion effects within the adlayers. The optimum interface can be found as a promising platform for bioaffinity sensing of proteins.

**REFERENCES:** <sup>1</sup> N.P. Huang, R. Michel, J. Vörös, M. Textor, R. Hofer, A. Rossi, D.L. Elbert, J.A. Hubbell, N.D. Spencer (2001) Langmuir 17:489-498.

<sup>2</sup> J. Vörös, J.J. Ramsden, G. Csucs, I. Szendrö, M. Textor, N.D. Spencer (2000) J. Molecular and Cellular Biology, submitted.

ACKNOWLEDGEMENTS: Financial contributions from the Swiss National Science Foundation (SNF, National Research Program NFP 47 "Supramolecular Functional Materials") and from the Swiss Federal Commission for Technology and Innovation (CTI, project no. 4620.1 MTS) are gratefully acknowledged.

### NEUROCHIPS FUNCTIONALIZED WITH ADHESION PROTEINS

H. Sorribas<sup>1</sup>, C. Padeste<sup>1</sup>, P. Sonderegger<sup>2</sup>, C. Stricker<sup>3</sup> <u>L.Tiefenauer</u><sup>1</sup>

<sup>1</sup> <u>Paul Scherrer Institut</u>, Villigen, Switzerland

<sup>2</sup> Institute of Biochemistry University of Zürich, Switzerland

<sup>3</sup> Institute for Neuroinformatics, Univ.& ETH Zürich, Switzerland

**INTRODUCTION:** Various types of microelectrode arrays (MEA) have been produced using photolithographic techniques. Such MEAs are used for stimulating and recording neural activity in slices of nerve tissues or of dissociated cultured neurons. In order to guide neurites of neurons to gold electrodes and also to achieve a close cell-electrode contact, we have generated patterns of novel neural adhesion proteins.

**METHODS:** Recombinant proteins from the two membrane proteins axonin-1 and NgCAM have been produced using protein engineering methods. These recombinant proteins have a C-terminal Cys, which allows the direct coupling to gold surfaces; alternatively a covalent immobilization on glass or oxides can be achieved using a silane and a heterobifunctional crosslinker. The cell-surface distance was determined using the fluorescence interference method [1]. Furthermore, photolithographic methods were applied to generate patterns of functional proteins [2]. The quality of these biopatterns was assessed by immunofluorescence microscopy of adhered neurons. Microelectrode arrays have been fabricated according to [3] and biofunctionalized with RGDC. These chips have been tested in first electrophysiological experiments.

**RESULTS:** On glass a line pattern of covalently immobilized axonin-1 was generated. Dissociated neurons spontaneously adhere to these lines (*Fig. 1*). The resulting network is not yet perfectly aligned and cell adhesion to the background may additionally be suppressed.

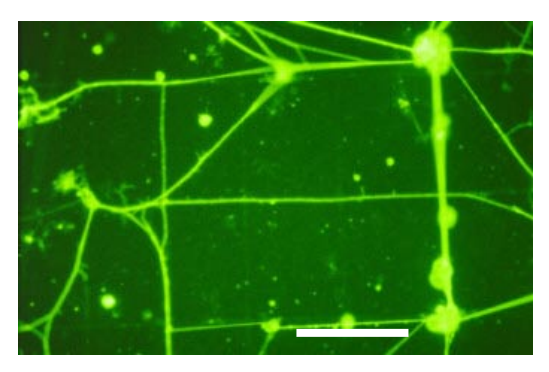


Fig.1: Primary neurons cultured on patterned Cys-axonin patterns (5 μm line width, immunostained with TRITC anti-axonin-1, scale bar 100 μm).

In *Table 1* mean lengths of outgrowing neurites and mean distances of the neuron cell membrane to the surface for different modifications are summarized. It is evident that the adhesion proteins axonin-1 and NgCAM promote neurite outgrowth and that the cell membrane is in a minimum distance to the material surface with these proteins. In addition it was found that on NgCAM and laminin 80% to 90% of all cells have outgrowths whereas only 20 % of the neurons form neurites on aminosilane (APTES). This result confirms the assumption that the adhesion protein strongly influences the biological reaction of cultured cells. Thus, depending on the intended application another adhesion molecule can be selected.

Table 1. Neuron cultured on various substrates

| Substrate  | Mean neurite | Cell-surface  |
|------------|--------------|---------------|
|            | length [µm]  | distance [nm] |
| Cys-axonin | 80±30        | 37±10         |
| Cys-NgCAM  | 231±86       | 47±8          |
| APTES      | 40±10        | 39±3          |
| RGDC       | 124±60       | 39 ±4         |
| laminin    | n.d.         | 91±4          |

Finally, the neurochips were tested in an electrophysiological experiment.



Fig.2: Differential interference contrast micrograph of a dissociated DRG culture (4d) with a gold electrode (black rectangular structure) for stimulation and impaled patch pipette for recording (scale bar 10 µm).

A microelectrode close to a neuron cell (Fig.2, white arrow) has been addressed and a current of

 $150~\mu A$  has been applied for  $100~\mu s$ . This stimulation induced the expected action potential of about 90~mV (see Fig. 3) as measured with a patch clamp electrode. This preliminary result confirms that our microelectrodes are useful for electrophysiological experiments.

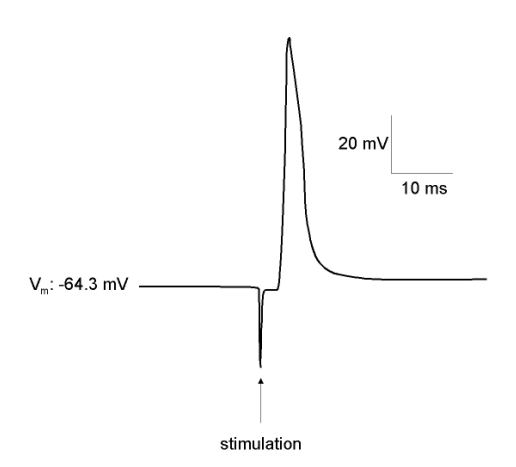


Fig.3: Action potential recorded intracellularly after extracellular stimulation.

**DISCUSSION & CONCLUSIONS:** The results demonstrate the potential of specific adhesion proteins immobilized in patterns on neurochips. Lines of adhesion molecules induce the adherence of cells to predefined areas and guide their outgrowths. Furthermore, some adhesion proteins can also provoke specific biological reactions. For instance, the induction of synapses at predefined location, preferentially on electrodes, is most interesting.

The techniques developed for neurochip production have also a potential for many other applications. Especially, micropatterns of functional proteins of interest can be generated and the functionality can spatially be controlled with a resolution of 1  $\mu$ m. The described photolithographic method allows us also to produce many chips on one wafer and is thus suitable for a mass production. Functional micropatterns may be required for multiplex sensing. The mentioned method can also be adapted to produce pixel gradients out of two different molecules. Such biosurfaces may be very interesting in order to investigate and control the migration of cells.

**REFERENCES:** <sup>1</sup>H. Sorribas, D. Braun, L. Leder, P. Sonderegger & L. Tiefenauer (2001) Adhesion proteins for a tight neuron-electrode contact *J. Neuroscience Methods* 104:133-141. <sup>2</sup> H. Sorribas, C. Padeste & L. Tiefenauer (2001) Photolithographic generation of protein micropatterns, *submitted for publication to Biomaterials.* <sup>3</sup>H. Sor-

ribas, L. Leder, D. Fitzli, C. Padeste, T. Mezzacasa, P. Sonderegger & L. Tiefenauer (1999) Neurite outgrowth on microstructured surfaces functionalized by a neural adhesion protein *J. Mater. Sci. Mater. Med.* 10:787-791.

**ACKNOWLEDGEMENTS:** This work was supported by the SNF SPP Biotechnology, Module Neuroinformatics. We thank L. Leder for the preparation of the adhesion proteins axonin-1 and NgCAM.

### FUNCTIONAL BIOASSAY ON G PROTEIN-COUPLED RECEPTORS USING TOTAL INTERNAL REFLECTION FLUORESCENCE

K. L. Martinez, E. L. Schmid, R. Hovius, H. Vogel

Laboratory for Chemical Physics and Polymer membranes, Dept. of Chemistry, EPFL, Switzerland

INTRODUCTION: The ability of organisms, or individual cells to sense and react to different external signals (light, hormones, odorants, taste) is crucial for their survival. External signals interact with cell surface receptors which transduce the signals across the membrane and activate a variety of intracellular processes leading to the cellular response. G protein-coupled receptors (GPCRs) constitute a major class of membrane receptors<sup>1</sup>. They transmit extracellular stimuli by activating intracellular heterotrimeric GTP-binding proteins, called G proteins. In their resting state, G proteins bind to guanosin diphosphate (GDP). The exchange of GDP by GTP is promoted by the formation of a trimeric ligand-receptor-G protein complex, which is induced by ligand binding to the receptor. Binding to G protein in turn triggers dissociation of the G protein heterotrimer into its functional units: the GTP-complexed alpha and the betagamma subunit. The intracellular concentration of small signalling molecules (cAMP, cGMP, diacylglycerol, inositoltrisphosphate, Ca2+, K+) is then modulated by the conteration of both parts with the respective enzymes or ion channels. The GPCRs are therefore the target in the human body for the majority of clinical used drugs.

Today, functional investigations of GPCRs are mostly based on detection of indirect events occurring upon activation of the receptors. There is a high demand for both fundamental research and for different screening purposes in the pharmaceutical research and industry to detect the ligand binding events and the subsequent molecular interactions on the target membrane directly. Since optical evanescent wave techniques offer on-line detection of molecular interactions without additional separation steps, they are of great interest in this context. Here we propose to develop a generally applicable procedure for assessing G protein activation by its receptor using Total Internal Reflection Fluorescence (TIRF) spectroscopy<sup>2-3</sup>.

**RESULTS:** We choose the neurokinin (tachykinin)-1 receptor (NK1R) as a model of a GPCR. It is activated by the natural tachykinin peptide Substance P. The immobilization of this

member of the superfamily was performed using the high specificity of biotin-streptavidin interaction. The quartz surface was first covered with biotynilated BSA and then with streptavidin. Native membrane fragments containing mutant NK1R protein, genetically modified with a biotin tag<sup>4</sup> were finally added to the surface. The immobilization of these fragments on several surfaces was shown to be reproducible.

The binding of a fluorescent agonist (substance P labelled with fluorescein) to the NK1R at different ligand concentrations was followed. The specificity of the binding was controlled using a competitive antagonist non fluorescent. It allowed the establishment of the binding curve of the fluorescent agonist, which is in good agreement with the pharmacological features of the receptor in its native environment and in solution, suggesting that the immobilization of the protein doesn't affect its binding features.

It was thus possible to perform a pharmacological study on few amounts of protein, coming from crude cellular extracts, without further purification.

#### **REFERENCES:**

- 1- Gudermann T., Kalkbrenner F., and Schultz G. 1996. Annu. Rev. Pharmacol. Toxicol. 36:429-59.
- 2- Thompson N.L., Pearce K.H., and Hsieh H.V. 1993. Eur. Biophys. J. 22:367-78.
- 3- Schmid E.L., Keller T.A., Dienes Z., and Vogel H. 1997. Anal. Chem. 69:1979-85.
- 4- Lundstrom K., Vargas A., and Allet B. 1995. Biochem. Biophys. Res. Commun. 208:260

## MECHANICAL PROPERTIES OF INDIVIDUAL MICROTUBULES MEASURED USING AFM

A. Kis<sup>1\*</sup>, S. Kasas<sup>2</sup>, A. Kulik<sup>1</sup>, L. Forró<sup>1</sup>

<sup>1</sup> Swiss Federal Institute of Technology, <u>EPF-Lausanne</u>, Switzerland <sup>2</sup> Institut de Biologie Cellulaire et de Morphologie, University of Lausanne, Switzerland

**INTRODUCTION:** Microtubules (MT) are self-assembling cylindrical protein structures that are present in almost all living cells as part of the cytoskeleton. Building a network across the cytoplasm, they perform various vital functions like providing mechanical support for the cell thus determining its shape; acting as a transport network; pulling apart chromosomes during cell division; involvement in movement of cells e.g. sperms etc. – they are essential for life.

Changes in the structure of microtubules under the influence of various diseased states and chemical agents could be probed by measuring their mechanical properties. Despite the inarguable importance of the knowledge of MTs stiffness and a significant number of performed experiments, there doesn't seem to be a consensus on the actual numerical values – values reported in the literature range between 1 MPa [1] and 1 GPa [2].

**METHODS:** using AFM, a method has been developed for elastically deforming microtubules (Figure 1). It consists of depositing microtubules on a porous surface and elastically deforming it with an AFM tip. Various procedures for fixing microtubules on substrates have been investigated and measurements in different conditions have been performed.

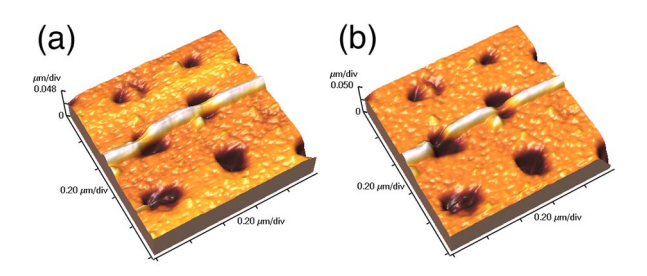


Fig. 1: Pseudo-3D renderings of a microtubule lying on a porous substrate under two different loading forces: (a) F = 200 pN (b) F = 400 pN

**RESULTS:** Two different kinds of elastic moduli have been reproducibly measured: bending and radial compression moduli. Furthermore, measurements on different temperatures between 5°C and 42°C have been performed. Results (Figure 2.) show a dramatic stiffening of microtubules on cooling. This effect can be explained by changes in the interaction between

the protofilaments building microtubules due to conformational changes of tubulin molecules.

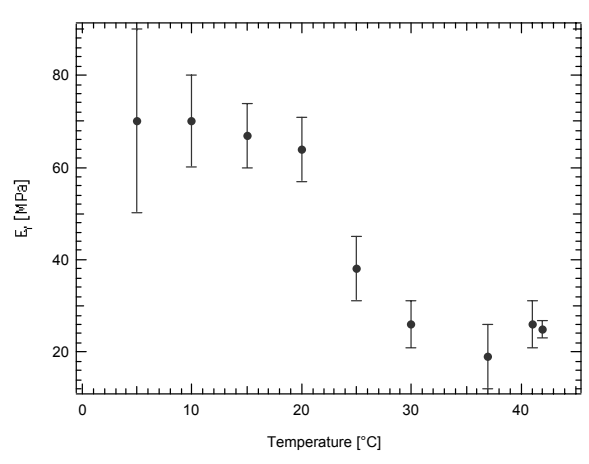


Fig. 2: Dependence of the bending modulus of microtubules on the temperature.

**REFERENCES:** <sup>1</sup>A. Vinckier et.al. (1996) Journal of Vacuum Science and Technology B **14:** 1427-1431. <sup>2</sup>M. Elbaum, D. K. Fygenson and A. Libchaber (1996) Physical review letters 76, 4078-4081

**ACKNOWLEDGEMENTS:** We thank G. Beney, EPFL-DP-IGA for producing the substrates. Also great thanks to Prof. Benoit and Prof. Zuppirolli (same address) for many interesting discussions and continuing support.

#### AMINO ACID ADSORPTION ON TIO<sub>2</sub>(110)

A.G. Thomas, W.R. Flavell, G. Thornton\*

Department of Physics, UMIST, P.O. Box 88, Manchester, M60 1QD, UK \*Department of Chemistry, Manchester University, Oxford Road, Manchester M13 9PL, UK

**INTRODUCTION:** The adsorption of glycine on the TiO2(110) surface has been investigated by LEED and HREELS (High Resolution Electron Energy Loss Spectroscopy). The glycine appears to form a disordered multilayer at high exposures with the glycine in the zwitterionic form. Heating of the multilayer to around 80 °C results in all but the last few zwitterionic glycine layers being desorbed from the surface. Heating above 80°C removes all of the glycine layers to reveal a methylamine-like fragment directly adsorbed on the TiO2(110) surface. At no point does LEED suggest the formation of an ordered overlayer. Low exposures also result in the formation of the methylamine fragment without heating of the substrate suggesting the decomposition is substrate induced. LEED again suggests no ordering of the adsorbate on the surface.

Finally the effects of preadsorption of water and coadsorption of water are discussed

### FORMATION OF PROTEIN-CONTAINING SUPPORTED LIPID BILAYERS ON SiO<sub>2</sub>.

A. Graneli <sup>1,2</sup>, F. Höök <sup>1</sup>, J. Rydström <sup>2</sup>, <u>B. Kasemo</u> <sup>1</sup>

<u>Chemical Physics Group</u> Department of Applied Physics, Chalmers, Göteborg, Sweden

<sup>2</sup> Department of Biochemistry and Biophysics, Göteborg University, Sweden

INTRODUCTION: One way to study transmembrane proteins is to mimic the membrane structure by incorporating the proteins into lipid membranes deposited on solid supports. The focus of this project is to combine spontaneous formation of lipid membranes on solid supports, known to occur on SiO<sub>2</sub> [1], with incorporation of transmembrane proteins. Understanding and mastering of this process has important implications field biosensors, in the of bioenergetics, biomaterials and for a basic understanding of membrane processes.

In this work we use small unilammellar proteoliposomes to form a lipid bilayer with incorporated transmembrane proteins on a hydrophilic SiO<sub>2</sub>-surface. The vesicle and protein adsorption is studied with the QCM-D technique where the frequency shift (mass adsorbed on the surface including the mass of water coupled to the molecules bound to the surface) and the energy dissipation shift (reflecting the viscoelastic properties of the overlayer) are measured simultaneously [2]. Proton translocating nicotinamide nucleotide transhydrogenase (TH) is used as a model protein. The presence of TH in the supported lipid bilayers was detected by trypsin-cleavage of water soluble subunits of the protein.

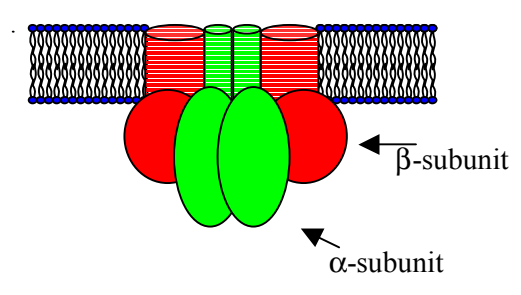


Fig. 1. TH in the lipid membrane. The enzyme consists of two subunits. In the cell membrane it is a dimer.

**METHODS:** The purified TH comes from *E-coli*, it is the wild-type enzyme and it is purified according to Meuller et al [3]. The liposomes consists of 50% bovine heart PE, 45% egg-PC and 5% bovine heart PS and has been prepared by sonication, followed by ultra-centrifugation [4]. The lipids are purchased from Sigma-Aldrich.

The TH is reconstituted by mixing pre-formed liposomes, Triton X-100 and protein. The Triton X-100 is removed by bio-beads SM-2, Bio-Rad. The 1 inch diameter, piezoelectric quartz sensor crystals, with gold electrodes, used in the QCM-D experiments are purchased from Maxtec,. 3 nm Titanium followed by 100 nm SiO<sub>2</sub> are evaporated onto the sensor electrodes to constitute the bilayer forming SiO2 surface [ref]. The sensors are cleaned with detergent and UV-Ozon-treatment. The buffer used trough the entire experiment is 100 mM NaCl, 10 mM Tris-HCl, pH 8,0. The bilayer is incubated with trypsin for 30 minutes with and without the presence of the substrate for the β-subunit of TH, which is NADPH [5]. When trypsin is added to the bilayer without NADPH only the  $\alpha$ -subunit is cleaved off. When NADPH is present both soluble subunits are cleaved off.

**RESULTS:** The supported lipid bilayers containing protein are spontaneously formed onto the silicon wafers when exposing them to the proteoliposomes. When the protein concentration is too high, the desired total transformation of the proteoliposomes to bilayer doesn't occur. Instead there are some intact proteo-liposomes remaining on the surface, indicated by the final higher frequency and dissipation shift compared to the results of the fusion of the liposomes in fig 2.

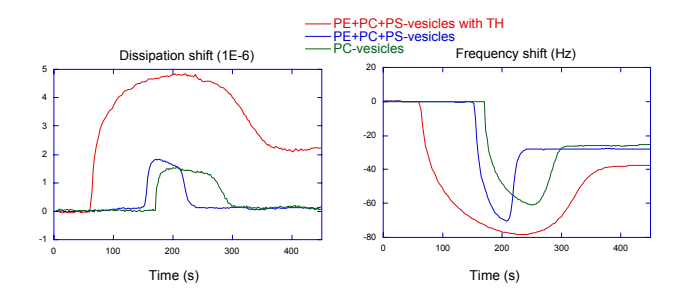


Fig 2.QCM-D results. Comparison of frequency and dissipation shifts between liposomes containing different kinds of lipids and proteoliposomes. The maximum and minimum of the curves show the collapse of the liposomes and proteoliposomes where the mass and energy dissipation of bound water inside the liposomes are lost.

When the protease Trypsin is added to the formed bilayer, containing incorporated proteins, the soluble subunits are cleaved off resulting in complete transformation of the vesicles to a bilayer. See fig 3 where the loss of mass and energy dissipation is shown when the subunits are cleaved off.

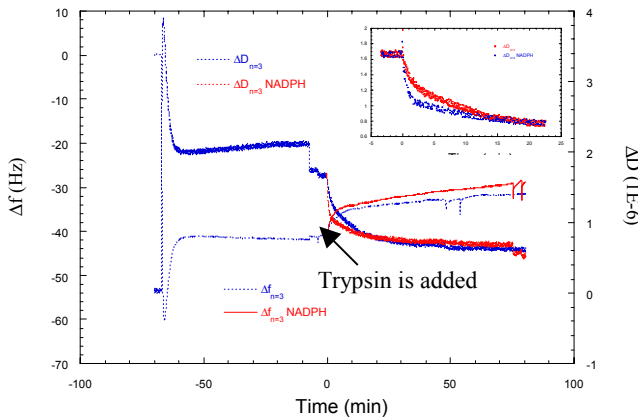


Fig 3. Trypsin cleaving of subunit  $\alpha$  and  $\beta$  of TH in supported membrane

**REFERENCES:** <sup>1</sup>Keller, C.A. and B. Kasemo, Surface specific kinetics of lipid vesicle adsorption measured with a QCM. Biophys J 1998. 75(3):1397-1402.

<sup>2</sup> Rodahl, M., et al., Simultaneous frequency and dissipation factor QCM measurements of biomolecular adsorption and cell adhesion. Faraday Discuss., 1997. **107**: 229-246.

<sup>3</sup> Meuller, J., et al., Properties of the cysteine-free proton-pumping nicotinamide nucleotide transhydrogenase. Biochemical Journal, 1997. **324**: 681-687.

<sup>&</sup>lt;sup>4</sup> Barenholz, Y., et al., A Simple Method for the Preparation of Homogenous Phospholipid Vesicles. Biochemistry, 1977. **16**(12): 2806-2810.

<sup>&</sup>lt;sup>5</sup> Fjellström, O., et al., Mapping of Residues in the NADP(H)-Binding Site of Proton-translocating Nicotinamide Nucleotide Transhydrogenase from Escherichia coli: a Study of Structure and Function. Journal of Biological Chemistry, 1999. 274(10):6350-9.

#### SURFACE IMMOBILIZATION OF RECEPTORS FOR BIOASSAY DEVELOPMENT

A-F Sévin-Landais, <u>E.Schmid</u>, <u>A-P.Tairi</u>, <u>R.Hovius</u>, H.Vogel Laboratory of Physical Chemistry of Polymers and Membranes, EPFL, Lausanne, Switzerland

**INTRODUCTION:** Incorporation of membrane receptor proteins in supported membranes for the study of receptor-ligand interactions and signal transduction events by surface sensitive evanescent wave techniques necessitates a method to immobilise these receptors in a manner that preserves all their functional features. Here we present two complementary approaches for the functional surface immobilization of membrane receptor proteins.

Immobilization via affinity tags: A detergent solubilised, His-tagged 5-HT3 serotonin receptor was fixed to quartz slides; the surface of the quartz slides was modified with NTA, a metal-ion chelating group, allowing the reversible attachment of the His-tagged receptor proteins (Fig.1, left panel). The specific binding of a fluorescently labelled antagonist to the receptor was detected by total internal reflection fluorescence (TIRF). The immobilized receptor exhibited identical ligand binding pharmacology as the native receptor in brain tissues, indicating that surface immobilization did not effect these properties of the receptor <sup>1</sup>. The TIRF assay is extremely sensitive; a few cells express sufficient receptor to perform ligand screening.

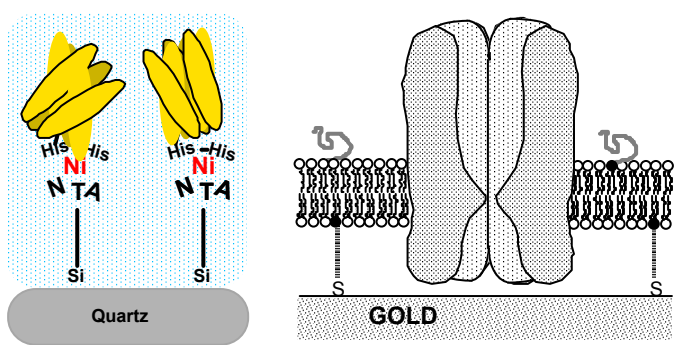
Immobilization in tethered membranes: The nicotinic acetylcholine receptor (nAchR) was reconstituted into vesicles containing a mixture of thiolipids and conventional lipids by detergent dialysis. The thiolipids, bearing in the headgroup a thiol group attached to the terminus of a long polyethyleneoxide spacer, bind covalently to the gold surface of surface plasmon resonance (SPR) nAchR containing sensor. The supported membrane is attached to the surface via the long spacer forming an aqueous compartment between the surface and the membrane, giving space to the extramembraneous parts of the nAchR (Fig.1, rigth panel).

The ligand binding site of the nAchR was predominantly native and facing the solution in the flow cell, as determined using epitope specific monoclonal antibodies. The pharmacological properties of the surface-immobilised receptor, tested by the competition of binding between certain ligands and a monoclonal antibody specific for the ligand binding site, were in good agreement

with the values found in radioligand binding assays <sup>2</sup>.

These results demonstrate that the nAchR-containing supported membranes can be applied for ligand screening by SPR.

Fig. 1: Immobilisation of membrane protein receptors onto sensor surfaces. Detergent-



solubilised His-tagged 5HT3 receptors were reversibly attached to NTA-modified quartz slides (left). The nicotinic acetylcholine receptor was reconstituted in tethered membranes onto a gold surface using so-called thiolipids, which serve both to covalently anchor the membrane to the surface and to decouple the membrane from the surface to accommodate the extramembraneous parts of the receptor protein (right).

**DISCUSSION & CONCLUSIONS:** We believe that the methods developed in this study are generally applicable for membrane receptor proteins and will be important for the discovery of new pharmacologically active compounds.

**REFERENCES:** <sup>1</sup>E. Schmid, et al., (1998) *Anal. Chem.*, **70**: 1331-1338. <sup>2</sup>A. Sévin-Landais, et al., (2000) *Biophys. Chem.*, **85**, 141-152.

**ACKNOWLEDGEMENTS:** This work was financially supported by the Swiss National Science Foundation (project 31-57023.99).

### PPS-PEG BLOCK COPOLYMERS RENDER HYDROPHOBIC SURFACES PROTEIN AND CELL RESISTANT

<u>J. Bearinger</u> <sup>1,2</sup>, A. Napoli<sup>1</sup>, M. Graf <sup>1</sup>, M. Textor <sup>2</sup>, and <u>J. Hubbell</u> <sup>1</sup>

<u>Institute for Biomedical Engineering</u> and <sup>2</sup> <u>Laboratory for Surface Science Technology</u>,

Swiss Federal Institute of Technology, ETH-Zürich, Switzerland

INTRODUCTION: Poly Ethylene Glycol (PEG) has been used in numerous biomedically motivated systems to aid in minimization of protein adsorption and cell adhesion. Typical approaches rely on silane based chemistries, electrostatic interactions, and plasma treatments. Hydrophobic interactions are the focus of this research, chosen for the simplistic nature a coating deposition allows. Asymmetric PEG chains separated by a polypropyl sulfide (PPS) block provide a facile molecule that is both protein and cell resistant.

**METHODS:** PPS-PEG block copolymers<sup>1</sup> were synthesized from a PEG thioacetate block of approximately 16 units. Deprotection of the macrothiol, followed by propyl sulfide living end polymerization, led to a second block of 25 PPS units. End capping with an acrylate PEG of 7 units provided an asymmetric triblock copolymer.

The polymer was added to methanol (1 mg/ml) and sonicated to create a slightly opaque colloidal dispersion. The dispersion was first applied to hydrophobic and hydrophilic surface coatings on waveguides suitable for Optical Waveguide Light Spectroscopy (OWLS) to quantify adhesion of Human Serum Albumin (HSA) and/or serum. The substrates used were Teflon AF1600. Octadeclyphosphate (ODP), and clean waveguides (a SiTi sol gel coating). Coating solution was adsorbed onto surfaces for 30 minutes. Surfaces were then rinsed in methanol, and then in HEPES Z1 buffer before exposure to protein solutions. Uncoated similar surfaces served as controls. The coating was next applied in a similar fashion to similar hydrophobic and hydrophilic surfaces (Teflon, Dodecyl phosphate (DDP), polystyrene (PS), SiO<sub>2</sub>, and tissue culture polystyrene (TCPS)) to test the effect of plating Human Foreskin Fibroblasts (HFF) for 20 hours at a seeding density of approximately 20,000 cells per culture dish well.

**RESULTS:** Results indicate that PPS-PEG applied to hydrophobic, but not hydrophilic surfaces, renders surfaces both protein and cell resistant. Table 1 indicates the amount of HSA adsorbed onto waveguides. Figure 1 shows an OWLS plot of polymer adsorption, change in refractive index between MeOH and HEPES

buffer, and lack of HSA and serum adsorption (complete removal was observed upon a HEPES rinse). Fig. 2 contrasts cell activity over 20 hr between HFFs plated on PPSPEG treated hydrophobic PS and on untreated TCPS.

Table 1. Protein adsorption (HAS) measured with OWLS on PPSPEG treated and control substrates.

| Substrate | Treatment | HSA (ng/cm²) |
|-----------|-----------|--------------|
| Teflon AF | PPSPEG    | -            |
| Teflon AF | control   | 160          |
| ODP       | PPSPEG    | -            |
| ODP       | control   | 107          |
| SiTi      | PPSPEG    | replacement  |
| SiTi      | control   | 176          |

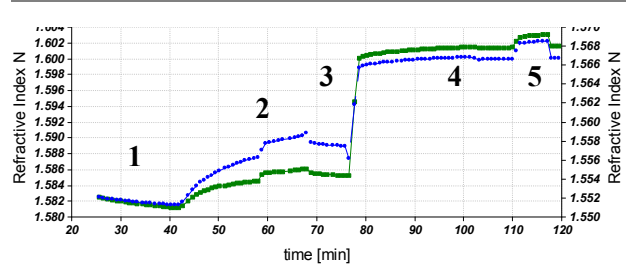


Fig. 1: PPSPEG adsorbed on Teflon AF coated waveguide shows no protein adsorption according to OWLS: 1)MeOH baseline, 2) PPSPEG adsorption, 3) transition from MeOH to HEPES buffer, 4) no HSA adsorption, 5) no serum adsorption (level back to aqueous baseline upon rinse with HEPES).





Fig. 2: PPSPEG adsorbed on PS (left) shows no HFF cell attachment after 20 hr, in contrast to TCPS (right) which shows rapid cell proliferation.

**CONCLUSIONS:** PPSPEG adsorbed in MeOH onto hydrophobic surfaces renders all surfaces tested protein and cell resistant for at least 20 hr.

**REFERENCES:** <sup>1</sup> A. Napoli, N. Tirelli, G. Kilcher, J.A. Hubbell (2001) *submitted to Macromolecules*.

**ACKNOWLEDGEMENTS:** Thanks to N. Tirelli, and G. Kilcher for synthetic efforts and helpful discussions.

### MICROFABRICATED SURFACES TO STUDY CELL-SURFACE INTERACTIONS

M.Winkelmann<sup>1</sup>, <u>G.Csúcs</u><sup>2</sup>, J.Vörös<sup>1</sup>, C.Scotchford<sup>3</sup>, M.Textor<sup>1</sup>, J.Gold<sup>4</sup>, N.Spencer<sup>1</sup>

<u>Laboratory for Surface Science and Technology</u>, <u>Laboratory for Biomechanics</u> Swiss Federal Institute of Technology, ETH-Zürich, Switzerland, <u>School of Biomedical Sciences</u>, University of Nottingham, Great Britain. <u>Chemical Physics Group</u>, Dept. of Applied Physics, Chalmers University of Technology, Gothenburg, Sweden

INTRODUCTION: Most artificial materials, once implanted in the patient's body, induce a cascade of reactions with the biological environment through interaction of the biomaterial with body fluid, proteins and various cells. The specific surface interactions determine the attitude the body takes towards the foreign material, the path and speed of the healing process and the longdevelopment of the biomaterial-body interface. As regards surface properties, both the chemical composition and the topography (structure, morphology) are known or believed to be important in bone, since they regulate type and degree of the interactions that take place at the interface. Microfabrication has proved to be a very valuable tool for producing geometric patterns of well-defined surface chemistry and/or topography. Such surfaces are ideal to study-in separate of experiments-the influence chemical composition and surface morphology and to learn how cells sense surfaces of biomaterials, in both in vitro and in vivo assays.

METHODS: Silitronix (100)-surface polished silicon 2" wafers were coated with 20nm of either Ti, Al, Nb or V in a thin film deposition system. Wafers were then spin-coated with 1.5mm thick photoresist (Shipley S-1813 Microposit). The samples were exposed to UV light (400 nm; Mercury lamp; 3.5 mWatt/cm2) with a contact printer through a chromium mask. Then developed (Shipley MF322 Microposit) to remove exposed photoresist. A second evaporation with a 20nm layer of either Ti, Al, Nb, or V was carried out. The remaining resist was then removed with acetone. Finally the wafer surface consisted of spatially patterned regions (Figure 1) of Ti, V, Al and Nb, representing models of heterogeneous titanium alloy surfaces currently used in orthopaedic and maxillofacial implants. The dimension of the patterns was varied between 0.5 and 150 mm.

Prior to testing and characterizing all samples were cut to 11x9 mm size, extensively washed in acetone-isopropanol-DI water, treated in an O2-

plasma for 5 min and then studied by AFM, XPS, ToF-SIMS, SEM measurements.

Studies of the attachment and spreading behaviour of human osteoblasts on these well-defined chemically patterned model surfaces have been carried out in collaboration with University of Nottingham.

Protein adsorption studies were done on the structured (and also non-structured) metal-oxide surfaces either by fluorescent microscopy or by OWLS. For the experiments we used either fresh human serum, or single proteins like fibronectin, human serum albumin, fibrinogen and human IgG. In microscopy the visualisation of proteins was done by using labelled antibodies.

**RESULTS:** AFM, XPS, ToF-SIMS, SEM indicated a well defined surface structure, corresponding to the expected/designed one. The metal film surfaces have been shown to be protected by natural oxide layers upon exposure to air. The most prominent stoichiometries have been found to be: TiO2, Al2O3, V2O5 and Nb2O5.

Cell Culture Tests show no significant difference between the long term (>18 h) adhesion/spreading behaviour of the osteoblasts on the metal-oxide surfaces. However, on the short time scale (90 min – 6 h) cells clearly preferred the V and Nb surfaces instead of Al on the structured Al/Nb, Nb/Al and Al/V, V/Al surfaces. The Ti/Ti showed no such differences.

Protein Adsorption Studies were performed in order to explain the observed cell behaviour. The results show that single protein studies are unable to solve the problem, more complex experiments using protein mixtures or full serum should be used. Preliminary results indicate that the amount (ratio) of Fibronectin compared to other serum proteins (like IgG) is higher on the V, Nb surfaces then on the Al surfaces.

#### DIFFERENT ECM SUBSTRATES INDUCE CELL-TYPE SPECIFIC MORPHOLOGY AND/OR DIFFERENTIATION.

<u>H.Hall</u>, H.Mohajeri <sup>1</sup> <u>J.A.Hubbell</u> *Institute for <u>Biomedical Engineering</u>, Department of Materials Swiss Federal Institute of Technology,* ETH-Zürich, Switzerland Department of Psychiatry Research, University of Zurich, Switzerland

INTRODUCTION: Cell adhesion and migration is dependent on specific interactions between substrates and cell surface expressed receptors that mediate the communication between outside and inside of the cell and induce appropriate reactions towards changing conditions (Humphries, 1990; Hynes 1992; Calderwood et al., 2000; Ivaska and Heino, 2000). Our study shows that providing different ECM-molecules as substrates for a single cell type leads to different morphology and probably also functionality. Providing a single ECM substrate to different cell types also induces different morphology. In this study we compared the effect of surface adsorbed ECM molecules such as matrigel and L1Ig6-modified fibrin on the morphology of human umbilical vein endothelial cells (HUVECs) and on neuronal stem cells (NSCs). Both cell types are known to interact with different ECM-substrates through their integrin receptors expressed on the surface.

METHODS: HUVECs were purchased from PromoCell, Heidelberg, Germany and maintained under low serum conditions (2%) in the absence of additional growth factors. NSCs were obtained.... Both cell types were cultured on the surface of TCPS adsorbed matrigel (Pharmingen) and on covalently L1Ig6-modified fibrin matrices (Hall et al., submitted) at 50000 cells/ml for 24h at 37°C and 5% CO2. Effects of collagen I and plain fibrin are not shown here. Living cells were fluorescently labelled with fluorescein diacetate (FDA) as described by Hall et al. (submitted) and the morphology of cells was analysed by fluorescence microscopy.

**RESULTS AND DISCUSSION:** Cell-matrix interactions are responsible for cell-type specific morphology and/or differentiation. Both cell types survive on matrigel and on L1Ig6-modified fibrin as demonstrated by staining of living cells by FDA. However, the morphology of HUVECs and NSC cultured on matrigel and on L1Ig6-modified fibrin was very different. HUVECs on matrigel form tube-like extensions that are interconnected. They have been described as first indications towards the angiogenic differentiation (Pepper et al., 1996). NSCs cultured on matrigel extend neurites. Interactions between NSCs and matrigel are mediated by integrins and laminin-1, the major component of matrigel. When grown on L1Ig6modified fibrin, an artificial matrix designed to interact specifically with  $\alpha v \beta 3$ -integrins on angiogenic HUVECs, HUVECs show a similar morphology as observed on matrigel. HUVECs extend processes that can be interconnected with each other. The same substrate is not very adhesive for NSCs, since they do not express ανβ3-integrins and therefore can not interact with L1Ig6-modigied fibrin. The cells stay round and do not attach and spread on the surface.

Our experiments indicate that communication between a cell-type and ECM-molecules is very specific and is mediated by receptors on the cell surface. These include integrins, cell adhesion molecules, cadherins and selectins that are expressed in a cell-type specific manner and, most important, can be addressed specifically to induce a certain reaction of the cell, such as inducing the angiogenic phenotype of HUVECs by triggering αvβ3-integrin.

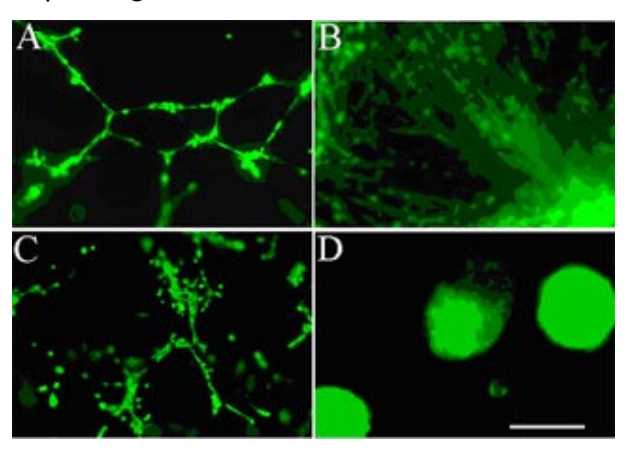


Fig 1: HUVECs were cultured for 24h on matrigel (A) and on L1Ig6-modified fibrin (C), and NSC on matrigel (B) and L1Ig6-modified fibrin (D), respectively. The scale bar represents  $200 \square m$ .

REFERENCES Humphries, 1996, Curr. Opin. Cell Biol. 8, 632-640. Hynes, 1992, Cell, 69, 11-25. Calderwood et al., 2000, J. Biol. Chem. 275, 22607-22610. Ivaska and Heino, 2000, Cell Mol. Life Sci. 57, 16-24. Pepper et al., Enzyme Protein, 49, 138-163. Hall et al, submitted.

### CELL ADHESION PHENOMENA ON PATTERNED SUBSTRATES PREPARED WITH MICROCONTACT PRINTING

D. Lehnert, M. Bastmeyer

Department of Biology, <u>University of Konstanz</u>, Germany

**INTRODUCTION:** Cell adhesion, the interaction of cells with each other or with the extracellular matrix (ECM), is a complex process that plays a fundamental role during development and maintenance of the fate of multicellular organisms. The initial phase of cell/matrix interactions is characterized by the binding of specific receptors on the cell surface to ECM molecules and the assembly of the receptors at the contact sites. This leads to the induction of intracellular signalling cascades that cause the assembly of specific linker molecules at the contact sites and a reorganization of the actin cytoskeleton<sup>1</sup>. We are interested in achieving a better understanding of the basic process of cell adhesion by confronting cells with chemically defined and regularly patterned substrates. What are the minimal requirements for initial cell adhesion? What is the maximal distance between two ECM-coated areas that can be bridged by a single cell? What is the minimum size of an ECM-coated area to induce intracellular signalling cascades, an assembly of linker molecules and a reaction of the cytoskeleton?

METHODS: We used micro contact printing (µCP)<sup>2</sup> to create well defined structures of proteincoated regions in the micro- and nanometer scale. With this method we were able to produce patterned substrates of **ECM** molecules (fibronectin, vitronectin, laminin) consisting of squared dots (3µm, 1µm, 800nm, 500nm, 300nm) separated by nonadhesive regions of variable distances (2µm-30µm). Cells were cultivated on the patterned substrates for 1 h, fixed and fluorescently labelled for actin, focal adhesion associated molecules (integrin, paxillin, talin, vinculin) and markers for intracellular signalling (phosphotyrosine, FAK), and analysed.

**RESULTS:** When cells are cultured on a homogeneous fibronectin substrate prepared with  $\mu$ CP, they show a typical morphology characterized by flat lamellipodia. Cells seem to interpret dots of any size as a homogeneous substrate if the distance between dots is smaller than 5 $\mu$ m. With increasing distance between dots (10-25 $\mu$ m), cells react by orienting their cell shape according to the dot pattern, forming lamellipodia with straight edges and right angles. A distance of 30 $\mu$ m between two dots can no longer be bridged

by a single cell, resulting in ball-shaped cells adhering to a single dot. The actin cytoskeleton reacts to dot sizes down to 500nm by forming straight bundles between dots (Fig. 1a). Integrin, focal adhesion associated molecules and markers for signal transduction accumulate in regions of the cell overlying ECM-dots (Fig. 1b) down to 300nm in side length.

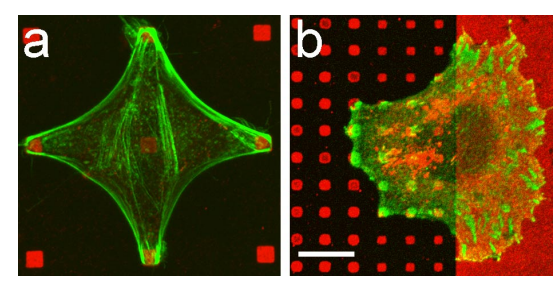


Fig. 1: (a) The actin-cytoskeleton (green) of a B16 melanoma cell on a patterned fibronectin-substrate (red). (b) BRL-fibroblast stained for phosphotyrosine (green) at the border of a homogenous and a patterned fibronectin-substrate (red). scale bar 10μm.

**DISCUSSION & CONCLUSIONS:** μCP in combination with cell culture is a powerful technique to study basic principles of cell adhesion and migration. We show, that an ECM-coated area of  $0.25 \mu m^2$  is sufficient to induce a functional focal contact and that cells can bridge non-adhesive distances of  $25 \mu m$ . We are currently using transformed cell lines expressing GFP-fluorescent proteins (integrins, tubulin, actin) to investigate the dynamics of focal adhesion formation on patterned substrates in living cells.

**REFERENCES:** <sup>1</sup>S.M. Schoenwaelder and K. Burridge (1999) *Curr. Opinion in Cell Biol.* 11:274-286. <sup>2</sup>M. Mrksich and G.M. Whitesides (1996) *Ann.Rev.Biophys.Biomol.Struct.* 25:55-78

**ACKNOWLEDGEMENTS:** We thank C. David (PSI, Villigen) for preparing the wafer, V. Eck (University Heidelberg) for the ethyleneglycolterminated alkanethiols and C. Schäfle (University Konstanz) for help during initial printing problems. GFP-transfected cells were provided by B. Wehrle-Haller and B. Imhof (CMU, Genf) This work is supported by the DFG (SFB 513).

# DYNAMIC MEASUREMENTS OF BOUND WATER IN PROTEINS AND PROTEIN-RESISTANT POLYMERS: A COMBINED OWLS AND OCM-D STUDY

<sup>1</sup>J. Vörös, <sup>1</sup>S. M. DePaul, <sup>1</sup>I. Reviakine, <sup>2</sup>C. Galli, <sup>2</sup>M. Collaud Coen, <sup>1</sup>M. Textor, <sup>1</sup>N. D. Spencer <sup>1</sup>Laboratory for Surface Science and Technology, Swiss Federal Institute of Technology, ETH-Zürich, Switzerland <sup>2</sup> Solid State Physics Research Group, University of Fribourg, Switzerland

**INTRODUCTION:** Water is known to play an important role in biological systems, but the time-dependent variation of the amount of bound water during adsorption processes has not been fully characterized. To elucidate the role of water in protein and polymer adsorption, comparative studies were carried out using two different, but complementary, *in situ* techniques: optical waveguide light mode spectroscopy (OWLS) and the quartz crystal microbalance with dissipation measurement (QCM-D).

To study the behaviour of bound water during protein adsorption, the model proteins human serum albumin (HSA), fibrinogen, immunoglobulin, and haemoglobin were adsorbed onto titanium-oxide coated substrates.

In addition, the role of water in adsorbed poly (L-lysine)-g-poly(ethylene glycol) (PLL-g-PEG) was examined. Such graft-copolymers, like other PEGylated coatings, have been shown to be remarkably resistant to protein adsorption [1] and the cationic poly(L-lysine) backbone allows for facile and rapid adsorption to metal oxide surfaces (such as titania and silica) that are negatively charged at neutral pH. This makes these polymers highly suitable for biosensing applications.

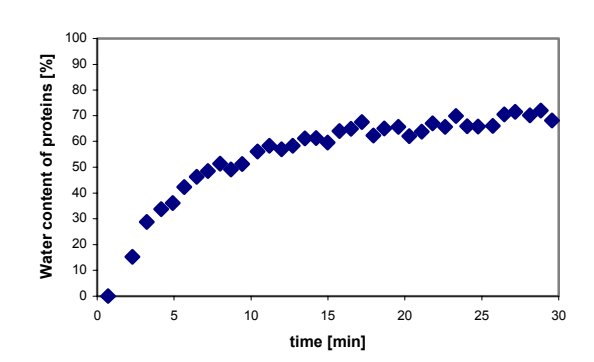
**METHODS:** The OWLS technique involves the incoupling of a He-Ne laser into a planar waveguide generating an evanescent field which allows for the direct online monitoring of macromolecule adsorption. It is highly sensitive (i.e. ~1 ng/cm²) up to a distance of 100 nm above the surface of the waveguide. The mass of an adsorbed layer can be calculated from the thickness and refractive index values derived from the mode equations.

The QCM-D technique is based on the pulsed excitation of shear oscillations in piezoelectric quartz crystals. Changes in the resonance frequency of these shear oscillations as a function of time provide information about adsorbed masses, and the decay rate of the oscillation amplitude after the pulse gives insight into the viscoelastic nature (i.e., mechanical properties) of the adsorbed layer.

Whereas the adsorbed mass calculated from OWLS measurements reflects only the mass of the polymer or protein, the mass calculated from the QCM experiments contains an additional contribution from the mass of the water that is immobilized within the adlayer [2]. The two techniques thus provide complementary information.

Both the OWLS and QCM-D techniques have the advantages of being able to monitor real-time kinetics and of not requiring labelled samples.

RESULTS AND DISCUSSION: The water content was found to be characteristic for the investigated proteins. An example of a typical experiment, shown in the figure below, demonstrates the evolution of the water content of HSA during the adsorption process onto a TiO<sub>2</sub> surface. The water content of HSA is low during the initial phase of adsorption indicating a different conformation than at the end of the adsorption process.



Adsorption and water content of PLL-g-PEGs with different molecular weights and grafting ratios were also examined on several different metal oxide surfaces.

**REFERENCES:** <sup>1</sup> G. L. Kenausis, J. Vörös, D. L. Elbert, N. Huang, R. Hofer, L. Ruiz, M. Textor, J. A. Hubbell, N. D. Spencer, *J. Phys. Chem. B* **104**: 3298-3309, 2000.

<sup>2</sup> F. Höök, M. Rodahl, J. Vörös, R. Kurrat, P. Böni, J.J. Ramsden, M. Textor, N. D. Spencer, P. Tengvall, J. Gold, B. Kasemo, *Colloids and Surfaces B*: in press 2001

### DIFFERENTIAL CELL ADHESION TO PHOSPHORYLCHOLINE POLYMERS WITH VARYING CATIONIC CHARGE.

S.F.Long, A. L. Lewis\*, G. W. Hanlon & A. W. Lloyd School of Pharmacy and Biomolecular Sciences, University of Brighton, UK \*Biocompatibles Ltd, Farnham, UK

INTRODUCTION: The adhesion and proliferation of cells to biomaterials is key to the biological acceptance and integration of many medical devices within a host. Kottee-Marchane et al 1996 showed that the success of vascular stents is greatly improved following adhesion and growth of vascular endothelial cells over the stent surface. This study evaluates the adhesion of cells to a series of phosphorylcholine (PC) polymer coated materials in order to assess whether cationic charge would modulate adhesion of specific cell type.

**METHODS:** Phosphorylcholine polymers containing varying amounts of cationic charge were coated on to poly(ethyleneterephthalate) (PET). The adhesion of rabbit corneal epithelial cells, mouse fibroblast cells and bovine vascular endothelial cells were investigated by incubating the materials with 6000 cells cm-2 in 5% CO2 at 37°C for up to 3 days. At daily intervals, cells adherent to the material surfaces were fix with methanol and stained with DAPI stain. The number of adherent cells was quantified manually under a fluorescent microscope at x 400 magnification.

**RESULTS:** Figure 1 shows the adhesion of corneal epithelial cells to the different substrate surfaces. Results indicate that both cell adhesion and proliferation is dependent on material composition. Samples with 0% charge showed no cell adhesion. No clear pattern in cell adhesion was seen with varying cationic charge although the number of cells adherent to PC polymers with 20 and 30% charge was generally lower than samples with 5, 10 and 15%. Figure 2 shows the adhesion of fibroblast cells to the different substrate surfaces. Results indicate that both cell adhesion and proliferation is dependent on material composition. Samples with 0% charge showed little to no cell adhesion. As cationic charge increase to 10% the number of adherent cells also increased, with then number of cells generally increasing with time. Above 10% little difference between samples is seen in the number of adherent cells. Figure 3 shows the adhesion of endothelial cells to different substrate surfaces. Results indicate that both cell adhesion and proliferation is dependent on material composition. All samples showed little to no cell adhesion.

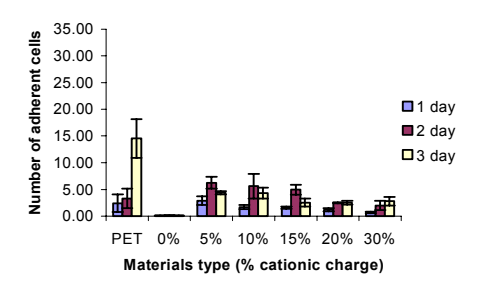


Fig. 1. Corneal epithelial cell adhesion to phosphorylcholine polymers varying in cationic charge.

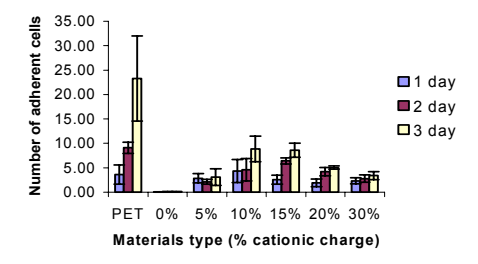


Fig.2. Fibroblast cell adhesion to phosphorylcholine polymers varying in cationic charge.

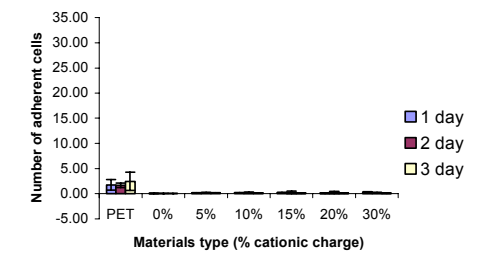


Fig. 3 Endothelial cell adhesion to phosphorylcholine polymers varying in cationic charge.

Conclusion: Adhesion to biomaterials is dependent on both material composition and cell type. The addition of cationic charge to the PC polymer appeared to increase the adhesion of both fibroblast and epithelial cells. This is consistent with other studies; Kishida et al 1991 and Dekker and Beugeling 1991 showed that cationic charge encourages cell adhesion. Cationic charge did not however increase the adhesion of endothelial cells in this study. Increasing cationic charge does not increase epithelial and fibroblast cell adhesion beyond a maximal value. This may be attributed to

the adsorption of proteins onto the cationic surface.

References: 1.Kottee-Marchane et al 1996 Journal of Biomedical Materials Research 30, 209-220

- 2. Kishida et al 1991 Biomaterials 12 786-792
- 3. Dekker and Beugeling 1991. In 'Modern aspects of Protein Adsorption on Biomaterials' 25-
- 28 Missirlis Y. F. and Lemm W. (eds). Kluwer Academic Publishers. Printed in the Netherlands

# TEMPORAL AND SPATIAL CONTROL OF CELL-GLYCOPOLYMER SURFACE INTERACTION: REGULATION OF HEPATOCYTE CELL SIGNALING BY GLYCOPOLYMER

S-H. Kim<sup>1</sup>, J-H Kim<sup>2</sup>, T. Akaike<sup>1</sup>

<sup>1</sup> Dept. of Biomolecular Engineering, Tokyo Institute of Technology, Yokohama 226-8501, Japan <sup>2</sup> Dept. of Chemical Engineering, Korea Advanced Institute of Science & Technology, Taejon 305-701, Korea

**INTRODUCTION:** Cell adhesion to extracellular matrixes (ECMs) plays pivotal role in a wide of variety of biological process such as proliferation, differentiation and metastasis in animal tissue. Synthetic biomimetic materials have designed to stimulate cell adhesion and specific cellular functions in tissue engineering [1]. Cell adhesion to materials is initialized by cell surface molecules, while cooperating with material surface molecules through biological recognition or nonspecific interaction. Carbohydrate-mediated cell recognition has been applied to enhance selective interactions between the materials and cell surface. developed carbohydrate-We initially the derivatized polystyrenes, poly-(N-p-vinylbenzyl-4-O-β-D-galactopyranosyl)-D-gluconamide (PVLA) poly-(N-p-vinylbenzyl-6-O-α-Dand galactopyranosyl)-D-gluconamide (PVMEA), that have multivalent galactose moieties. The polymers were excellent in mammalian primary hepatocyte mediated by asialoglycoprotein recognition receptor (ASGPR) of the cell surface [2]. Recently, we designed a novel glucose-derivatized polystyrene, poly-(N-p-vinylbenzyl-Dglucuronamide (PV6Gna), which also recognized by ASGPR [3]. In this study, we used the glycopolymers as a cell adhesion matrix to integrin-mediated control cell signaling, elucidating the events that take place at surface or interface of biological system and synthetic materials.

**METHODS:** Preparation of glycopolymers Amphiphilic sugar-carrying polystyrenes were synthesized by a simple method which couples glycolactone with N-p-vinylbenzyl amine followed by radical polymerization [4, 5]. Molecular structure of hepatocyte-recognizable glycopolymers, PVLA, PVMEA, and PV6Gna, is shown in Fig 1.

Atomic force microscopy (AFM)

AFM image was taken by a scanning probe microscopy (SPM; NanoScope IIIa, Digital Instruments, U. S. A.). SPM was performed in air with an etched 125 µm silicon cantilever operating in TappingTM mode with a scan size of 200 nm.

Fig. 1 Molecular structure of glycopolymers

Western blot analysis and immuno-precipitation Cultured hepatocyte was solubilized in lysis buffer. The lysate was precipitated with primary antibody-conjugated agarose, then the precipitate was separated by SDS-PAGE and analyzed by western blot with horseradish peroxidase-conjugated anti-mouse or anti-rabbit secondary antibody (Jackson ImmunoResearch Lab.) and the ECL method was used (Amersham Pharmacia Biotech) using standard techniques.

**RESULTS:** Initial adhesion affinity of hepatocyte for glycopolymer surfaces was increased with an increase of the concentration of coated-PVLA, PVMEA, or PV6Gna. However, the hepatocyte adhesion strength at 30 min after adhesion was not paralleled to initial cell adhesion affinity. Rapid initial adhesion was followed by ASGPRprocess independent post-adhesion glycopolymer surfaces. Atomic force microscopy (AFM) was performed in order to characterize the geometric structure of the coated-PVLA and -PV6Gna. PVLA was coated to PS surface with different geometric structure depending on the coating concentration, as presented Fig. 2. The

post-adhesion process was controlled by microenvironmental distribution of ASGPR-glycopolymer interaction, which had been dependent on geometric structure of coated-glycopolymer surface, as presented in Fig. 3.

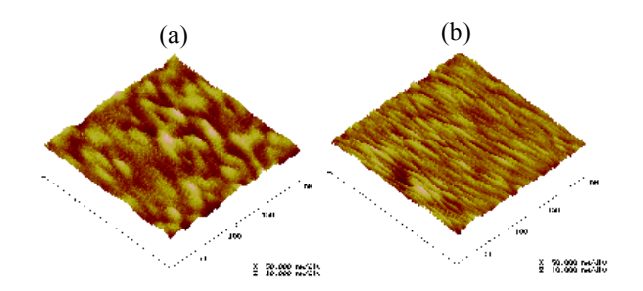


Fig. 2. 3-D AFM image of PVLA-coated PS surfa 0.5  $\mu$  g/ml, (b) 100  $\mu$  g/ml. Yellowish domains point PVLA.

Integrin-mediated signaling, such as cell growth, anti-apoptotic ability, and cell spreading, was restricted in the hepatocyte cultured on the glycopolymer surface, for example on PVLA surface at high coating density, which had induced the clustered ASGPR-glycopolymer interaction at the site of the initial adhesion contact. We suggest that integrin-mediated signaling is a part of post-adhesion processes on the glycopolymer surfaces and can be controlled temporally and spatially by employing glycopolymer surface as an adhesion matrix.

DISCUSSION & CONCLUSIONS: Sugar-carrying polystyrene was a good model for assessment of the role of carbohydrate on hepatocyte cell adhesion to synthetic glycopolymers.

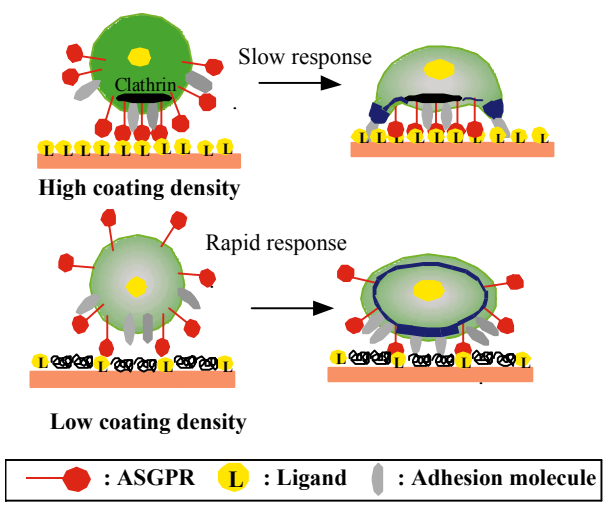


Fig. 3. Illustration of behavior of hepatocyte adhered to glycopolymer surface.

We found a well-defined culture system by controlling hepatocyte adhesion temporally and spatially, while interpreting hepatocyte behavior on the synthetic glycopolymers. These observations could be helpful for basic study of integrin-independent cell signaling for normal hepatocyte and for improved design of cell transplantation devices and cell culture substrate for tissue engineering.

**REFERENCES:** <sup>1</sup> J. A. Hubbell (1995) Bio/Technol. 13: 565-576. <sup>2</sup>K. Kobayashi, et al. (1994) Carbohydrate-containing polystyrene in Neoglycoconjugates (eds Y. C. Lee and R. T. Lee) Academic Press 262-282. <sup>3</sup>S.-H. Kim, et al. (2001) J. Biol. Chem. In press. <sup>4</sup>K. Kobayashi, et al. (1983) Polymer J. 15: 667-671. <sup>5</sup>S-H. Kim, et al. (2000) Biotech. Lett. 22: 1049-1057

# CONTROL OF SPATIALLY PERIODIC PATTERNS OF CELL AGGREGATION ON SOFT ECM SUBSTRUTA: EXPERIMENT VERIFICATION OF MECHANOCHEMICAL MODEL

I.Harada T.Akaike

Department of Molecular Design, Tokyo Institute of Technology, Japan

**INTRODUCTION:** Development of spatial pattern and form is one of the central issues in embryology and is included under the general morphogenesis. Turing name mathematically how certain combinations of chemical reaction kinetics and diffusion rate should lead to chemical instabilities, capable at least in principle of producing the desired type of spontaneous morphogenesis [1]. Subsequently, some actual combinations of chemicals have been found which spontaneously generate patterns in approximately the desired way, and the general principles underlying all such 'reaction-diffusion system' have become the major concept of morphogenesis.

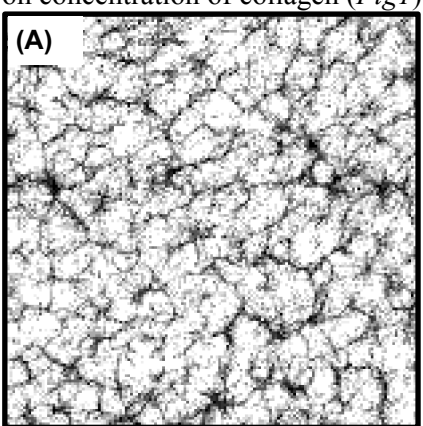
Rather contrast to this view point, Harris et al have found the generation of spatial patterns created by mechanical instabilities [2]. When fibroblasts were cultured on the collagen gel, and the contraction of the gel as a whole is physically restrained by attachment of its margin to a plastic substratum, then the effect of the fibroblasts' traction is to break up the cell-matrix mixture into a series of aggregations of cells and compressed matrix. These aggregations are interconnected by linear tracts of collagen fibres aligned under the tensile stress exerted by fibroblast traction. Oster Murrav showed mathematically and mechanical force between fibroblast and collagen gel germinated cell aggregation, and they predicted distribution of fibroblasts on the collagen gel become periodic pattern [3]. Although their theory was formulated in terms of measurable quantities such as cell densities, forces, and so on, there seems to be no established experiment fact to prove their theory. In this study, we have observed varieties of geometric patterns of fibroblast (3T3 Swiss albino) distribution, when they were cultured on collagen gel attached on plastic substrata.

**METHODS:** To clarify periodic structure of the distribution pattern of the cell, we have observed the wide area of collagen gel. 9cm diameter of collagen gels were prepared on polystyrene Petri dishes with kept attached to the dish. Then the measurements were taken at 2cm x 2cm square center of the gel using CCD camera to obtain

images of cell distributions. Images were analyzed by using Fast Fourier Transformation (FFT) method to examine periodic structure of the geometric patterns.

#### **RESULTS:**

The patterns generated spontaneously on the collagen gels vary depending on initial cell population densities and concentration of collagen gels. Geometric shapes of patterns were depended on concentration of collagen (*Fig1*).



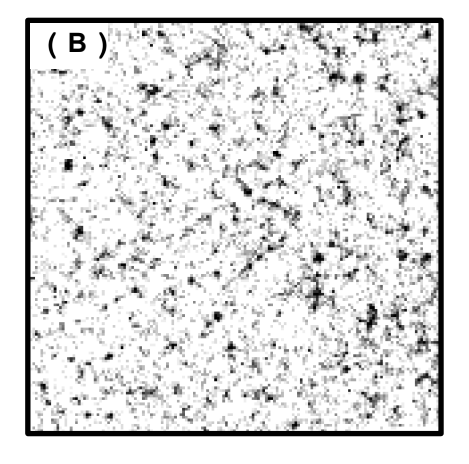


Fig1: Cell aggregation pattern generated on collagen gel. Each figure shows fourth day after cell seeded. Concentration of collagen gels are A) 0.3mg/ml, B) 3.0 mg/ml.

When the concentration of collagen was low (0.3 to 1.0(mg/ml)), cell aggregation formed 'Network like'

shape. As increasing concentration of collagen (3.0(mg/ml)), cell aggregation formed 'island like' shape. FFT method revealed all the patterns

European Cells and Materials Vol. 2. Suppl. 1, 2001 (page 54-55) generated on collagen gels have periodic structure. The wavelength of patterns was only depended on initial cell population density, and the initial cell populated density were increased; the wavelength of patterns was decreased. Size of wavelength was approximately seven times larger than average distance between the cells initially populated.

**DISCUSSION & CONCLUSIONS:** From these results and analysis, range of cell-cell mechanical interaction through the collagen fibre only depends on initial cell populated density and this can be explained by Murray's theory qualitatively. Also, we suggested the cause of different geometric shapes of pattern formed on different concentration of the gels was asymmetry of the cell-cell interaction was remarkable when concentration of gel decrease.

**REFERENCES:** <sup>1</sup> Turing, A.M.(1952) Phil. Trans. Roy. Soc. B237:37. <sup>2</sup>Harris, A.K., Stopak, D., and Wild, P. (1984) J. Embryol. exp. Morphol. 80:1. <sup>3</sup>Murray, J.D., Oster, G.F, and Harris, A.K. (1983) J. Math Biol. 17:125.

#### ENGINEERING THE EXTRACELLULAR MATRIX: SYNTHETIC PROVISIONAL HYDROGELS FOR WOUND REGENERATION

M.P.Lutolf, A.B. Pratt, N. Tirelli and <u>J.A.Hubbell</u>

<u>Institute of Biomedical Engineering</u>, ETH and University of Zurich

**INTRODUCTION:** The extracellular matrix (ECM) of connective tissue plays an essential role in the regulation of cell behaviour and tissue formation, providing both biophysical and biochemical cues for the cells in contact. The remodelling and repair of tissues - involved in many physiologic and pathologic situations - is highly cell-controlled. Cells locally express or activate proteases that cleave the surrounding macromolecules thereby degrading the ECM.

The goal of this project was to design synthetic extracellular matrices that can be used as alternatives for naturally occurring matrices such as fibrin or collagen, which require difficult purification procedures and carry the risk of disease transmission. The poly(ethylene glycol)-(PEG) based hydrogels described herein contain a combination of biological signals, namely ligands for cell adhesion and migration and susceptibility to cell-secreted matrix metalloproteases (MMPs), which allow them to undergo cell-mediated remodelling.

MATERIALS AND METHODS: PEG's (Shearwater Polymers, USA; 4arm, Mw: 10, 15 and 20kD) were end-functionalised with vinylsulfone. Crosslinker peptides with different enzymatic activity (kcat/Km) were designed bearing a cysteine (for X-linking reaction with vinylsulfone under physiologic conditions) on both ends of a matrix metalloproteinase (MMP) substrate sequence [1], e.g. GCRD-GPQGIAGQ-DRCG. Hydrogels in contact with cells were also functionalised with pendant adhesion peptides (RGDSP). Cell-induced proteolytic degradability of the gels was analysed as a function of time by measuring the radial distance that human foreskin fibroblasts migrated through the networks from an embedded cell-fibrin cluster. Gels with different network architectures (Mw of PEG) as well as various adhesivity and enzymatic degradability were tested.

**RESULTS AND DISCUSSION:** Fibroblasts cultured inside adhesive and MMP-sensitive hydrogels migrated over large distances (Fig. 1). Cell migration did not occur when a) a peptide without enzymatic activity was incorporated, b) nonadhesive peptides (RDGSP) were used or c) in the presence of an MMP inhibitor (GM6001, Chemicon, USA). Moreover, the cell invasion speed responded to the protease substrate activity (Fig. 2), the adhesion site density or the network architecture.

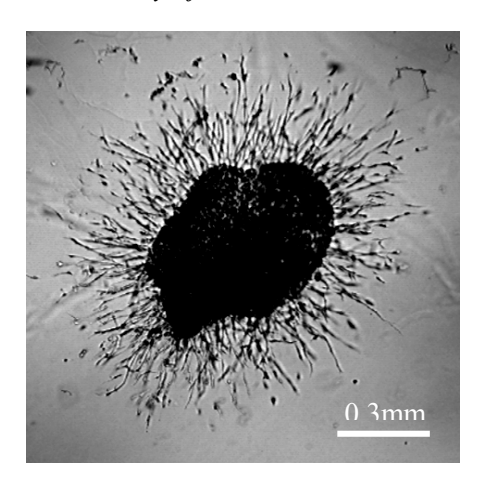


Figure 1. Within networks containing adhesion sites and MMP-sensitive peptides, fibroblasts were able to migrate over long distances.

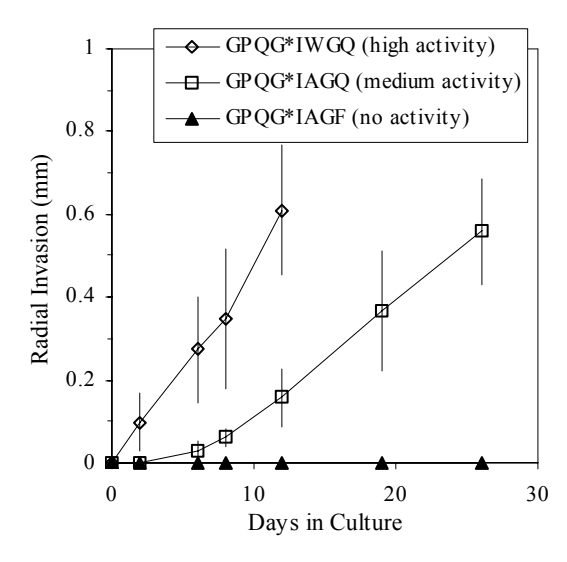


Figure 2. Cell invasion rate can be tailored by the activity (Km/kcat) of the incorporated MMP substrate.

**CONCLUSIONS:** The key characteristics of natural extracellular matrices can be rationally engineered into a synthetic material, allowing cells to migrate in response to the action of cell-secreted MMPs. Moreover, the migration speed can be tailored through several characteristics of the matrix. We believe that such hydrogels have a strong potential as provisional scaffolds to guide tissue reconstruction.

**REFERENCES:** [1] H. Nagase and G.B. Fields (1996), *Biopolymers (Peptide Science)*, **40**: 399-416.

#### 3-D CHARACTERIZATION OF FIBROBLAST CULTURES ON PET-**TEXTILES**

P.Thurner <sup>1,2</sup>, E.Karamuk <sup>1</sup>, B.Müller <sup>1</sup>

Dept. of Materials Science, Swiss Federal Institute of Technology, ETH-Zürich, Switzerland.

Federal Institute for Materials Testing and Research, Dübendorf, Switzerland

INTRODUCTION: Cell culture experiments are typically performed as in vitro studies based on 2-D seeding and characterization. Here, the procedures can be kept relatively simple. With respect to the in vivo situation, however, 2-D models are often inappropriate due to the 3-D character of living tissue in nature. Consequently, 3-D in vitro systems should better resemble the natural situation. For the 3-D in vitro studies suitable scaffolds have to be chosen and methods for 3-D characterization have to be adapted. Micro-tomography using X-rays (μCT) belongs to most promising techniques characterization. Using synchrotron radiation sources, the spatial resolution can be extended down to the sub-micrometer range and individual cells can be made visible. Since the samples consist mainly of light elements, the cells have to be labelled by the use of highly absorptive agents, well known from electron microscopy, to obtain enough contrast in the most frequently used absorption contrast modus. Contrary to electron microscopy, µCT does not need vacuum conditions making experiments in the hydrated state possible. The aim of the current study is the optimisation of µCT to uncover cell shape and cell distribution on porous scaffolds, which can be even opaque, in the hydrated environment.

METHODS: Tomography is a technique to nondestructively reconstruct a 3-D image of a solid state from a set of filtered 2-D projections. Using the parallel beams of a synchrotron radiation source, the sample is precisely rotated stepwise to 180°, and after each step a projection is recorded. Because the contrast mechanism is X-ray absorption, one gets a representation of the local absorption coefficients.<sup>1</sup> This means that the constituents have to differ in X-ray absorption to allow segmentation.

The samples, rat tendon fibroblasts seeded on texturized poly-ethylene-teraphtalate (PET) multifilament yarns (30 filaments with a diameter of 20 µm each) embedded in a hydrated matrix, were held in low absorbing glass or plastic containers. Since the fibroblasts show low X-ray absorption as the surrounding embedding and scaffold material it is inevitable to stain the cells with a higher absorbing contrast agent. For first experiments, OsO<sub>4</sub> has been used. The sample preparation procedure was identical to that used for scanning electron microscopy, just interrupted before dehydration: The rat tendon fibroblasts were fixated in 3% glutaraldehyde in phosphate buffered saline (PBS) overnight. After washing them once they were post-fixed with 0.1% and 0.01% OsO<sub>4</sub>, respectively, for 1 h. Subsequently, the samples were washed twice with PBS. At HASYLAB at DESY the samples were transferred into glass capillaries (diameter 0.7 mm, wall thickness about 10 µm) and PBS was added to keep the samples in a hydrated environment. The tomograms are generated from 720 projections obtained at the photon energy of 9 keV with a spatial resolution of 1.4 µm.

**RESULTS:** First, the porosity of the scaffold (textile) is extracted from tomograms of the PETtextiles without any cell. The advantage of µCT with respect to well-established techniques for porosity determination is the length scale accessible ranging from about 1 µm to 1 mm. In addition, one does not only obtain mean values but the whole 3-D micro-architecture necessary to study phenomena like cell migration and supply. Current limitation is the huge amount of data (Gigabytes) to be treated.

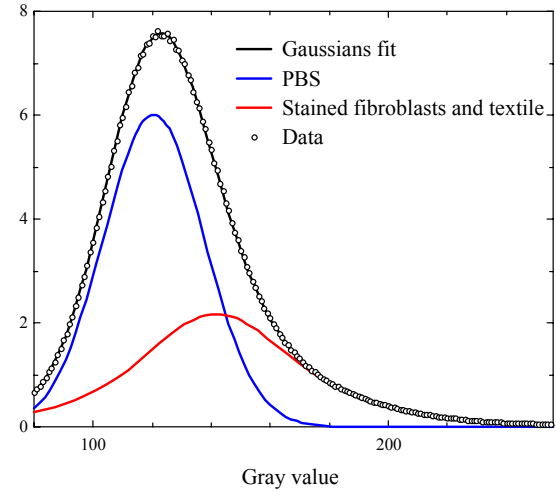
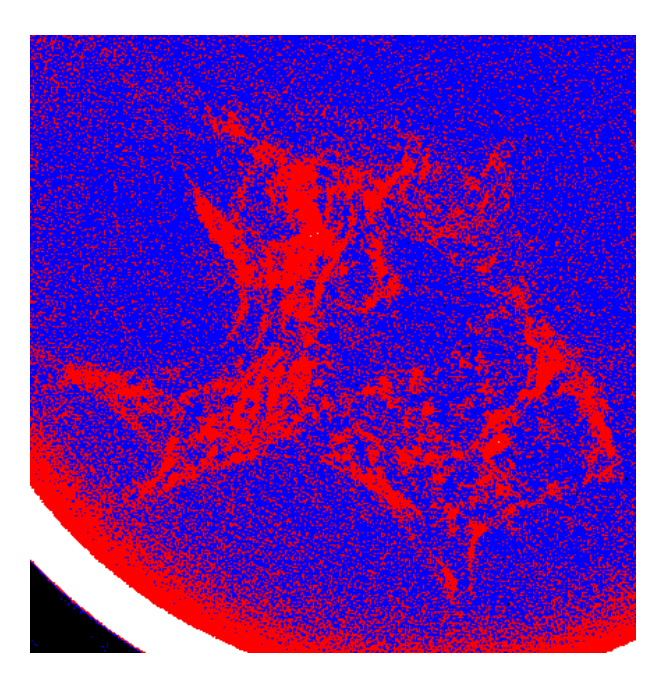
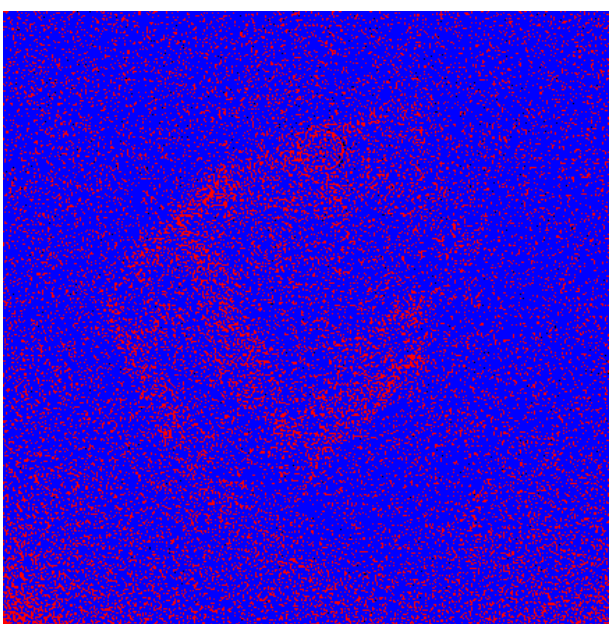


Fig. 1: Histogram for sample with high stain concentration; data, multiple Gaussians fit, gray level distributions (from fit) for PBS as well as for stained fibroblasts and the textile are shown. with samples the different concentrations were reconstructed with success, although bubble formation due to X-ray exposure was sometimes present.





*Top: Slice of the sample with high OsO*<sub>4</sub> concentration, segmented using two colours, blue (grey levels 70-131) and red (132-246). In the lower left corner, a part of the sample container is visible (white). Bottom: Slice of the sample with low OsO<sub>4</sub> concentration, segmented using two colours, blue (60-120) and red (121-246). The obtained tomograms reveal that the higher staining concentration results in sufficient contrast and gives rise to images with similarities to micrographs from electron microscopy. For the lower staining concentration, however, the image contrast was insufficient to segment the fibroblasts, since the grey values for the stained cells strongly overlap with those of the background. The two slices presented in fig. 2 were coloured according to the histogram of the

individual datasets. The threshold between red and

Fig2.: Image sizes: 631 μm x 644 μm

blue corresponds to the mean value of the two peak positions (cp. fig: 1).

DISCUSSION & CONCLUSIONS: µCT, a nondestructive technique is used in materials science to uncover the microstructure of composites avoiding surface preparation artefacts. The same holds for composites consisting of porous materials and biological matter. Only recently µCT has been applied to samples containing soft tissue cells. Their visualization was successful. Although many details as detected by electron microscopy are not uncovered, the shape of individual cells can be made visible. Therefore, it is possible to investigate the in-growth of cells into porous scaffolds in all 3 spatial directions. The cell behaviour can be adjusted by the choice of scaffold porosity and microstructure. Consequently,  $\mu CT$  is a valuable visualization technique to optimise scaffolds for the desired application. By the use of appropriate contrast agents and concentrations µCT may even be used for in vivo investigations. This requires the coordination of the composite materials, the photon energy and label concentration, not vet optimised for the present study. The availability of synchrotron radiation sources with high coherence enables us to take advantage of different contrast mechanisms.<sup>2</sup> For example diffraction enhanced imaging helps to determine internal and external interfaces, as we show by PET-textiles measured at ESRF in Grenoble. Here, changes of the refractive index are mapped. The adaptation of synchrotron-radiation-based µCT to biological samples on the cellular level opens up a new possibility to study cell-substrate interactions in 3-D even on opaque porous scaffolds.

**REFERENCES:** <sup>1</sup> U. Bonse F. Busch. (1996) X-ray computed microtomography (μCT) using synchrotron radiation, *Annu Rev Mater Sci* **22**:133-69, <sup>2</sup> A. Snigirev, I. Snigireva, (2000) On the possibilities of x-ray phase contrast microimaging by coherent high-energy synchrotron radiation *Rev Sci intrum* **66**:5486-92.

**ACKNOWLEDGEMENTS:** We are indebted to F. Beckmann from HASYLAB at DESY and T. Weitkamp from ESRF providing facilities for data acquisition and reconstruction. We acknowledge the financial support of the Swiss National Science Foundation (grant 2153-057127.99).

### STRUCTOPLATE: A NEWLY DEVELOPED 3D-MICROSTRUCTURED SURFACE IN MULTIWELL TISSUE CULTURE PLATES

B. Saad <sup>1,2,3</sup>, T. Callenbach <sup>4</sup>, K. Brander <sup>5</sup>, M. Welti<sup>2</sup>, G.K. Uhlschmid <sup>2</sup> and U.W. Suter <sup>1</sup>

<sup>1</sup>Dept. of Materials, Institute of Polymers, ETH, CH-8092 Zurich, <sup>2</sup>Research Division, Dept. of Surgery, University Hospital, CH-8091 Zurich, <sup>3</sup>Arab American University Jenin-PA, <sup>4</sup>H. Weidmann AG, CH-8640 Rapperswil, <sup>5</sup>Integra Biosciences Holding AG CH-6274 Eschenbach

**INTRODUCTION:** The currently available conventional tissue culture devices are not suitable to form tissue-like aggregates, that require high cell density. Therefore, the engineering of a new generation of substrates that enable cultured cells to grow at higher cell density and to maintain more *in vivo*-like cell-to-cell interactions is very important in order to obtain more reliable results *in vitro*. To evaluate the cell-compatibility and the usefulness of Structoplate as new substrate for routine cell cultures, the cell behaviour on 6 well and 24 well Structoplate was investigated.

**METHODS:** Primary isolated rat osteoblasts and rat chondrocytes, the macrophage cell line J774, the osteoblast cell line MC3T3-E1 and the fibroblast cell line 3T3 were used to examine the cell-compatibility of the newly developed Multiwell Structoplate (Integra Biosciences Holding AG, Acherfang, 6274 Eschenbach). Cells were added to the Structoplate (6 well and 24 well plates) at a density of 5 x  $10^4$ ,  $10 \times 10^4$ ,  $1.5 \times 10^5$ , 2  $^{1}$  x  $10^{5}$  and 2.5 x  $10^{5}$  cells per well in 2 ml (for 24) well plates) or 5 ml (for 6 well plates) of their respective culture medium and allowed to attach at 37°C. For the measurement of cell attachment, cells were washed twice with PBS to remove nonadherent cells and the number of attached and viable cells was determined 4h after cell seeding with the MTT assay. To examine cell growth, cell density was determined 1, 2, 4, and 6 d after cell seeding using the MTT test and by counting the cell number. As a control, cells were plated onto 6well tissue-culture plates (Costar) or 24 well plates (Nunc).

The content of collagen type I and Type II osteocalcin, and chondroitin sulphate was determined in ELISA tests. The alkaline phosphatase activity (ALP) was measured spectroscopically at 405 nm with p-nitrophenyl as substrate.

**RESULTS:** Enhanced cell morphology: The visibility under microscope was identical between Structoplate and conventional plates. The topography of the microstructures permits

unlimited observation of the adhered cells. which showed that the unique surface topography affected the cell spreading: cells seeded on Structoplate exhibited more rounded cell morphology than cells on conventional plates. Apart from macrophages, both primary isolated cells and cell lines built confluent cell multilayers.

#### 6-fold higher cell densities on 24 well plates:

The cell densities of fibroblast cell line 3T3 and rat osteoblasts was measured 48 hours after seeding on 24 well Structoplate and conventional 24 well plates. Cell aggregation and cell detachment were found at higher cell densities only on conventional 24 well plates but not on Structoplate. Also, at high cell densities the number of attached cells was up to 6 fold higher on Structoplate compared to control plates.

Phenotype and markers: In addition to the strong attachment and high growth rate, osteoblasts preserve their specific phenotype. There were no significant differences in ALP activity, collagen type I, and osteocalcin produced by primary isolated rat osteoblasts.

**DISCUSSION & CONCLUSIONS:** The newly developed 3D-microstructured Structoplate provide the cultured cells with *in-vivo* like structures and enhanced surface area which results in 1.7 – 6 fold higher cell densities. The topography of the microstructures supports homogeneous spreading of the cells as well as the formation of cell multi-layers which results in improved phenotypes and stronger attachment to the growth surface. Structoplate demonstrated its ability to enhance cell cultures in various ways and may be a valuable alternative for biochemical coating of cell culture devices.

### PLASMA TREATMENT OF SOLID SURFACES FOR BIOMEDICAL APPLICATIONS

H.Biederman<sup>1,2,\*, F</sup>.Carney<sup>2</sup>, P.Chabrecek<sup>1</sup>, J.Vogt<sup>1</sup>, R.Houriet<sup>3</sup>, H.Hofmann<sup>3</sup>, Y.Chevolot<sup>3</sup>, N. Xanthopoulos<sup>3</sup>, H.J.Mathieu<sup>3</sup>

<sup>1</sup>Ciba Vision AG (Novartis), Advanced Research Unit, Basel, Switzerland <sup>2</sup>Ciba Vision Corp. (Novartis), Business Technology Innovation, Atlanta, USA. <sup>3</sup> Materials Science & Engineering Dept. Swiss Federal Institute of Technology, EPF- Lausanne, CH

**INTRODUCTION:** Functional surfaces are very important for biomaterial technology. Among the various methods used for surface modification of biomedical devices plasma process shows significant advantages [1, 2]. In particular, some reactive surfaces obtained by glow discharge down-stream plasma polymerisation of functional vinyl monomers show tailorable functionalities [3-6]. The aim of this study was to prepare specifically functionalised surfaces by means of plasma polymerisation of 4,4-dimethyl-2-vinyl-oxazolinone or isocyanatoethyl methacrylate and to demonstrate superior reactivity of these surfaces.

**METHODS:** Substrates included silicone-hydrogel contact lenses (Lotrafilcon A, CIBA Vision) [7], silicone wafers, polished glass, soft silicone elastomer sheets (GoodFellow). In addition highly porous tricalcium phosphate (b-TCP) coated PES membranes, prepared at the Powder Technology Laboratory of EPFL in Lausanne using a Lina-Spark<sup>TM</sup> atomizer [8, 9], were used for surface fictionalisation.

Plasma polymerisation process was carried out in a glass reactor custom built in collaboration with ACR GmbH, Germany (power supply). Rf power (27.12 MHz) was capacitively coupled to the plasma using a ring electrode from outside the glass wall and earthed bottom metal base plate flange. The electrode arrangement and power supply allowed us to work in the both CW and pulsed modes. In this reactor the samples were placed outside of the plasma zone at variable distances in down stream direction. We focused on the variation of selected plasma parameters, mainly on the distance between the plasma zone (electrode gap) and the substrate position, on the input power and variable duty cycles. Argon was used as plasma gas and as carrier gas for the "afterglow-feed" of the monomers used.

The structure of the plasma coatings was examined using XPS on silicone wafers and FTIR-ATR analysis on all kind of substrates, mainly on highly porous b-TCP coated PES membranes and silicone elastomer. The coatings' morphology and thickness were measured by AFM on polished

glass pieces and by quartz microbalance thickness monitor.

The density of the functional groups on the substrate surfaces was determined as follows: 5biotinpentylamine was quantitatively coupled on VAL functionalised Lotrafilcon A contact lenses and the amount of biotin present on the surface was detected using the avidin-HABA reagent (ImmunoPure, Pierce). When 2-(4'hydroxyazobenzene) benzoic acid (HABA) is added in excess of avidin, an absorption band at 500 nm is observed and a change in colour occurred from yellow to red. This absorption decrease proportionately when biotin is added since biotin displaces the HABA dye due to its higher affinity for avidin. Several molecules of biotin can react with a plasma functionalised surface which in turn can each bind a molecule of avidin. This greatly increases the sensitivity of many assay procedures. Since the biotin is a relatively small molecule, the avidin-biotin interaction is the strongest known noncovalent, biological interaction (Ka=1015 M-1) between protein and ligand. The bond formation between biotin and avidin is very rapid and, once formed, is unaffected by wide extremes of pH, temperature, organic solvents and other denaturing agents [10]. A complementary method, implementing ESR, for surface functionality quantification was utilized after derivatising the functional groups with 4amino-2,2,6,6-tetramethylpiperidinyl-

-oxy free radical (NH2-TEMPO) in acetonitrile. For ESR experiments only contact lenses and soft silicon elastomer were used, the amount of detected functional groups was slightly higher in case of silicon elastomer because of its higher micro roughness in comparison to the contact lens surface.

Analogous to the experiments with NH2-TEMPO, the coatings with various bio/polymers were performed in ultra pure water, again on contact lenses and soft silicon elastomers.

**RESULTS & DISCUSSION:** The plasma modified surfaces were first characterized by FTIR-ATR. The spectra showed that the structure of the deposited polymer chains is, to a large

extent, identical to the structure of the polymer obtained through a non-plasma radical solution polymerisation of the respective functional vinyl monomers. Absorption bands of the azlactone ring at  $\sim 1820$  cm-1 (C=O) and at  $\sim 1673$  cm-1 (C=N) were still present. The absorption band of the C=C the monomer double bond in (vinylazlactone) at ~1599 cm-1 disappeared after the plasma induced polymerisation similar as in case of the conventional radical polymerisation. Using isocyanatoethyl methacrylate (IEM) as a monomer gas we observed a very intensive absorption bands belonging to isocyanato group (NCO) at ~2276 cm-1 and carbonyl from ester (C=O) at  $\sim$ 1731 cm-1 (Fig. 1).

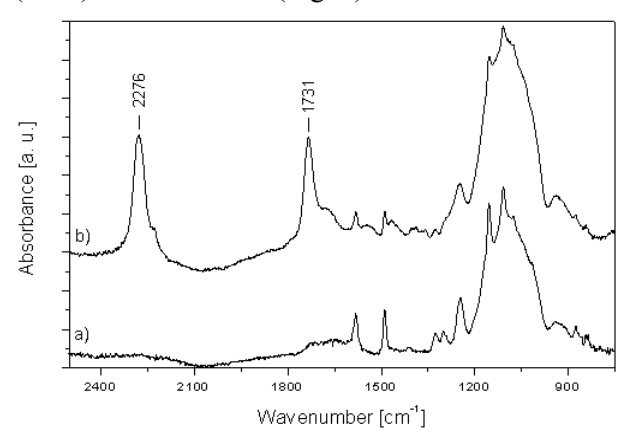


Figure 1. FTIR-ATR of IEM plasma polymer coated b-TCP a) in plasma zone, CW 40 W, b) 20 cm below plasma zone, CW 40W.

In comparison to the IEM plasma polymer coated in the down-stream position 20 cm below the plasma zone, IEM plasma polymer prepared in the plasma zone contains no functional groups that would be available for further chemical reactions. XPS analysis showed full surface coverage at all distances from 10 to 30 cm downwards from the plasma zone (Fig. 2). After spin-labelling of the groups with NH2-TEMPO, spectroscopy indicated a correlation between the substrates "downstream" distance and the density of the functional groups achieved. This was confirmed through the avidin-biotin coupling procedure. where 5-biotinpentylamine covalently linked to the lens surface and then detected using the modified avidin-HABA ImmunoPure test (Fig. 3). ESR spectroscopy showed an increase of the number of reactive groups from the lower edge of the plasma zone towards distance of 20 cm to 30 cm. Beyond 30 cm the amount of functional groups started slowly to decrease. The HABA test confirmed this trend a platform from 10 cm up to 30 cm, then a decrease of functionality was observed.

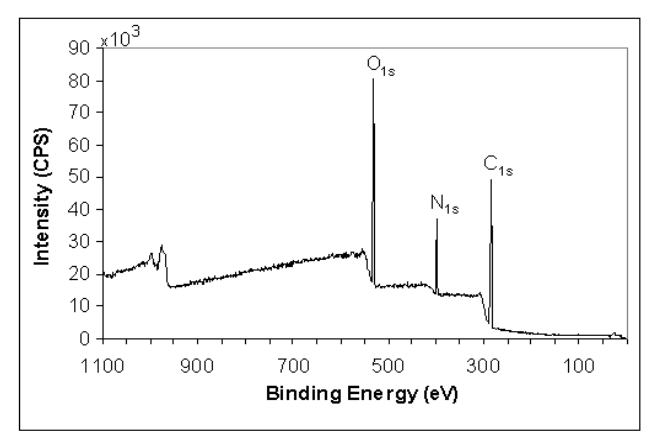


Fig.2Survey XPS spectrum of plasma polymerised IEM on Si wafer, Distance = 30 cm

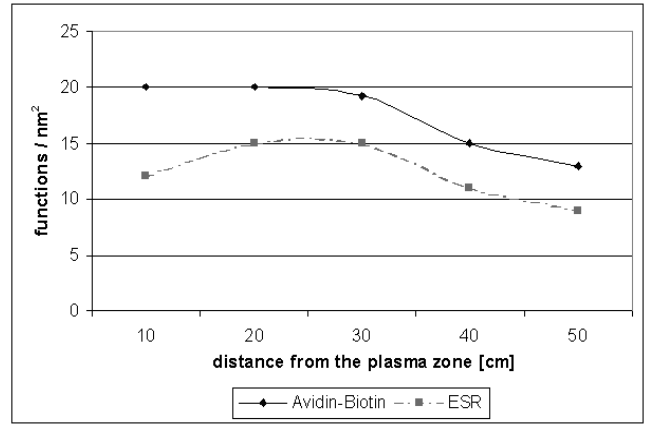


Fig.3Results from avidin-biotin assay compared to the ESR analysis of VAL plasma coated contact lens at various distances (macroscopic area)

High resolution XPS spectra and IR spectra showed that when the sample was prepared directly in the plasma zone a considerable part of the original monomer molecule was destroyed by energetic particles such as positive ions (mostly Ar+) that directly had impact on the surface of the growing layer (Fig. 1a). At higher distances the photons still could reach the film, however energetic particles not. This could explain the disordered structure of the film grown in the plasma zone. ESR spectroscopy confirmed that the amount of accessible reactive groups on the surface prepared in the plasma zone is quite low. observations indicated that fragmentation of organic monomer species, usually occurring under conventional plasma conditions, was largely avoided at higher distances. Radical polymerisation of 4,4-dimethyl-2-vinyloxazolinone (often called vinylazlactone, VAL) or of isocyanatoethyl methacrylate (IEM) has been identified as the predominant process under the conditions used.

The optimal substrate distance downstream from the middle of the plasma zone for VAL and IEM plasma induced polymerisation was found to be between 20 and 30 cm. At this distance we did not observe any delamination of the plasma generated polymer. At greater distances 100% coverage was not achieved as proven by XPS analysis. On one hand shortening the distance between the plasma zone and the position of samples and/or increase of plasma power increased the likelihood of covalent binding of the deposited polymeric chains. On the other hand, as indicated from FTIR-ATR spectra, decrease in sample - plasma distance or a further increase of the plasma power caused some structural changes of the deposited VAL or IEM polymer layers.

Various binding experiments were performed on contact lenses or silicon elastomer, functionalised either with VAL or IEM, which led to highly hydrophilic secondary coatings. Thus, secondary coatings made with 10% aqueous solutions of poly-(allylamine- co -N-allyl-gluconamide 1:1) (Mw ~ 150000) showed excellent surface wettability; the dynamic water/air contact angles were 0° [11]. The coating thickness significantly increased over 300 nm, as determined by AFM. Sterilization by autoclaving did not cause any detrimental effects. Other polymers which were successfully coated on lens surfaces were Jeffamine M-2070, polyethyleneimine, albumin (human) and elastin (5% aqueous solutions). The coating with elastin revealed a good water film break-up time, and the contact angles were 28° adv. / 18° rec. We did not observe any difference between the use of contact lenses and soft silicone elastomer as a substrate for preparation of secondary coatings.

**CONCLUSIONS:** Downstream plasma polymerisation vinylazlactone and of isocyanatoethyl methacrylate proofed to give a good control of substrate surface properties. The new highly functional coatings showed firm adherence, appropriate stability as well as a high potential for the covalent attachment of a large number of polymers, biopolymers and bioactive principles. The results obtained confirm that the down-stream plasma technique provides a valuable extension of conventional methods for surface fictionalisation.

#### **REFERENCES:**

- [1]H.Yasuda Plasma Polymerisation, Academic Press, Orlando, FL (1985).
- [2] H. Biederman, Y. Osada Plasma Polymerisation Processes, Elsevier, Amsterdam, 1992
- [3] P. Chabrecek, D. Lohmann Surface Modification of Extended Wear Contact Lenses by Plasma-Induced Polymerisation of Vinyl Monomers, Fundamentals and Applied Aspects of

- Chemically Modified Surfaces, 223-234, The Royal Society of Chemistry (1999).
- [4] P. Chabrecek, D. Lohmann Reactive Coatings, U.S. Pat. WO9828026, CIBA Vision Corp. (1998).
- [5] L. M. Han, R. B. Timmons Pulsed-Plasma Polymerisation of 1-Vinyl-2-Pyrrolidone: Synthesis of a Linear Polymer, J. Appl. Pol. Sci., 36, 3121-3129 (1998).
- [6] Ch. L. Rinsch, X. Chen, V. Panchalingam, R. C. Eberhart, J.-H. Wang, R.B. Timmons Pulsed Radio Frequency Plasma Polymerisation of Allyl Alcohol: Controlled Deposition of Surface Hydroxyl Groups, Langmuir, 12, 2995-3002 (1996).
- [7] P.C. Nicolson, R.C. Baron, P. Chabrecek, et al. Extended wear ophthalmic lens, U.S. Pat. 5,760,100 (1998).
- [8] R. Houriet, R. Vacassy, H. Hofmann, W. Vogel Thin film growth using ablation of ceramics with a Lina-Spark<sup>TM</sup> Atomizer, Materials Research Society Symposium Proceedings, MRS, 526, 117-122 (1998).
- [9] R. Houriet, R. Vacassy, H. Hofmann Synthesis of powders and films using a new laser ablation technique, NanoStructured Materials, 11, 1155-1163 (1999).
- [10]N.M. Green Avidin, In Adv. In Protein Chemistry, 29, 85-133 (1975)
- [11] M. Miyama, Y. Yang, T. Yasuda, T. Okuno, H. Yasuda Static and Dynamic Contact Angles of Water on Polymeric Surfaces, Langmuir, 13, 5494-5503 (1997).

ACKNOWLEDGEMENTS: The authors are grateful to Amina Wirth and Uwe Pieles of Technical University Muttenz for AFM measurements and multiple scientific communication.

### **EX-VIVO** TRABECULAR BONE PERCOLATION SYSTEM: DEVELOPMENT FOR EVALUATION OF IMPLANT SURFACES

C.M.Davies<sup>1</sup>, D.B.Jones<sup>2</sup>, M.Alini<sup>1</sup>, C.Archer<sup>3</sup>, R.G.Richards<sup>1</sup>

1 AO Research Institute, Davos, CH. <sup>2</sup> Experimental Orthopaedics & Biomechanics, Phillips University Marburg Germany. <sup>3</sup> Cardiff School of Biosciences, Cardiff University, Wales (GB)

**INTRODUCTION:** Numerous studies with implant materials are carried out in vivo using sheep models. To reduce the amount of animals used for biocompatibility studies of implant surfaces we are developing the use of a novel ex vivo culturing/bioreactor system for the sheep model. The system "Zetos" was devised by David Jones (Marburg, Germany) and Everett Smith (Madison, USA). Zetos is a percolated loading system that maintains trabecular bone cores viable for up to 40 days<sup>1</sup>. It is a closed cross flow perfusion system that allows vertical loading of the longitudinal axis, to mimic the in vivo situation. It consists of a number of individually crafted bone chambers and a computer controlled loading device. The first studies are to confirm that bone formation and resorption occurs in the system with sheep bone. At the same time the loading device will be fully calibrated so that the displacement measured on the loading device is related to the displacement that the bone receives. The system has great potential to evaluate cancellous bone implant surface interactions.

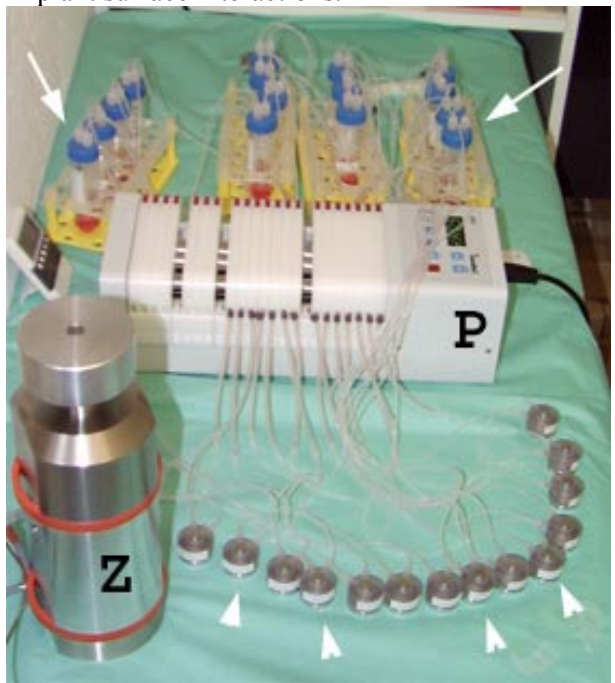


Fig. 1: Zetos System (Z) in  $37^{\circ}$ C room. Bone Chambers (arrowheads), Microprocessor controlled low pulsation dispensing pump (P), Media filled test tubes (arrows)

**METHODS:** Femurs from a Swiss Mountain sheep are excised and cut at the epicondyle into 7 mm thick sections with a band saw. Cancellous

bone cores, 10 mm in diameter, are removed and then cut parallel to the height of 5 mm with an annular saw. The bone is constantly irrigated with sterile saline to limit damage caused by heat and to stop the bone from drying out. Implants are inserted transversely or longitudinally through the bone cores, which are then washed in medium and antibiotics for 30 minutes before being inserted into the chambers. assembled system is allowed to settle for 36 hours at 37 °C (Fig.1). Bone cores are deformed daily with compressions of 20 µm and 5 µm in a rectangular waveform at 1 Hz for 300 cycles. This is achieved by the expansion and contraction of a piezo stack under high voltage, placing a force on the piston of the chambers. This force, in turn causes a deformation (compression) of the bone cores that mimic in vivo loading patterns. The expansion/contraction of the piezo is controlled by a sensor that acts in a feedback loop to control the amount of force applied to each chamber, which in turn controls the amount of deformation the bone cores receives.

has been demonstrated previously to maintain bovine bone cells (osteoblasts, osteoclasts, osteocytes, bone marrow) viable for 40 days and that bone growth and resorption occurs Jones *et al* 2001<sup>2</sup>. Our preliminary results show viability of sheep bone cells, the samples currently undergoing histological analysis. The system will be used to study the effect of implant surfaces on cancellous bone ingrowth / ongrowth and resorption.

**REFERENCES:** <sup>1</sup> E. L. Smith, F. Martens, K. Koller, W. Clark, D. B. Jones. The Effects of 20 Days of Mechanical Loading Plus PTH on The E-Modulus of Cow Trabecular Bone *Abstracts 22nd annual meeting ASMBR 2000 SAP* 07<sup>2</sup> D.B.Jones, U.Boudriot, M.Kratz, F. Martens, K. Koller, E. L. Smith (2001) A Trabecular Bone and Marrow Bioreactor. *European Cells and Materials* Vol. 1. Suppl. 2, 2001 (page 53)

**ACKNOWLEDGEMENTS:** The research is funded by the 3R Foundation grant # 78/01. Marita Kratz, Eckhard Brokemann, and Torsten Pohl, Philips University, Marburg, for setting up the system in Davos. Iris Keller and Patrick Schlegel, AO, Davos, for help with bone preparation.

### FIBROBLAST MORPHOLOGY AND ADHESION ON CALCIUM PHOSPHATE SURFACES.

L. C. Baxter<sup>1</sup>, V. M. Frauchiger<sup>2</sup>, M. Textor<sup>2</sup>, I. ap Gwynn<sup>1</sup>, R.G.Richards<sup>1</sup>

AO Research Institute, Davos, Switzerland. <sup>2</sup>Laboratory for Surface Science and Technology, Swiss Federal Institute of Technology Zürich, Switzerland.

**INTRODUCTION:** Studying the morphology and adhesion of cells on different metal surface coatings can give an indication as to the biocompatibility of the coating and its suitability for possible further applications on orthopaedic implants. The adhesion of either soft or hard tissue cells to implant materials is essential to the success or failure of an implant and is also important for the prevention of infection. Implant surface topography and chemistry are important factors in the adhesion of cells to surfaces.

The adhesion and morphology of fibroblast cells was studied on titanium discs coated with either: calcium phosphate, deposited using anodic plasma-chemical treatment (APC) at current densities of 200mA and 290mA; phosphoric acid (H<sub>3</sub>PO<sub>4</sub>) at temperatures of 25°C and 75°C; hydroxyapatite; anodisation at 57V. Thermanox culture plastic discs were also investigated.

**METHODS:** Balbc/3T3 fibroblasts were used throughout this study and were cultured in DMEM containing 10% foetal calf serum at 37°C. Approximately 20,000 cells were seeded onto each sample 24 hours before fixation and immunolabelling. All the fixation and labelling protocols were conducted at room temperature (22°C).

The cells used for morphological studies were fixed in 2.5% glutaraldehyde and were post-fixed in 0.5% osmium tetroxide. The cells were dehydrated through an acetone series, critical point dried, coated in chromium (10nm) and imaged with a Hitachi S-4700 Field Emission Scanning Electron Microscope.

Immunolabelling was used to identify adhesion areas. Cells were permeabilised with 0.1% Triton X-100 (1 minute) and fixed with 4% paraformaldehyde (5 minutes). Non-specific binding sites were blocked (30 minutes) and the vinculin (an integral focal adhesion protein) immunolabelled using an indirect labelling method with the secondary antibody attached to 5nm gold labels (primary antibody 1 hour and secondary antibody 2 hours). The cells were fixed with 1% glutaraldehyde (5 minutes). Gold enhancement

was performed using a kit from Nanoprobes for 7 minutes. The cells were post-fixed with 1% osmium tetroxide (1 hour), dehydrated through an acetone series and critical point dried before coating and imaging. After imaging samples were embedded in LR White resin. The resin was polymerised and separated from the discs by rapid cooling, on a copper block immersed in liquid nitrogen, so that the cells remained in the resin. The undersurface of the cells was then directly imaged within the resin using backscattered electron imaging.

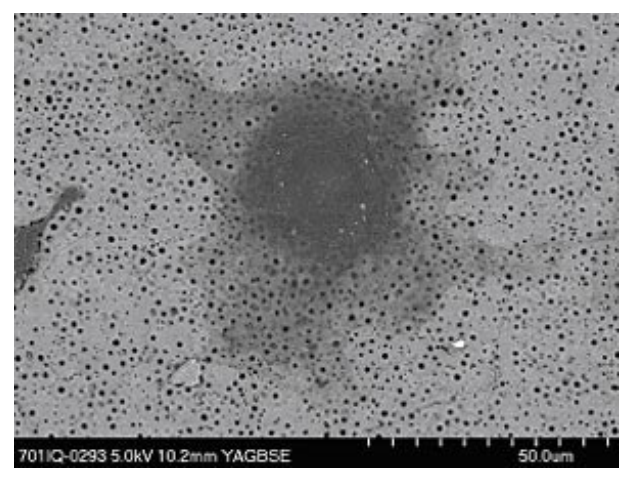


Fig 1. A well spread out fibroblast on the calcium phosphate (APC) surface (anodic plasma-chemical treatment at 75°C).

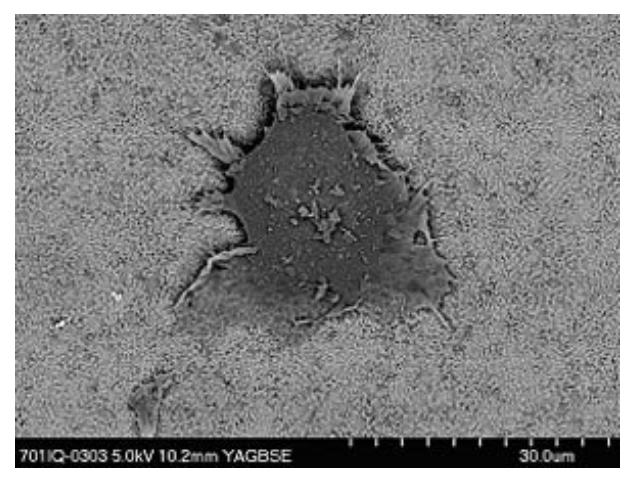


Fig 2. Fibroblast attached to the phosphoric acid surface, which is not spread and is slightly raised compared to cells on the APC surface.

**RESULTS:** Studies of the cells on the different surfaces revealed variations in the morphology of the cells. Cells on the anodised titanium, Thermanox plastic and the calcium phosphate (APC) surfaces were very spread out, especially on the calcium phosphate (APC) surfaces On these APC surfaces the cells were extremely flat and extremely spread with few features on the surface of the cells. On the APC surface the majority of the cells tended to have very few or no filopodia.

The cells on the hydroxyapatite and the phosphoric acid surfaces were much less spread with numerous filopodia and many folds and blebs on their surface. They were closer to the expected size of fibroblasts but did not look as if they were comfortable i.e. their ventral surface was raised from the surface.

There were no observable differences between the two calcium phosphate (APC) surfaces. The cells on the phosphoric acid surfaces also did not appear to be noticeably different from each other.

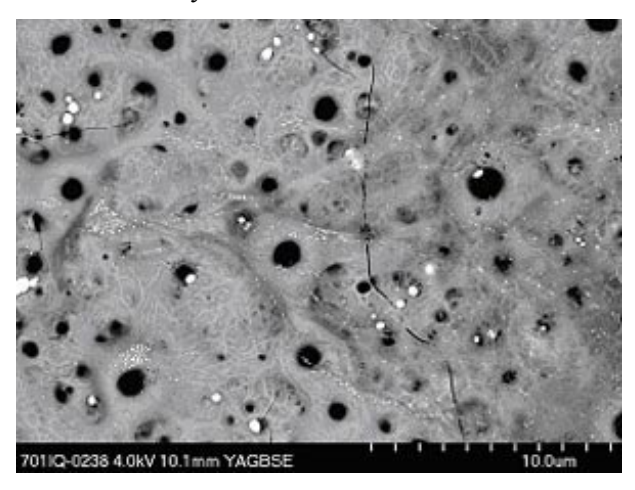


Fig 3. The periphery of an immunolabelled fibroblast on the calcium phosphate (APC) surface showing the gold label attached to the adhesion sites.

Cell adhesion sites were seen on all the surfaces at the cell periphery using immunolabelling. The adhesion sites for cells on the calcium phosphate (APC) surface appeared to be situated on and around the rough areas on the "volcanic like" structures. There were no particular areas of preference that could be seen for the other surfaces. Qualitatively "by eye" there were more adhesion sites on the APC surface than the other test surfaces (not including the Thermanox or anodised titanium).

**DISCUSSION & CONCLUSIONS:** The morphology and the adhesion of the cells indicate that the fibroblasts prefer the calcium phosphate (APC) surface to the other test surfaces

(hydroxapertite and phosphoric acid surfaces) and show similar morphologies to the cells on the Thermanox plastic and the anodised titanium discs. However, the cells used for this study are fibroblastic, soft tissue cells, which are known to spread more on smoother surfaces<sup>1</sup>. For osteoblast proliferation and differentiation in an *in vivo* situation a three-dimensional matrix structure is essential<sup>2, 3</sup>. Therefore an *in vitro* osteoblast adhesion study should also be undertaken on these surfaces. *In vivo* studies are currently being undertaken to assess the adhesion and osteointegration of all the surfaces when applied to screws for orthopaedic use.

The cells do adhere to all the surfaces and show adhesion patterns on and around the periphery of the cells. The adhesion sites for the calcium phosphate (APC) surface appear to be located on the rougher surface texture indicating that the actual adhesion of the cells may be related to the micro-topography<sup>4</sup>. Quantitative analyses of the adhesion sites are currently being conducted.

**REFERENCES:** 1. Könönen, M. et al (1992). J. Biomed. Mat. Res. **26**: 1325-1341. 2. Bellows, c., G. et al (1986). Calcif. Tiss. Int. **38**: 143-154. 3. Casser-Bette, M. et al (1990). Calcif. Tiss. Int. **46**: 46-56. 4. Richards, R., G. et al (1997). Cells and Materials. **7** (1): 15-30

**ACKNOWLEDGEMENTS:** We would like to acknowledge Mathys Foundation and Stratec Medical KTI/Medtech 4729.1 for the implant materials and funding.

## CELL ADHESION VARIATION DURING THE CELL CYCLE MEASURED

USING IMMUNOLABELLING AND AUTORADIOGRAPHY TECHNIQUES

D.O.Meredith, <sup>1</sup>, G.Rh Owen, <sup>1</sup>, <u>LapGwynn</u>, <sup>2</sup>, & <u>R.G.Richards</u>

1 AO Research Institute, Davos, Switzerland <sup>2</sup> Institute of Biological Sciences, The University of Wales, Aberystwyth, Wales, GB.

**INTRODUCTION:** In the case of orthopaedic implants, one indicator of implant material compatibility is the adherence of soft tissue to the material in question. An in vitro investigation. initiated previously, focused on cell adhesion as a determination of 'implant surface-soft tissue' compatibility (Richards et al, 1997). Adherent cells (in this instance - fibroblasts) attach to substrates using unique sites known as focal adhesions. The aim of deriving a material compatibility status from quantifying the amount of focal adhesions expressed by a cell could not be met. This was thought to be due to practical shortcomings of the identification method used. Osmium tetroxide was used to stain the focal

adhesions. It primarily stains proteins; focal adhesions become distinct due to their high protein content. The staining produced inconsistent shading, thus distinguishing regions of interest using similar image analysis threshold levels could not be performed for each sample. A more specific method of immunolabelling a constituent protein of the focal adhesion was introduced. The protein chosen for labelling was vinculin, an integral component protein of the focal adhesion. The vinculin, as an antigen, is known to be highly resistant to both permeablisation and fixation methods utilised in immunolabelling. For electron microscopy purposes a gold label provides an easily identifiable marker, attached indirectly to the vinculin antigen during the labelling procedure. For image analysis reproducibility, the gold has a distinct greylevel making it easily identifiable at the 'thresholding' stage.

In the study by Richards et al (1997) cell adhesion patterns varied considerably on the same substrate, making the quantification of the cells' adhesion area unreliable. Observations have been made connecting adhesion variation to cell morphology and to cell cycle position. Hunter et al (1995) found cells with the greatest number and area of focal adhesions were well spread and flattened whilst those with the least number of focal adhesions were more rounded and less spread. Cross & ap Gwynn (1987) showed that for cellcell adhesion, cells within the S-phase of the cellcycle were most adhesive. Associated to what is known about the cells' morphology (grown on a substrate) during the cell cycle, it can be proposed that the cells' adhesion area will change radically during the cycle - primarily a marked increase in adhesion area density of cells in S-phase.

The goal of this study was to continue the development of the in vitro cell adhesion quantification test to remove variability from staining methods and the influence of the cell cycle. In addition, S and non S-phase cell adhesion was investigated using the developed immunogold labelling methods.

MATERIALS & METHODS: Swiss Balb c/3t3 fibroblasts were cultured Thermanox on (Polyethylene tetrapthalate) discs in DMEM media supplemented with 10% foetal calf serum at 37°C for 2 days. S-phase cells were labelled by a pulse of <sup>3</sup>H thymidine (2nCi/ml) in the culture medium for 30min. Cells were cultured for a further 2 hours in normal media before being processed for immunogold labelling of vinculin. For scanning electron microscope (SEM) visualisation of the adhesion sites on the whole cell, the gold label was enlarged with gold enhancement. Postfixation and staining was performed with osmium tetroxide. Samples were dehydrated through a graded ethanol and critically point dried. autoradiography (Owen et al. 2000) the discs were coated with 4nm of carbon by evaporation, and then covered with a thin layer of photographic emulsion in a dark room. They were left in a light tight box at 4°C for 7 days before developing the emulsion. Samples were embedded in LR White resin and the substrate was removed. The of undersides cells were imaged using backscattered electron (BSE) imaging. A general view of the cells at a high accelerating voltage (kV) visually differentiated S phase from non Sphase cells (the S-phase cells had distinctly labelled nucleuses). A lower kV was used to visualise the immunolabelled focal adhesions of the identified cells.

**RESULTS & DISCUSSION:** The focal adhesion sites were clearly marked with the gold label and the higher density of gold distinguishes it from any other element or stain (e.g. osmium) present within the cell (see *Figure 1*). An increased precision of the quantification is attained as the probe only labels one constituent of the focal adhesion, unlike the osmium stain, which marked all the proteins within the focal adhesion. The labelling revealed that vinculin is also found in locations other than the focal adhesion, such as near the nucleus deeper within the cell body. At high kV the cells embedded in resin showed labelling throughout (see *Figure 2 (a)*), while the low kV of the same sample revealed labelling from only the area where the cell was in contact with the substrate (see *Figure 3 (b)*).

Image analysis results were calculated to assess cell adhesion density. The value was a percentage calculation of the adhesion area quantified in relation to the actual cell/substrate contact area. The results showed that the S-phase cells had significantly less adhesion density than non S-phase cells  $(1.3 \pm 0.1 \text{ vs. } 2.3 \pm 0.2, \text{ mean} \pm \text{S.E}, p=0.002)$ . It was also observed that the adhesion density varied significantly less for S-phase than non S-phase cells.

For *in vitro* compatibility tests comparing cellular adhesion on varying surfaces and materials, it should be considered to only quantify cells identified to be in the S-phase, due to the narrower distribution of results. Currently, we are investigating various biomaterials using this immunolabelling method.

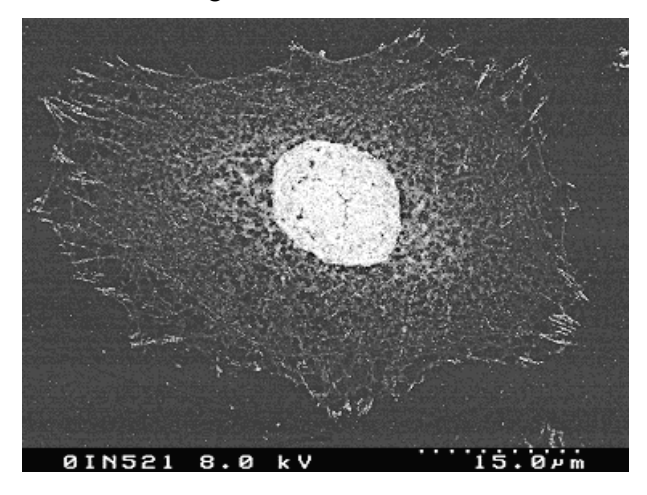
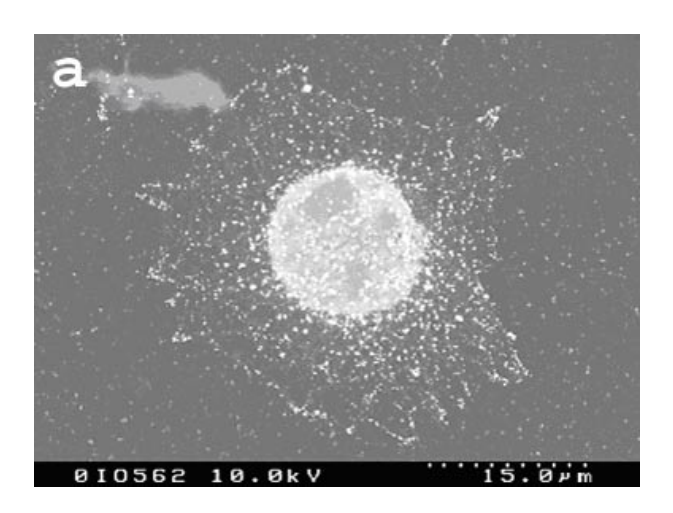


Figure 1. Adhesion sites of a fibroblast visualised by immunogold labelling of the vinculin. In this spread cell the label is mainly observed at the periphery.



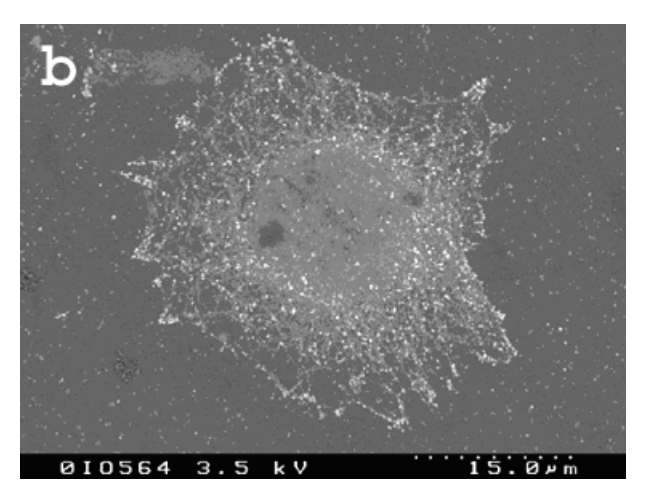


Figure 2(a) A fibroblast, immunolabelled with gold markers at the adhesion sites, can be identified as being in the S-phase by the silver deposit situated directly above the nucleus. The cell was imaged at high kV, so both the immunolabel and autoradiography label are visible. (b) The same cell imaged at a lower kV, in this case only the gold label is visible on the ventral surface of the cell.

#### **REFERENCES:**

Cross & ap Gwynn (1987) Cytobios 50, 41-62.

Hunter et al (1995) Biomaterials. 16, 287-295.

Richards et al (1997). Cells and Materials 7,15-30.

Owen *et al* (2000) European Orthopaedic Research Society, 10,135.

### FRETTING CORROSION OF IMPLANTS: AN ELECTROCHEMICAL APPROACH

S.Barril, S.Mischler, D.Landolt

<u>Laboratory of Metallurgical Chemistry</u>, Materials Department,

Swiss Federal Institute of Technology of Lausanne, EPF-Lausanne, Switzerland.

**INTRODUCTION:** Fretting corrosion of implants arises from micro motions occurring at the bone/implant interface. It is known to cause degradation of femoral stems of metallic implants leading to the release of wear particles and oxidized products into the body. Depending on their amount and size, wear fragments can lead to inflammation of the surrounding tissue and to loosening of the implant. The extent of fretting corrosion depends on many factors and synergistic effects between electrochemical mechanical and degradation mechanisms (called tribocorrosion) are of crucial importance [1].

The main mechanical factors are the contact pressure, slip amplitude at the interface and the frequency of movement, the latter depending on the age and activity of the patient. Osteoporosis affects the mechanical properties of bone and thus influences the stiffness of the contact. In addition, chemical parameters are critical. Indeed, the presence of a passive oxide film at the surface of the metallic implant is at the origin of the good biocompatibility of titanium alloys. However, the periodic removal and reformation of the passive oxide film under fretting conditions can lead to a significant increase in corrosion and in the rate of formation of wear fragments.

There is a need to better understand the mechanism of generation of wear fragments under tribological conditions typical for bone-implant interfaces. For this reason, an experimental apparatus has been developed which permits to carry out fretting studies under controlled mechanical and chemical conditions in simulated biological environments. In particular, the apparatus allows one to carry out experiments under potential control using the implant material as an electrode in an electrochemical cell.

**METHODS:** The apparatus consists in a rigid stainless steel structure with a mobile beam. When the mobile beam is moved upwards, the flat surface of the metal sample (usually Ti6Al4V) enters into contact with an alumina ball (or another material) used as antagonist. The normal force is controlled by a rotating screw pressing the contact along the z axis via a spring of variable stiffness. The oscillation of the metal sample is controlled by a piezo-actuator,

which allows for different amplitudes and frequencies. A force sensor monitors the evolution of the normal and the tangential forces. The contacting surfaces subjected to fretting are immersed in a liquid electrolyte as shown in Fig.1. The metal sample forms the anode in an electrochemical cell. Critical mechanical and electrochemical quantities are monitored in real time. The biological medium is simulated by a solution of 0.9 %wt NaCl. Although the experimental device offers temperature control of the solution, all experiments described here were performed at room temperature. An anodic potential of 0.5 V was applied with respect to the Ag/AgCl reference electrode.

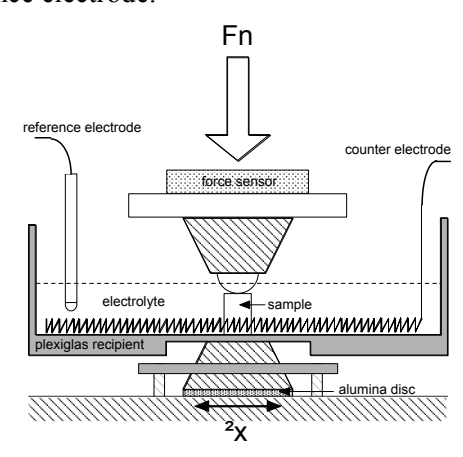


Figure 1: Schematic of the contact and the electrochemical cell.

**RESULTS:** As an illustration, Figures 2 shows the evolution (a) of the friction coefficient, (b) of the anodic current and (c) of the position of the antagonist with time. (amplitude: 150 μm, frequency: 1 Hz, normal force: 10 N, applied potential: +0.5 V). The monitoring of position of the antagonist permits to measure in situ the wear rate. In Fig. 2, rubbing starts at 300 s and stops at 900 s. To get more information on the nature of wear fragments formed under the present experimental conditions worn surfaces were observed with the scanning electron microscope. Fig. 3 shows a worn surface resulting from fretting for 5 hours at an amplitude of 150 µm, a frequency of 1 Hz, a normal force of 10N and an applied potential of 0.5 V

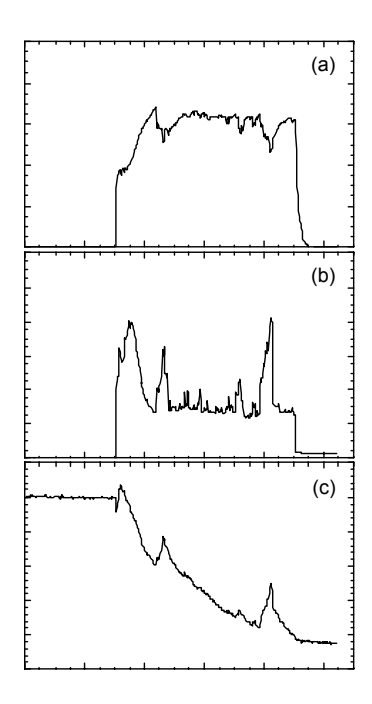


Figure 2: Friction coefficient (a), Current (b), Linear wear (c) measured during a fretting experiment (150  $\mu$ m, 1 Hz, 10 N, +0.5 V). Rubbing starts at 300 s. and stop at 900 s.

**DISCUSSION & CONCLUSIONS:** At the onset of rubbing the current increases markedly. This confirms that rubbing damages the passive film and leads to anodic metal oxidation. This electrochemical contribution to material loss can be calculated by integrating the measured current and applying Faraday's law, assuming that titanium oxidation to the four valent state is the only anodic reaction. Calculations for experiments carried out at a slip amplitude of 30  $\mu$ m and an applied potential of + 0.5 V show that the electrochemically oxidized material represents between 16 and 34 % of the total wear volume. Indeed, there seems to be a correlation between the current peaks, the friction coefficient variations and the wear rate shown in Fig. 2. These peaks can be explained by postulating that particles detach from the surface and form a third body. Their presence in the contact leads to a rise in the antagonist and a lowering of the friction coefficient. When these particles are ejected or disintegrate into smaller particles the contact behaves again as before. An explanation for the current increase would be that relatively large particles are formed at certain intervals due to fatigue wear. Detachment of such

plate like metal fragments from the surface would expose naked metal to the electrolyte. Reoxidation of the exposed metal surface would yield an anodic current peak. The plate like particles formed by fatigue may progressively be destroyed due to rubbing, and the small fragments formed may eventually be ejected from the contact.

The low magnification micrograph of Fig. 3a shows that wear fragments are present in the contact and distributed symmetrically at some distance around the contact. This confirms that wear particles are ejected during fretting. The high magnification micrograph of Fig. 3b suggests that the size of the ejected particles is on the order of a few micrometers, but they are in fact agglomerates of even smaller entities, of nanometer dimension. Wear particles of similar size and shape have been described previously in the literature and similar fragments have been observed in retrieved biological tissues. These observations support the idea that the present apparatus should be well suited for in-vitro simulation of physico-chemical phenomena at boneimplant interfaces.

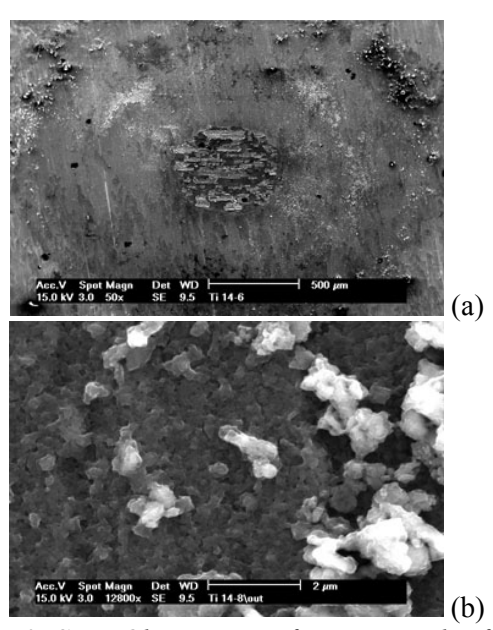


Figure 3: SEM Observation of wear particles formed after 5 hours (150  $\mu$ m, 1 Hz, 10 N, +0.5V). View of the wear scar (a). High magnification view of wear particles outside the wear scar (b).

**REFERENCES:** <sup>1</sup>S.Mischler, S.Debaud, D.Landolt, J.Electrochem, Soc., 145(3), 750-758 (1998)

**ACKNOWLEDGEMENTS:** 'Entwicklungsfonds Seltene Metalle' is acknowledged for financial support.

## DEGRADATION OF CoCrMo HIP IMPLANTS – A CORROSION, WEAR AND CLINICAL ANALYSIS

A.W.E Hodgson <sup>1</sup>, S. Mischler <sup>2</sup>, S. Virtanen <sup>1</sup>, A.O. El-Warrak <sup>3</sup>, B.von Rechenberg <sup>3</sup>

<sup>1</sup> Institute of Materials Chemistry & Corrosion, Dept. of Materials, Swiss Federal Institute of Technology Zurich-ETHZ, Switzerland. <sup>2</sup> Lab. of Metallurgical Chemistry, Dept. of Materials, Swiss Federal Institute of Technology Lausanne-EPFL, Switzerland. <sup>3</sup> Musculoskeletal Research Unit, Dept. of Veterinary Surgery, University of Zurich, Switzerland

**INTRODUCTION:** prerequisite Α understanding the reasons that may lead to implant rejection, exemplified typically by aseptic loosening, is a clear insight of the processes occurring at the metal biological interface and the influences that each environment plays on the other. Considering the very different nature of the environments and the disparate interactions between these, it is essential to approach the problem from different directions corresponding to different competence fields. In this study, an animal model for interface tissue formation in cemented CoCrMo hip replacements [1] was exploited to investigate the processes occurring at the implant-biological interface. In contrast to most studies reported, in which the task in hand is approached from either a biological, clinical or material angle, here we seek to investigate the interaction of the different processes by combining competence from medicine, biology, corrosion and tribology. [2]

METHODS: The degradation of CoCrMo ASTM-F75-92 hip implants as a result of wear and dissolution processes was investigated. Total hip arthroplasty of the cemented type was carried out on 12 sheep and observed over a period of 8 <sup>1</sup>/<sub>2</sub> months. Radiography was employed to analyse the stability of the implant and the presence of possible fractures in the cement mantle. Upon euthanasia, the explants were retrieved for analysis of the surfaces and evidence of degradation (optical stereomicroscopy, SEM and non-contact laser profilometry), whilst tissue from the interface regions was harvested for chemical analysis and evidence of Co, Cr and Mo content (ICP-MS). Histological analysis was also performed.

**RESULTS:** Clinical analysis and histology. The surgical procedure was successful in all 12 experimental animals. From the radiographs, differences in bone resorption and periosteal reaction were observed according to the clinical looseness of the implants. Severe cracks in the PMMA cement mantle were observed in cases where the implant was severely loose and could be

removed from the shaft with ease. During explantation of the bone and prostheses extraction procedures, the subjective clinical evaluation of the stability of the shaft of the implant within the femur showed differences between implants, and the degree of fixation was categorized as well fixed, fixed and loose. This classification reflected the degree of mobility of the prostheses within the cement mantle and the ease with which the latter could be removed at the time of euthanasia Macroscopic analysis of transverse bone sections revealed an interface tissue with scar-like, dark red coloration between the PMMA mantle and the bone. The latter was considerably more prominent in sheep with clinically more loose implants. In the clinically fixed implants, an immediate contact between bone and cement was present without interposition of an interface tissue.

Metal release in tissue. In Figure 1 results of chemical analyses of tissue samples from the PMMA-cortex interface are shown, plotted as a function of the ranking of the implant stability within the cement mantle at the time of retrieval. In all experimental sheep tissue analysed, the metal concentrations measured exceeded those found in blank tissue, indicating that a release of metal from the prostheses took place in all cases.

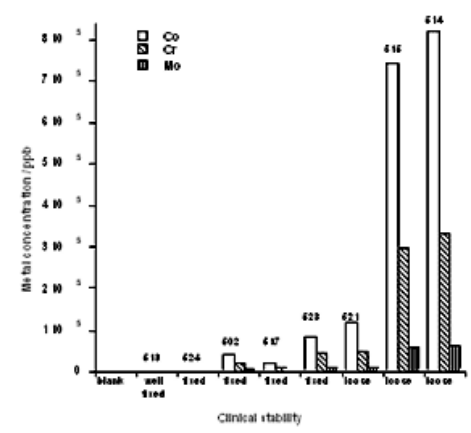


Fig. 1: Plot of absolute concentration of Co, Cr, Mo measured in interfacial membrane samples versus clinical stability of the implant within the bone at the time of retrieval.

In addition, the concentrations of all three metal elements measured increased with increasing clinical instability of the implant, as exemplified by sheep 513 with a very well fixed prosthesis, where the concentration of Co in the interface tissue was 141 ppb, and in sheep 514 with a very loose implant, where the concentration of Co reached a value of 820845 ppb. Of particular notice were the relatively constant concentration ratios of 1Mo:2Cr:100Co found, which do not reflect the composition of the alloy or that of the passive film, suggesting that the nature of the metal release process occurring could be a combination of cyclic mechanical de-passivation and chemical re-passivation.

Surface damage of implants. Optical and secondary electron (SEM) microscopies were used to identify surface modifications resulting from wear, such as scratches or presence of debris and from corrosion events such as pitting. SEM images of implant 514, compared to an as-received sterilized hip prosthesis, revealed a systematic mechanical flattening of the microscopic asperities forming the original surface topography, in addition to the observation of debris particles. This suggested that during clinical use repeated sliding conditions were locally established between the prosthesis and the PMMA cement mantle leading to wear of asperities.

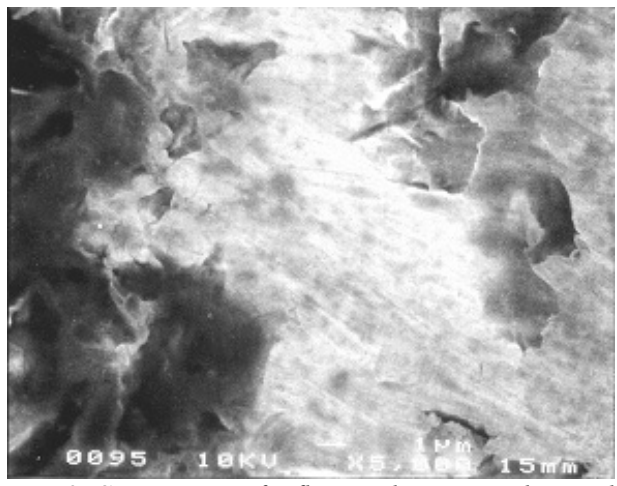


Fig. 2: SEM image of a flattened asperity observed on a loose implant (514) as the results of sliding wear events.

A variable length scale analysis of selected roughness profile lines measured using laser profilometry was carried out systematically on most of the implants to quantify the extent of asperities flattening and thus of wear damage. An influence of clinical use on surface structure was clearly noted when roughness was quantified over small interval distances (<100 µm) corresponding

to the typical size of the asperities. This was in agreement with SEM observations. However, no significant difference between fixed and loose implants could be identified, thus indicating that all the implants underwent similar wear damage.

**DISCUSSION & CONCLUSIONS:** From the results it was evident that a good degree of correlation exists between the clinical evaluation of the implant stability and the chemical analysis of the interface tissue. In particular, it was found that the quantity of interface tissue grown between the cement and the cortex closely reflected the degree of fixation of the implant shaft, and concomitantly the degree of metal release from the The presence of prominent interface allov. membrane was often accompanied by more pronounced resorption and an abnormal new bone formation including increased vascularity within the bone cortex. Moreover, it was also found from measurements of the surface roughness along the stem that a certain degree of wear occurs in all implanted prostheses, irrelevant of the degree of fixation of the implant within the PMMA, indicating that fretting wear does take place.

In conclusion, it was clear from the collected explant surface- and retrieved tissue chemicalanalysis data, that generation of metal particles, or alloy degradation mechanism, involving a mixture of wear and tribo-corrosion took place in all implanted hip prostheses. However, the absence of evident correlation between the surface morphology and roughness data with either the degree of fixation of the implants, or with the tissue chemical analysis classifications suggested that the modes of mass transport between the implant surface and the tissue play an as important role as the surface degradation mechanism of the metal. The mode and degree of mass transport might depend on the presence of cracks or defects in the bone cement as well as on the local physiological constitution.

**REFERENCES:** <sup>1</sup>A.O. El-Warrak. M.L. Olmstead, H. Noetzli, M. Akens, B. von Rechenberg, (2001). <sup>2</sup>A.W.E. Hodgson, S. Mischler, S. Virtanen, A.O. El-Warrak, M.L. Olmstead, B. von Rechenberg, (2001) *J. Biomed. Mat. Res.* in print.

**ACKNOWLEDGEMENTS:** The authors thank the Foundation "Entwicklungsfonds für Seltene Metalle", Switzerland, for financial support of the project. The authors would also like to thank Professor D. Günther and K. Hametner for their help in the chemical analysis and B. Senior and P. Mettraux for their help in SEM. analysis.

#### ELECTROCHEMICAL CHARACTERISATION OF TITANIUM ALLOYS FOR BIOCOMPATIBLE APPLICATIONS

A.W.E Hodgson, S. Virtanen

<u>Institute of Materials Chemistry & Corrosion</u>, Dept. of Materials, Swiss Federal Institute of Technology Zurich, ETH-Zurich, Switzerland

**INTRODUCTION:** Titanium alloys are regarded as highly biocompatible materials and are hence widely employed in the fabrication of prostheses. Their high corrosion resistance is due to the spontaneous formation of a protective oxide film, the integrity of which has been strongly correlated to the chemical and mechanical stability of implants. Despite the fact that total hip arthroplasty is a successful and world-wide accepted modern surgical operation, every year up to 20 % of human patients require revision surgery due to complications. These are often associated with the formation of a synovial-like tissue at the interface between the bone and the implant in response to the interaction of mechanical, electrochemical and biological processes. In this work [1], the electrochemical properties of Ti, TiAlV and TiAlNb were investigated under experimental conditions resembling the in vivo biological environment. Particular focus was placed on TiAlV, the currently more frequently employed alloy for hip prostheses.

METHODS: The electrochemical properties of the Τi samples were investigated using potentiodynamic, impedance AC and photoelectrochemical techniques. The experimental conditions selected consisted of buffered simulated body fluid solutions, thermostatted at 37°C. The effects of parameters such as pH, temperature and time were studied as well as the effects of different ionic species contained in simulated body fluid.

**RESULTS:** The influences played by the composition of the electrolyte solution on the formation and growth of the oxide film on TiAlV and modifications in the latter, as a result of selective ion inclusion or adsorption was investigated. Of particular interest were the effects of calcium and phosphate ions, as these ions are thought to be the first ions to interact with the metal surface amongst the different ions contained in body fluid. In situ measurements were carried out employing AC impedance and photo-electrochemistry in order to monitor changes at the metal-electrolyte interfaces and in the electronic properties of the semi-conductive oxide layer. AC impedance studies showed that these ions interact with the surface and change the passive film with time. This could be best monitored from changes in the phase diagrams with time. In fact the appearance of a second overlapping phase shift was observed with time in the presence of either calcium ions or phosphate ions in electrolyte solutions containing 0.14 M NaCl. In the absence of added ions, only one phase shift was observed irrelevant of the time of exposure of the sample to the solution. Changes in the phase shifts in the presence of calcium and phosphate ions were not observed at room temperature. Photoelectrochemical experiments revealed an absorption at 250 nm in all simulated body solutions tested, but the photocurrents measured varied quite considerably in the presence of calcium and phosphate ions compared to NaCl. Differences were also observed between the three different metal samples investigated.

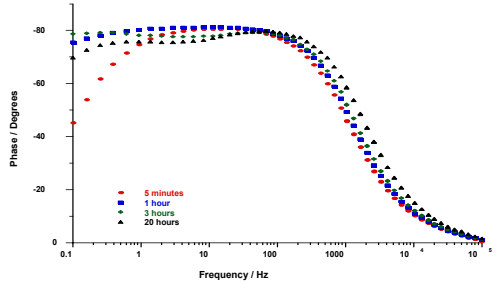


Fig. 1: AC phase shift spectra of TiAlV in 0.14 M NaCl containing 10 mM KH<sub>2</sub>PO<sub>4</sub> adjusted to pH 7.4; T = 37°C;  $E_{Pol} = E_{Corr} \pm 10$  mV.

DISCUSSION & CONCLUSIONS: Upon placing a metal implant in a biological environment, changes in the properties of the metal oxide film may occur as a result of interactions between the two environments. First results have shown that the use of in situ techniques such as ACimpedance photoelectrochemistry enable the monitoring of changes in the passive film with time under different simulated conditions. It was found that calcium and phosphate ions are both responsible for interacting with the Ti surfaces and altering the passive film shortly after contact. Other ions contained in body fluid do not appear to have the Surface modifications, however, same effect. appear to occur to a different extent or mechanism on pure Ti and on the two Ti alloys investigated. **REFERENCES:** <sup>1</sup> A.W.E. Hodgson, Y. Müller,

**REFERENCES:** A.W.E. Hodgson, Y. Müller, D. Forster, S. Virtanen, *Corr. Sci.* submitted.

**ACKNOWLEDGEMENTS:** The Foundation "Entwicklungsfonds für Seltene Metalle", Switzerland, for financial support of the project.

## IMPLANT USED AS DRUG DELIVERY SYSTEM: INFLUENCE OF PARTIAL BIOCAOTING ON THE BONE REMODELING

B. Peter <sup>1, 2</sup>, D.P. Pioletti <sup>1, 2</sup>, A. Terrier <sup>2</sup> and L.R. Rakotomanana <sup>3</sup>

<sup>1</sup> Bone Biophysics Group, Orthopaedic Hospital, Lausanne

<sup>2</sup> Biomedical Engineering Laboratory, EPF-Lausanne

<sup>3</sup> IRMAR Rennes, France

#### Introduction

There is an actual trend to propose cementless hip implants to younger patients. The long term performance of implants has thus to be increased in particular for this type of patients. Beside the development of new materials with better wear properties, another way opens up with systemic pharmaceutical treatments targeting resorption e.g. [1]. However, this systemic therapy presents some drawbacks as important side effects e.g. (throat damage for bisphosphonates) or difficulty to determine appropriate dosage. To overcome these limitations, we propose a new concept of orthopedic implant which would be used not only as a mechanical supporting structure, but also as a drug delivery system. To this end, the stem of a cementless implant could be biocoated with a combination of carrier and drug (for example hydroxyapatite and bisphosphonate) that would enable to locally control the peri-implant bone remodeling.

In the present study, we propose first to theoretically validate the new concept of implant as drug delivery system using a bone remodeling model [2]. Secondly, we will evaluate the effect of a partial coating in order to gain a better control of the peri-implant remodeling.

#### **Material and Methods**

Bone adaptation model. The adaptation model relates the rate of bone density  $\square$  to the mechanical stimulus  $\square$  (plastic yield stress) by a trilinear function:  $\not = v_d(\psi - \psi_d)$ , when  $\psi \ge \psi_d$  (densification);  $\not = v_r(\psi - \psi_r)$ , when  $\psi \le \psi_r$  (resorption). Otherwise, the rate is zero when  $\square$  is in the equilibrium zone defined by  $\psi_r$  and  $\psi_d$ .  $v_r$  and  $v_d$  are the rates for resorption and densification. The bone remodeling parameters  $\psi_r, \psi_d, v_r$  and  $v_d$  were experimentally determined in a previous work [3].

Model of biocoating effects. Drugs used to control the disease of bone metabolism (e.g. bisphosphonate) affect the bone turnover [4]. These effects are modeled in the present study by changing the bone remodeling parameters  $\psi_r, \psi_d$ ,  $v_r$  and  $v_d$  with the following relation:  $v_r(\kappa) = v_r + v_r^{\kappa} \kappa$ ,

where  $v_r(\kappa)$  is the drug altered slope of resorption rate,  $v_r^{\kappa}$  is the weight parameter representing the influence of the drug on the resorbtion rate and  $\square$  is a value between 0 and 1. The dependencies for  $\psi_r(\kappa)$ ,  $\psi_d(\kappa)$ , and  $v_d(\kappa)$  are defined in exactly the same way. The factor  $\square$  which is defined for each location in the bone, could be dependent upon the drug concentration or other biological properties. We use in the present study parameters  $(v_r^{\kappa} = -v_r, \psi_r^{\kappa} = -\psi_r, \text{ and } \kappa = 0.5)$  corresponding to a drug concentration involving a two fold decrease of the bone resorption parameters,  $\psi_r$  and  $v_r$ .

Application to hip arthroplasty. We simulate the remodeling of bone surrounding a femoral stem using a finite element model [5]. This model accounts for major muscle forces corresponding to daily activities as gait cycle. Three different situations are simulated: A) the *standard case* corresponds to the stem without biocoating; B) the *full biocoating case* corresponds to a two fold decrease of the bone resorption parameters,  $\psi_r$  and  $\nu_r$  over the entire stem surface; C) the *partial biocoating case* corresponds to a two fold decrease of the bone resorption parameters,  $\psi_r$  and  $\nu_r$  on the proximal stem surface (Gruen zones 1 and 7).

#### **Results**

The biocoating has significant effects on the perimplant bone remodeling (Figure 1).

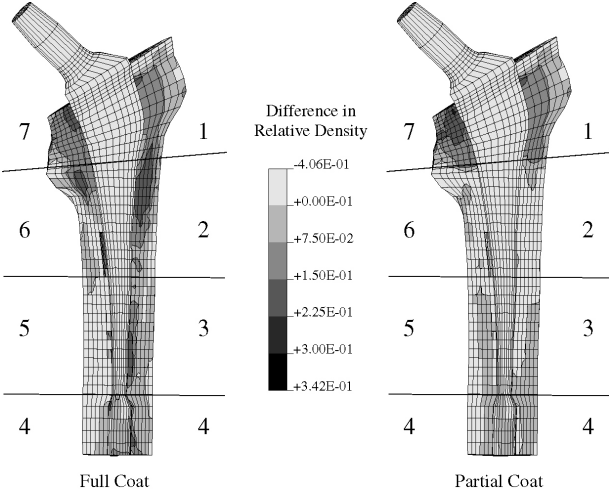


Fig. 1: Difference in relative bone density between the biocoated cases and the standard case

In both cases most regions have a higher density than in the standard case. The main differences between standard and biocoated stems appeared in the proximal region. The fully biocoated case results in a bone slightly denser in the medial proximal bone next to the implant and in the lateral distal outer region of the bone. The main difference between full biocoated and partial biocoated cases resides in the zones 2 and 6 and in particular in the lateral region next to the implant where the bone with a fully biocoated stem is 10 % denser. For the locally biocoated stem, a higher density in the Gruen zones 1 and 7 is achieved compared to the full biocoated stem. In the regions 3, 4 and 5, the fully biocoated stem results in a denser bone mainly located in lateral part with the higher increases next to the implant.

#### **Discussion**

The presented results show that the developed model of biocoating allows us to simulate a boneimplant system with locally altered remodeling behavior. This work enables to validate the usefullness of the new concept of implant as drug delivery system. The numerical results clearly show that the bone density increases when the stem is fully biocoated in comparison to the standard case. This study also shows that a partial biocoating results in a more favorable bone remodeling situation. Indeed, in the case of full stem biocoating the major increase is located in the zones 1 and 7 but is inferior to the increase in density for the local stem biocoating. Moreover the full stem biocoating presents a higher bone density in the lower part of the implant which is not mechanically advantageous.

In conclusion, this concept of implant as drug delivery system seems a promising approach [6].

### References

<sup>1</sup>A.S. Shanbhag (1997), *Clin Orthop* **344**:33-43.

<sup>2</sup>A. Terrier (1997), *Comp Meth Biomech Biomed Eng* **1**:47-59., 1997; 

<sup>3</sup>A. Terrier (1999), Thesis #2048 EPFL. 

<sup>4</sup>H. Fleisch (1995), Bisphosphonates in bone disease. 

<sup>5</sup>N. Ramaniraka (2000) *JBJS* **82**:297-303. 

<sup>6</sup>Pending International Patent #PCT/CH 00/00382.

## "SULFAMERS"-B'ASED POLYMERIC VESICLES FOR DRUG DELIVERY APPLICATIONS

A. Napoli, N. Tirelli, J.A.Hubbell

Institute for Biomedical Engineering, Department of Materials, ETH Zürich

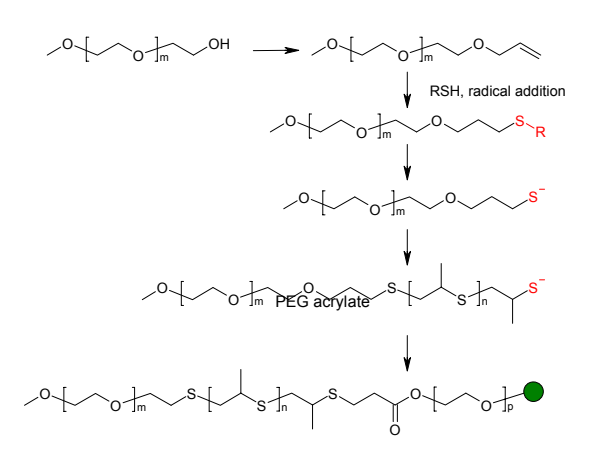
**INTRODUCTION:** The growing interest devoted to amphiphilic polymers and to their self-assembling in aqueous environment, brought to extensive investigations for the block copolymers of the Pluronic series, and in more recent years to poly(ethylethylene)-*bl*-poly(ethylene glycol) (PEG)<sup>1</sup>, poly(styrene)-*bl*-PEG<sup>2</sup> and some others. In most cases the phase behaviour in water showed high complexity and a variety of structures were detected. Indeed only in a few literature examples amphiphilic synthetic polymers were shown to form vesicles<sup>3</sup>, and they are generally demanding in synthesis, difficult to functionalise with bioactive molecules and/or degradable groups and present only AB or ABA structures.

In this communication we report on a new method for the synthesis of amphiphilic polymers that can be used for the preparation of AB, ABA, ABA' (A' chemically analogous, but physically different than A), ABC, ABCBA and other structures, where B is the hydrophobic part and A, A' and C the hydrophilic ones. Those block copolymers were able to form vesicles in water in a wide range of concentrations.

**METHODS:** The synthetic path is based on the anionic ring-opening polymerisation of episulfides, initiated by a thiolate group. The initiator is generated in situ from a PEG chain containing a protected thiol (a thio- or dithioester), avoiding the use of free thiols and thus the problems arising from disulfide formation.

The living anionic process produces a polysulfide chain with a reactive thiolate end, which was used to couple the polymer with an acrylate-terminated PEG through Michael-type addition. The mild character of the end-capping reaction allows the insertion of sensitive biological groups, e.g. peptides.

**RESULTS:** In water environment these structures have been proved by Freeze-Fracture TEM to form lamellar phases and, upon dilution and extrusion, unilamellar vesicles having a diameter of 100-200 nm. Preliminary encapsulation studies were performed using a dye (crystal violet). In the picture is shown a Freeze-Fracture TEM image of



Scheme 1: One-pot reaction scheme of ABA' "Sulfamer"

the vesicle suspension that retained the colour after dialysis.

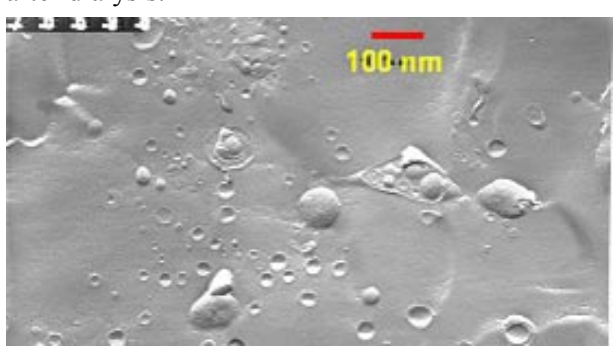


Fig. 1 FF-TEM picture on the CV- $EO_{16}PS_{25}EO_8$  vesicles suspension.

**DISCUSSION & CONCLUSIONS:** We believe that vesicles based on those block copolymers are ideal candidates for controlled and targeted drug delivery systems. Their stability over much longer time, when compared to phospholipid vesicles is an additional advantage allowing the study of their biostability *in vitro* and *in vivo*.

**REFERENCES:** (1) Won, Y.-Y., Davis, H.T., Bates, F.S. Science **1999**, 283, 960-963. (2) Eisenberg, A., Yu, K Macromolecules **1998**, 31, 3509.

(3) Nardin, C., Hirt, T., Leukel, J., Meier, W. Langmuir **2000**, 16, 1035-1041.

## SYNTHESIS AND CHARACTERISATION OF γ-Fe<sub>2</sub>O<sub>3</sub> PARTICLES

M.Chastellain, A. Petri, M.Hofmann, H.Hofmann

Powder Technology Laboratory, DMX, EPFL, Lausanne, Switzerland

**INTRODUCTION:** Nanoscaled particles showing a superparamagnetic behaviour have been intensively studied these past years for biomedical applications. Nevertheless, in vivo as well as in vitro applications still suffer from the lack of well-defined particles. One of the major challenges remains the synthesis of particles with a narrow size distribution.

**METHODS:** The aim of this work is to synthesize and characterise improved ferrofluids for cell separation and drug delivery. The size-controlled precipitation of iron oxide particles and the coating step are the two main parts of the project. The nanoparticles are synthesized by coprecipitation of iron-based salts in different media. The use of various compounds such as dextran, polyvinyl alcohol (PVA), starch, dodecylsulphate (SDS) and silica allows to obtain stable colloids. The particles composition and morphology are characterized using TEM, XRD and FTIR. SQUID magnetometery is used to investigate the magnetic characteristics of the particles but this technique is discussed more in detail in the presentation D5.

**RESULTS:** TEM pictures show ellipsoidal particles. A statistical analysis based on hundred particles per sample lead to an average size of less than 10nm with an ellipse aspect ratio of about 1.2. XRD patterns show a wide amorphous background due to the presence of polymer, nevertheless typical peaks, which can be attributed to nanocrystalline magnetite (Fe<sub>3</sub>O<sub>4</sub>) or maghemite (γ-Fe<sub>2</sub>O<sub>3</sub>) are also present. The size calculated from these data using the Scherrer formula confirms the TEM results. FTIR spectrometry led to the conclusion of a defect magnetite structure with a lattice parameter in between the one of bulk maghemite and magnetite.

DISCUSSION & CONCLUSIONS: Up to date, the studies revealed that stable ferrofluids at ambient temperature and neutral pH could easily be synthesised using "bio-compatible" compounds as stabilisers. The next step is to try and get a firmly attached coating around each particle. The study of the coating step is in progress and the conformation investigation of some polymers at the particles surface is planned. The size distribution of iron oxide particles is still too broad but should be improved by using a Segmented Flow Tubular Reactor (SFTR) for the synthesis.

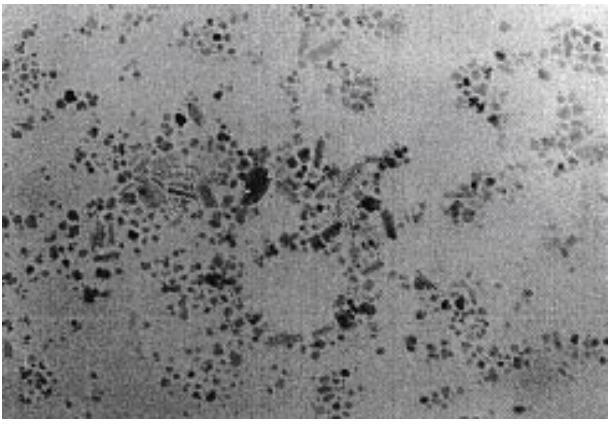


Fig. 1: Bright field TEM image of iron oxide particles stabilised with SDS. The sample consists of stable colloids at physiological pH, diluted and dried on a copper grid. The agglomerated structure is thought to be mainly due to the drying step

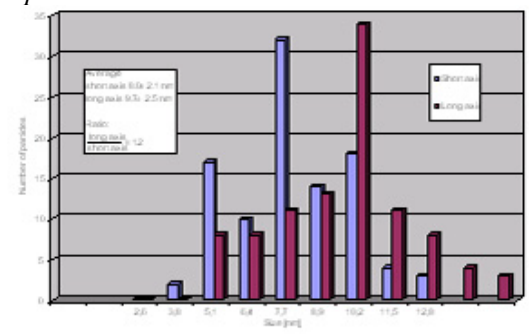


Fig. 2: Length distribution of the two axes of the particles (considered as ellipsis) from the TEM picture.

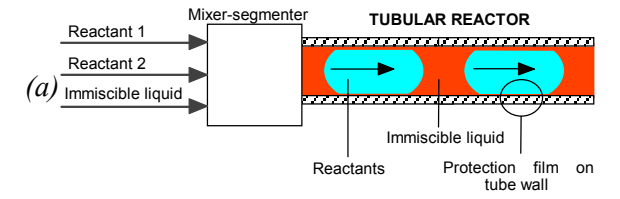




Fig. 3: Principle of a Segmented Flow Tubular Reactor (a) and setting in use (b). Such a setting allows a continuous synthesis with the advantage of producing identical particles over time.

### Studies on Zinc sulfide - Synthesis and Characterization

A. Petri<sup>1</sup>, Y. Axmann<sup>1,2</sup>, A. Lentz<sup>2</sup>, H.Hofmann<sup>1</sup>

<sup>1</sup>Powder Technology Laboratory, Swiss Federal Institute of Technology, CH-1015 Lausanne <sup>2</sup>Department of Inorganic Chemistry and Crystallography, University Ulm, D-89069 Ulm

INTRODUCTION: The poster describes new findings of an investigation of semiconductor nanoparticles for processing size, surface properties, and functionalisation of the surface. It is understood that the control of the surface is the key to highly luminescent nanocrystals. Organic capping yields very high quantum efficiency already at room temperature. The ligands act as passivators and, at the same time, allow functionalisation which turns the nanocrystals into chemical reagents. However, matching extensive ligands with the compact packing of the nanoparticle still remains difficult. Furthermore, for a biomedical application, these quantum dots have to be water-dispersible so as to be compatible with the biological environment. We describe the synthesis of ZnS and manganese doped ZnS nanoparticles by organic and inorganic methods. The two methods are compared here, the development and optimisation of the synthesis is presented on the poster.

**METHODS:** : ZnS and ZnS:Mn nanoparticles have been synthesized in aqueous solution and organic solvent (chloroform).

Inorganic synthesis: relevant synthesis parameters such as pH, concentration, the type of zincprecursor, temperature, and  $Zn^{2+}/S^{2-}$ -ratio have been investigated and optimised. Furthermore, different stabilizers (e. g. thioglycerol, cellulosederivates, polymers) and their influence on the reaction have been tested. The general synthesis follows a similar route for most inorganic synthesis: a metal salt is dissolved in water in the presence of the stabilizer and the chalcogen source is added.

Organic synthesis: ZnS nanoparticles have been synthesized using bis(trimethylsilyl)sulfide as "sulfide-source" and trialkylphosphine as "stabilizer". Manganese doped ZnS is produced similarly. The properties of the obtained particles have been studied so far by UV-VIS and fluorescence spectra, X-ray diffraction spectra, electron microscopy (TEM) and PCS (Photon Correlation Spectroscopy).

**RESULTS:** The major results can be summarized in the following table:

Table 1. Results

| Organic Synthesis | Inorganic Synthesis       |
|-------------------|---------------------------|
| Narrow size       | Optimisation of existing  |
| distribution      | reaction parameters       |
| Stable over weeks | Improved quantum yield    |
| Efficient doping  | No doping possible so far |

All samples (organic and inorganic synthesis) show clearly resolved electronic transitions which are blue-shifted compared to the bulk material. Transition metal ion doping works very well for the organic synthesis:

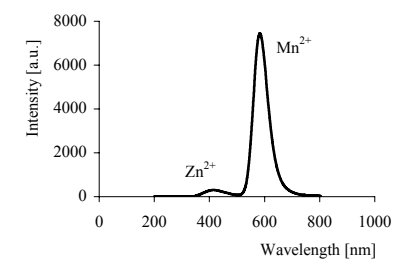


Fig.1:Photoluminescence spectrum of manganese doped zinc sulphide

These powders can be isolated and show an orange fluorescence upon UV-excitation:

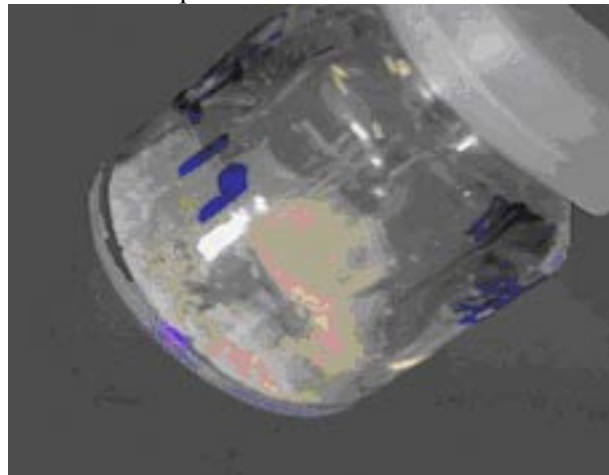


Fig. 2:ZnS:Mn powder

Recent work: Instead of removing the organic "shell" and capping the nanoparticles with an inorganic shell and a second layer for solubility and functionalisation, we immediately functionalised the phosphine by an organic synthesis. With this method we are able to obtain water-dispersable highly fluorescent nanoparticles and at the same time provide enough hydrophilic OH-groups for further treatment with biological active molecules.

studied various organic and inorganic methods to synthesize ZnS nanoparticles. In particular we focused on the influence of synthesis parameters. Existing methods could be improved leading to systems with reasonable narrow size distribution. Although we started to investigate the system, a detailed characterization has to be carried out. For example the influence of Mn<sup>2+</sup> concentration is not yet clear and the concentration and crystallographic environment of the Mn<sup>2+</sup> -ion has not yet been determined.

**REFERENCES:** <sup>1</sup>R. Vacassy, S.M. Scholz, H. Hofmann et al. (1998) *J. Am. Chem. Soc.* 81(10): 2699-2704. <sup>2</sup>J. Leeb, V. Gebhardt, G. Müller et al. (1999) *J. Phys. Chem. B* 103: 7839-7846. <sup>3</sup>R. Vacassy, S. M. Scholz, J. Dutta, H. Hofmann (1998) *Mat. Res. Soc. Symp. Proc.* 50: xyz-xyz. <sup>4</sup>K. Sooklal, B. S. Cullum, S. M. Angel, C. J. Murphy (1996) *J. Phys. Chem.* 100: 4551-4555.

**ACKNOWLEDGEMENTS:** This work is part of the TOP NANO 21 Program and was done in collaboration with the Department of Inorganic Chemistry and Crystallography at the University of Ulm-Germany.

We thank M. Chastellain for the work at the TEM.

### MAGNETIC NANOPARTICLES FOR DRUG DELIVERY

M.Chastellain<sup>1</sup>, A. Petri<sup>1</sup>, H. Hofmann<sup>1</sup>, A. Gupta<sup>2</sup> and K.V. Rao<sup>2</sup>

<sup>1</sup> Powder Technology Laboratory, DMX, EPFL, Lausanne, Switzerland

<sup>2</sup> Department of Material Science and Engineering, Tmfy-MSE, KTH, Stockholm, Sweden

INTRODUCTION: Drug targeting to reach a site of action, where a magnetic carrier can recognize and bind the target and/or provide opportunities for therapeutic action is a growing field of interest. Such an approach results in enhanced dosage at a defined specific site in a living system, with reduced side effects but higher efficiency in handling crucial biological problems. Up to date functionalised magnetic carriers have been mostly used for MRI imaging but superparamagnetic iron oxide nanoparticles consist in an important and promising mean for targeted drug delivery because of their high intrinsic magnetic moment, which allows a good magnetic guidance inside biological systems while still retaining no magnetic remnants.

METHODS: The aim of this research is to synthesize and characterize biocompatible particles before developing a setting for actual drug delivery application. The nanoparticles are synthesized by a chemical route namely coprecipitation of iron-based salts in aqueous medium. The obtained colloids are stabilised using various compounds such as dextran, starch, polyvinyl alcohol (PVA) and silica. The particles composition and morphology are characterized using TEM and other methods described in poster D3. SQUID magnetometry as well as AC susceptometry is used to investigate the magnetic characteristics of the particles.

RESULTS: TEM pictures show ellipsoidal particles. A statistical analysis based on hundred particles per sample lead to an average size in the 10nm range. From SQUID measurements the effective magnetic particle size is found to be smaller. The difference in the particle size measured with TEM and SQUID is thought to be due to the presence of a so-called magnetic "dead layer" with effective non-magnetic property around the particles core. Field cooled (FC) and Zero field cooled (ZFC) graphs show a superparamagnetic behaviour with a noticeable size distribution.

**DISCUSSION** & **CONCLUSIONS:** The preliminary studies revealed that stable ferrofluids at ambient temperature and neutral pH could be synthesised using various "bio-compatible" compounds as stabilisers. The magnetic

characterisation mainly showed the existence of a "dead layer" around the particle core, which is an important point currently under study. The synthesis parameters need to be critically optimised in order to improve the particles size distribution and get a more homogeneous relaxation time of the superparamagnetic particle.

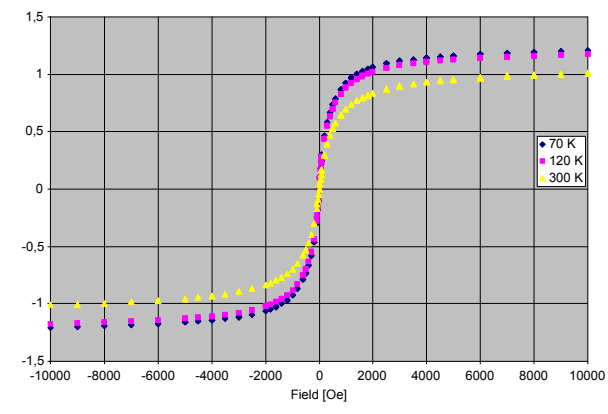


Fig. 1: The SQUID data measured at different temperatures show almost no hysteresis. The effective magnetic particle size is evaluated from the slope of initial curves around the origin.

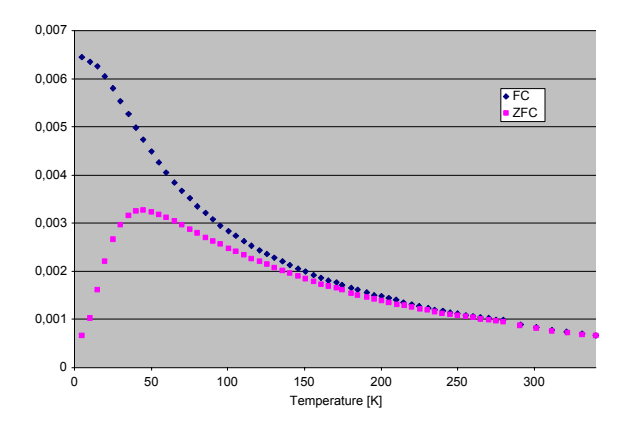


Fig. 2: FC and ZFC magnetisation curves are generally used to study superparamagnetic materials. Significant particle size distribution gives rise to the large difference between the maximum in the ZFC curve and the temperature at which the two curves overlap (around 170 K).

**ACKNOWLEDGMENTS:** This project is supported by EU - under the project MAGNANOMED - Magnetic Nanoparticles for Medical and Biological Diagnostics and Devices.

### LASER LITHOGRAPHY ON OXIDE FILM (I)

3D Titanium Object Micromachining

P.-F. Chauvy, D. Landolt

<u>Laboratory of Metallurgical Chemistry</u> (LMCH), Dept. of Materials, Swiss Federal Institute of Technology, EPF-Lausanne, Switzerland

INTRODUCTION: Due to its good mechanical properties and chemical inertness, titanium is the material of choice for implantable devices in medicine and dentistry. For many of these applications the surface topography must be carefully controlled to achieve optimum cell adhesion and differentiation [1]. Electrochemical micromachining is a useful method for the fabrication of well defined surface structures in the micrometer range [2]. Normally, dissolution is carried out through a suitably patterned photoresist, but the use of this technique is limited to planar surfaces. Certain applications. for example the production of biomedical implants, involve complex surface geometries to which a photoresist cannot be readily applied. Recently, it has been shown that a laser patterned anodic oxide film could assume the function of the photoresist [3]. In the present study this novel electrochemical micromachining method was applied to produce well defined microstructures on a titanium cylinder.

**EXPERIMENTAL:** The different steps of the process are presented on Fig. 1; results following each step are displayed on the right side. After anodic oxidation, the titanium sample is locally irradiated with a pulsed eximer laser. Next, Electrochemical dissolution takes place which results in isotopic etching. Ultrasonic cleaning is then sufficient to neatly break the free standing oxide bridge resulting from underetch. The final microstructure then reveals its shiny surface finish. **RESULTS:** A titanium hollow cylinder (diameter 1 cm, height 2 cm) was first electropolished and anodically oxidized, turning its colour to blue. It was then fixed on moving stages in front of the laser beam allowing lifting and rotating the sample during serial pulse writing. Displacement and laser parameters were set to pattern two areas of hole arrangement with two different spacings (50 and 100 µm). Laser writing was quite slow (27 min.) but this time could be drastically reduced using more elaborate optics [4]. Electro-dissolution was then carried out for 20 min., yielding well defined 40 µm diameter hemispherical holes (Fig. 2).

**CONCLUSIONS:** Laser lithography on oxide film followed by electrochemical dissolution allowed us to micromachine well defined microstructures on an electropolished titanium

cylinder. This demonstrates the feasibility to use this technique to produce fine topographies on implant surfaces.

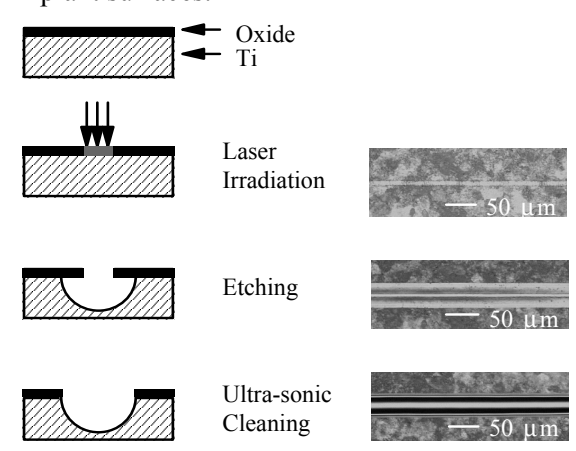


Fig. 1 Processing steps for laser electrochemical micromachining of titanium. After anodic oxidation, serial pulsed laser writing allows for flexible and rapid patterning. Selective electrochemical dissolution of the irradiated features is followed by ultra-sonic cleaning.

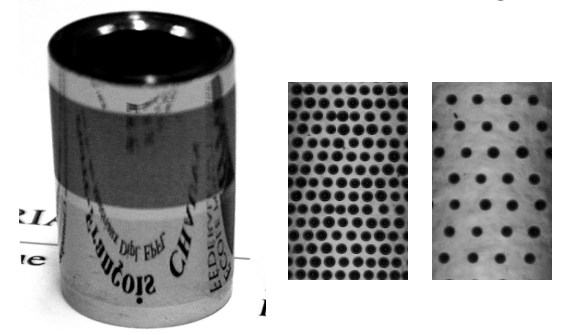


Fig. 2 Photograph of a microstructured cylinder; Blow-up shows two areas with different densities 50 and 100 μm spacing), holes are 40 μm in diameter.

#### **REFERENCES:**

<sup>1</sup>B. D. Boyan, T. W. Hummert, D. D. Dean and Z. Schwartz, *Biomaterials*, **17**, 137 (1996). <sup>2</sup>C. Madore and D. Landolt, *J. Micromech. Microeng.*, **7**, 270 (1997). <sup>3</sup>P.-F. Chauvy and D. Landolt, *Electrochem. Solid-State Lett.*, **4** (5), C31 (2001). <sup>4</sup>B. Kasemo and J. Gold, *Adv. Dent. Res.*, **13**, 8 (1999).

**ACKNOWLEDGEMENTS:** The authors thank P. Hoffmann (IOA/IMT/EPFL) for help with the laser installation. Financial support from the Fonds National Suisse is gratefully acknowledged.

# NOVEL ENZYME ASSAYS USING THE ATTENUATED TOTAL REFLEXION SPECTROSCOPY (ATRS)

T.S. Hug, M. Linnhoff and U.E. Spichiger-Keller

ETH, Centre for Chemical Sensors (CCS) and Chemical Information Technology (CIT), Technopark, Zürich, Switzerland

**INTRODUCTION:** Simple and fast enzyme assays are attractive for medical diagnostics, *e.g.* in haemostaseology, when the pro-thrombin time can be monitored at the patient's home. Within the project MIOSA (miniaturized integrated optical sensor application), novel enzyme assays using attenuated total reflexion spectroscopy (ATRS) as measuring technique on a chip are being developed. To exclude optical interference with haemoglobin from blood, near-infrared chromophore-labelled peptides as substrates for thrombin and other proteases needed to be synthesized. Here we present preliminary results such as the characterization of the measuring platform and the synthesis of near-infrared-(NIR)-labelled substrates for proteases.

**METHODS:** ATRS measures the absorption of light within a thin sensing layer in the order of a few nanometers in z-direction of the propagating light at the Ta<sub>2</sub>O<sub>5</sub>-waveguide on the optical chip. The NIR-dye is covalently linked to the substrates immobilized on the chip surface. On addition of the enzyme, the dye is first cleft from the immobilized peptide and then diffuses out of the sensing layer. The enzyme activity correlates with the increasing intensity of light, which is transmitted through the waveguide by total internal reflexion.

**RESULTS**: The sensitivity of the ATRS photometer prototype, developed by Metanor AG, Regensdorf and in cooperation with CCS, was tested and in all three cases the sensitivity of the optical chip used was found to be satisfactory:

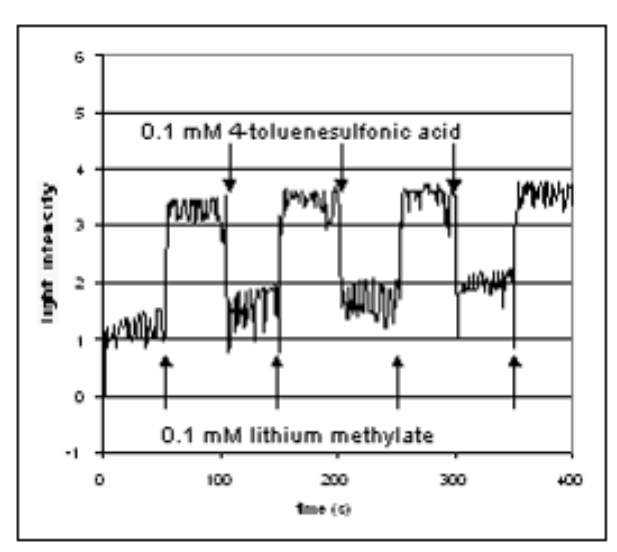


Fig. 1: The covalent immobilization of the NIR-dye on the  $Ta_2O_5$ -waveguide was tested by exposing the immobilized and pH-sensitive dye to two different methanol buffers (4-toluenesulfonic acid & lithium methylate) changing the detected light intensity of the ATRS-signal.

- 1) A lipophilic derivative of the same pH-indicator chromophore as used as label during synthesis of potential protease substrates was measured as indicator dye in its protonated form within methanol solutions. The detection limit, given by the signal to noise ratio, lay at about  $10^{-5}$  mol/l indicator at a propagation path length on the waveguide of 6 mm.
- 2) With regard to possible immobilization of chromophore-labelled substrates within a plasticised PVC membrane, the sensitivity of the set-up within a membrane disposed on the chip surface that contained the same indicator dye was investigated.
- 3) The chips were functionalised with amino groups, such that the  $Ta_2O_5$ -surface was completely covered (XPS). In the next steps, a linker was first chemically bound to the functionalised chip surface and secondly the dye was linked to the linker. The covalent immobilisation of the pH-sensitive-dye was tested by exposing the chip to different methanol buffer solutions leading to different absorption spectra of the indicator dye and different light intensities of the ATRS-signal.

Preliminary experiments to test the influence of immobilization on the substrate were performed in solution. A common substrate for trypsin was derivatized at the amino-terminus by caprinic acid (Caprinyl-Phe-Gly-Arg-pNA), showing remaining cleavability in kinetic measurements.

Chromogenic substrates for trypsin-like enzymes with the peptide sequence  $R_1$ - $R_2$ -Arginin-L-D ( $R_1$ ,  $R_2$ : amino acids; L: spacer [amino acid or phenylenediamin]; D: NIR-dye) were synthesized. Since modelling experiments had suggested a linker between substrate and NIR-dye to be necessary, substrates with and without different linkers ( $L_1$  &  $L_2$ ) were synthesized:

- BOC-Ser(Bn)-Gly-Arg-D
- BOC-Ser(Bz)-Gly-Arg-L<sub>1</sub>-D, L<sub>1</sub>=Phenylendiamine
- BOC-Ser(Bz)-Gly-Arg-L<sub>2</sub>-D, L<sub>2</sub>=Phenylalanin

Cleavability studies with these substrates are under investigation.

### **CONCLUSIONS:**

Substrates labelled with a NIR-chromophore likely to be cleft by trypsin-like proteases as suggested by modelling studies, could be synthesized.

ATRS on optical waveguides with immobilized substrates was shown to be sufficiently sensitive to realize miniaturized measuring devices.

#### **ACKNOWLEDGEMENTS:**

Synthetic contributions and helpful discussions with Fluka AG, Buchs, are gratefully acknowledged.

# SYNTHETIC, ENZYMATICALLY DEGRADABLE EXTRACELLULAR MATRICES FORMED FROM RECOMBINANT PROTEIN(POLY)ETHYLENEGLYCOL

S. C. Rizzi, S. Halstenberg, J. Hubbell <sup>1</sup>

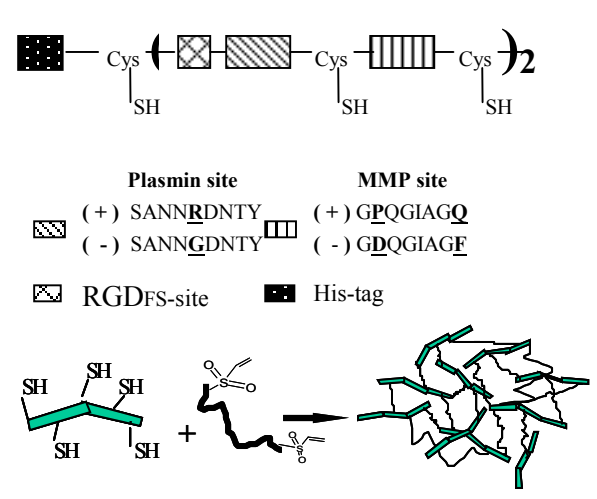
<sup>1</sup><u>Institute for Biomedical Engineering</u>, Department of Materials, Swiss Federal Institute of Technology, ETH-Zürich, Switzerland

INTRODUCTION: Our research addresses the clinical need for synthetic biomatrices as physical supports for the creation of functional tissue and as carrier vehicles for efficient and controlled delivery of drugs and growth factors. Here we describe the development of a novel class of biologically active synthetic hydrogel matrices that form through chemical cross-linking of polyethyleneglycol (PEG) with recombinant proteins. The design of our PEG-protein network is motivated by the function of the natural extracellular matrix (ECM) during tissue development and tissue repair. Towards this goal, we generated PEG-protein copolymers that carry some of the key functions of ECM such as the ability to mediate cell adhesion, cellular penetration and migration through proteolytic remodeling, as well as storage and cell-regulated release of growth factors. PEG was chosen for its well known biocompatibility and resistance to protein adsorption. Biological information was conferred to the copolymer backbone by the incorporation of recombinantly derived proteins that carry the cell adhesion motif RGD derived from fibronectin, and substrates for degradation by the cellular proteases plasmin and matrix metalloproteinase (MMP). The copolymer networks form in ageous solution by spontaneous reaction between thiols of cysteines in the protein backbone and vinylsulfone groups at the termini of PEG. The crosslinking reaction is highly self selective and can be carried out in situ in the presence of cells or tissue.

METHODS: Two artificial proteins of 116 amino acid length were created de novo by recursive PCR methodology using overlapping single stranded DNA fragments as templates. For the present study, two proteins that differ in their sensitivity to degradation by cellular proteases were produced (Fig. 1A). One protein construct was designed for degradibility by plasmin metalloproteinases (MMPs). A second control protein construct was generated in which cleavage sites for plasmin or MMP were mutated inactive. Both protein constructs contain the cell adhesion peptide motif RGD. Cysteines added within the protein backbone are designated cross-linking sites

with PEG divinylsulfone. A thrombin-cleavable histidine tag was added for purification by Nisequences chromatography. DNA affinity corresponding to monomeric proteins were dimerized double non-palindromic using restriction sites and were then subcloned into the E.coli expression plasmid PET 14b (Novagen). The resulting protein dimers were recombinantly expressed and purified in E. Coli. Purified proteins are visualized in figure 2, lanes 1 and 5.

Three-dimensional copolymer networks formed spontaneously within minutes under physiological condition by mixing aequeous solutions of recombinant protein and PEG divinylsulfone. A cartoon of the resulting network structure is depicted. The gels form via conjugate addition between thiol groups from cysteines in the protein with unsaturated double bonds present in PEG divinylsulfone (Fig. 1B).



Recombinant Protein + PEG divinyl sulfone = PEG-Protein-co-Polymer

Fig. 1 A and B: A) Generation of artificial recombinant proteins. B) Recombinant protein-PEG hydrogel formation

**RESULTS:** The principles of this biomaterial scheme were investigated in biochemical and in vitro cell culture assays. Purified recombinant proteins containing active sites for cleavage were specifically degraded by incubation with MMP-1 (Fig 2, lanes 2 to 4). Notably, degradation was almost completely absent in control proteins

containing mutant, inactive cleavage sites (Fig 2, lanes 6 to 8). Cell-derived proteolytic degradation was demonstrated in three-dimensional cell migration assays. Human fibroblasts embedded within degradable PEG-protein copolymers survived within the matrix, and were able to invade the matrix environment through their cellular activities. Cellular invasion was critically dependent on the degradability of the hydrogel (Fig. 3A and B).

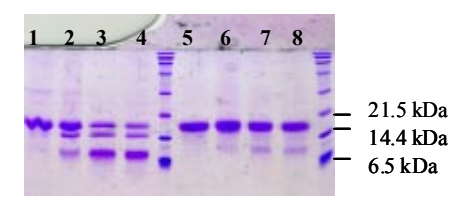
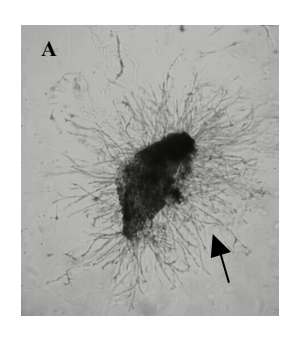


Fig. 2: Degradadation of recombinant protein by MMP-1. Fragmentation of the proteins was analyzed by 20% SDS-PAGE and subsequent Coomassie staining. Lanes 2 to 4 on the left panel show degradation of the MMP sensitive protein after 18h, 72h, 98h. Notably, little degradation was observed for protein containing the mutant, inactive MMP site (right panel, lanes 6 to 8).



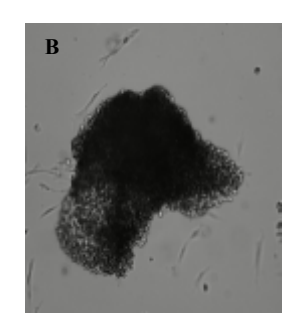


Fig. 3A and B: Cellular invasion of protein-PEG hydrogels is dependent on degradibility of the matrix. Fibrin clots containing human fibroblasts embedded within three-dimensional were degradable (A) or non-degradable (B) protein-PEG hydrogels. Cell migration into the synthetic hydrogel was analysed by phase-contrast microscopy at day 6 of cell culture. Massive cellular invasion was observed for degradable protein-PEG matrix, but was absent in control cultures non-degradable protein-PEG in hydrogels.

**CONCLUSIONS:** Together, our results have proven the functionality of PEG-protein copolymers as cell ingrowth matrices. Such matrices can be tailored toward specific medical needs and thus become potentially useful for the delivery of drugs and factors for regulated release by cellular activities.

# TITANIUM ELECTROCHEMICAL MICROSTRUCTURING APPLIED TO BIOLOGICAL MODEL SURFACES

O. Zinger, D. Landolt

<u>Laboratory of Metallurgical Chemistry</u> (LMCH), Dept. of Materials, Swiss Federal Institute of Technology, EPF-Lausanne, Switzerland

**INTRODUCTION:** Titanium and titanium alloys have attracted considerable interest in aerospace, chemical process and biomedical industry due to their biocompatibility, good mechanical properties and excellent corrosion resistance. The chemical stability of titanium results from the presence of a thin but stable surface oxide film, typically a few nanometer thick. In nonaqueous electrolytes containing perchloric or sulphuric acid, the oxide film is unstable and anodic polarization leads to titanium dissolution at high rate. Recently, a sulphuric acid based-methanol electrolyte has been developed for electrochemical polishing titanium [1,2]. Best polishing was obtained in an electrolyte containing 3 M sulphuric acid for applied potentials above 8 V corresponding to mass-transport controlled dissolution conditions [2]. Using this electrolyte, well-defined topographies in the micrometer range were produced on bulk titanium by electrochemical micromachining through a patterned photoresist [3]. This method involves high-speed selective metal dissolution from unprotected areas of a photoresist-patterned work-piece that is made an anode in an electrolytic cell. Compared to chemical etching, electro-chemical dissolution offers higher rates and better control on a microand macro-scale of shape and surface texture of anodically dissolved materials.

Biological performances of implantable titanium devices in medicine and dentistry have been shown to depend on their surface topography. This latter must be carefully controlled in the micro and nanometer range to achieve cell adhesion and differentiation [4]. Thus, through-mask electrochemical micromachining appears to be a useful method for the fabrication of well-defined surface structures on bulk titanium.

METHODS: The different steps of the process are shown on Fig. 1. The experimental details are described thereafter. Commercially pure titanium disks (Ti 99.6%) were mechanically polished to obtain a mirror finish surface. The polished titanium was coated with a negative polyimide based photoresist, which was exposed using a standard UV mask aligner and developed to reveal the initial patterns.

The dissolution of the titanium through the patterned photoresist was performed in a methanol based electropolishing electrolyte with 3 M sulphuric acid [3].

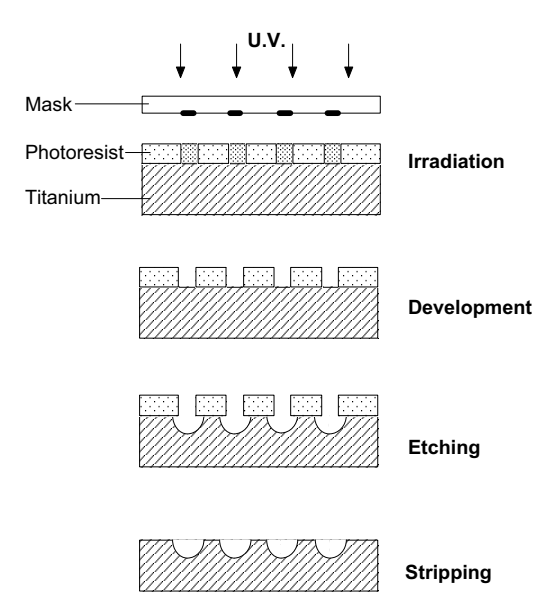


Fig. 1 Processing steps for through-mask electrochemical micromachining of titanium

**RESULTS:** To study the role of surface topography on the interactions of cells with implants, specific patterns were designed. Hexagonal arrangements of hemispherical holes of various size (10-100 µm) and various densities were chosen. Neat dissolution implies two contrary requirements: on one hand, one wants to work at high voltage to ensure rapid and uniform removal of the natural oxide film on the free titanium surfaces; and on the other hand, voltage should be kept as low as possible in order to avoid excessive Joule heating to obtain a good surface finish. This last requirement is especially true for patterns with a large etched surface area and/or high density. To reduce this effect, the electrolyte was cooled down to -10°C and ethanol was added to the methanol (50/50 mixture) to increase viscosity and decrease the anodic current.

For very high density, excessive Joule heating still resulted. To solve this problem, a special sample-holder cooled from the inside was developed; this allows better cooling and also direct temperature measurements through an imbedded thermocouple.

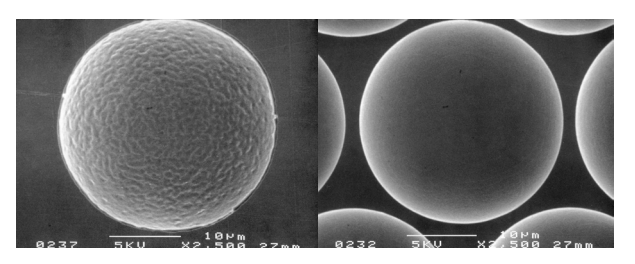


Fig. 2 SEM micrographs of holes (Ø 30 μm) dissolved with non-optimised and optimised parameters

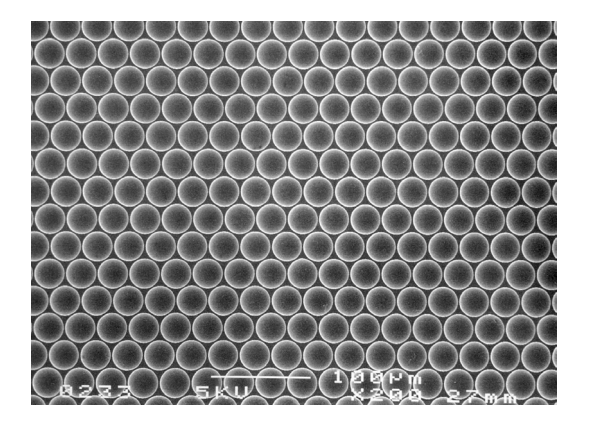


Fig. 3 SEM micrograph of an array of holes ( $\emptyset$  30  $\mu$ m) in hexagonal compact arrangement

With this new device electrochemical parameters were optimised. First, a short polarization of 40 V was applied to quickly remove the titanium oxide and to obtain a homogeneous dissolution from the beginning of the process; then, to reduce Joule heating effects, the potential was gradually decreased to 15 V and maintained at this voltage until the end of the dissolution. Fig. 2 presents a 30  $\mu$ m diameter hole with smooth surface texture and sharp edge obtained after optimisation in comparison with non-optimised conditions. Fig. 3 shows an array of the same 30  $\mu$ m diameter holes in hexagonal compact arrangement. The separation of the holes is 3  $\mu$ m and good definition is obtained over a long range.

**CONCLUSIONS:** The optimisation of electrochemical parameters and the use of a cooled sample-holder enabled us to produce dense and well-defined surface structures in the micrometer range on bulk titanium with smooth surface finish and good reproducibility. These structures will serve as model surfaces to study the role of the surface topography on the interactions of cells with implants.

### **REFERENCES:**

<sup>1</sup> O. Piotrowski, C. Madore, and D. Landolt, *Plat. Surf. Finish.*, **85**, 115 (1998) <sup>2</sup> O. Piotrowski, C. Madore, and D. Landolt, *J. Electrochem. Soc.*,

**145**, 2362 (1998) <sup>3</sup> C. Madore, O. Piotrowski and D. Landolt, *J. Electrochem. Soc.*, **146**, 2526 (1999) <sup>4</sup> B. D. Boyan, T. W. Hummert, D. D. Dean and Z. Schwartz, *Biomaterials*, **17**, 137 (1996).

### **ACKNOWLEDGEMENTS**

The authors thank B. Senior (CIME-EPFL) for the SEM pictures. Financial support of the Commission Fédérale de la Technologie et de l'Innovation (CTI) is gratefully acknowledged.

### LASER LITHOGRAPHY ON OXIDE FILM (II)

Multilevel Titanium Micromachining

P.-F. Chauvy, D. Landolt

<u>Laboratory of Metallurgical Chemistry</u> (LMCH), Dept. of Materials, Swiss Federal Institute of Technology, EPF-Lausanne, Switzerland

INTRODUCTION: Titanium finds increasing applications in medicine and dentistry such as implantable drug-delivery systems and microsurgery tools [1]. A distinct set of advantages make electrochemical dissolution a method of choice for the micromachining of titanium surfaces. The fabrication of certain devices such as implantable pumps requires etching of various sizes features at different depth levels. Multi level etching of titanium has successfully been achieved by several consecutive masking and dissolution steps [2]. Recently, it was reported that a laser patterned anodic oxide film could be used for electrochemical micromachining of titanium [3]. In the present study this novel method was applied to produce well defined complex multilevel microstructures.

**EXPERIMENTAL:** Laser lithography on oxide film is based on the following principle: local laser irradiation induces a depassivation of the oxide covered surface; this yields to selective dissolution during the subsequent etching step. Experimental detail of this technique have been presented elsewhere [3].

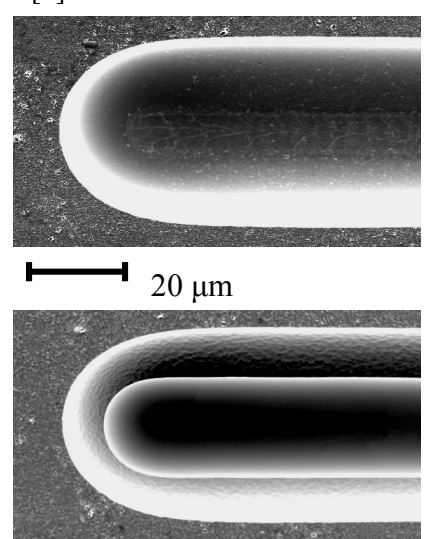


Fig. 1 SEM micrographs of the writing step and of the final appearance of a two level microstructure

After the etching and reoxidation of the first level, the sample has to be repositioned in front of the beam at its exact initial position in order to write the second level. This alignment is performed with the help of an optical sighting tube and the use of markers written on the surface. The precision of this operation is illustrated on the first SEM micrograph of Fig. 1 showing a laser line written at the bottom of an hemicylindrical groove. The second SEM picture presents the resulting two level microstructure with a small groove etched into the first one. This multi-step technique was used to create a complex two-level microstructure with a 'bio-chip' inspired design (not shown here). Results displayed thereafter present the creation of new kinds of cavity shapes.

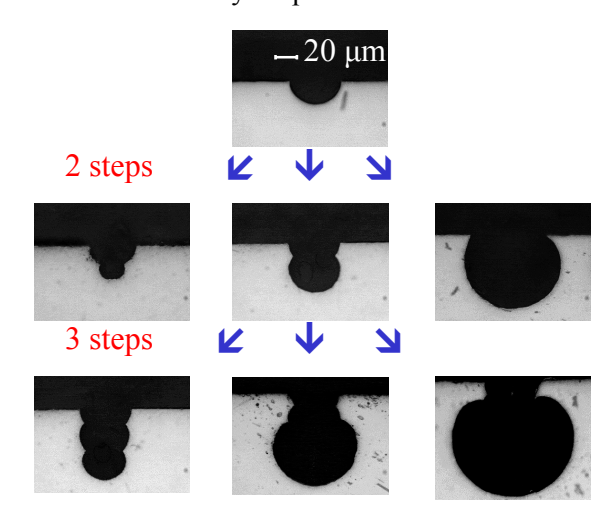


Fig. 2 Side views of microstructures produced by adding a second and a third level on the initial hemicylindrical groove.

**RESULTS:** Fig. 2 presents side views of microstructures realized with two and three steps of anodisation/irradiation/etching. Cavity shapes have been compared with good agreement to moving boundaries numerical simulations. High aspect ratio features are obtainable as well as large cavities with an inner diameter larger than the entrance one. Etching time can be quite high (more than 3 hours for the bottom right cavity), this provides a good illustration of the high chemical resistance of our oxide films.

**CONCLUSIONS:** Complex multilevel titanium microstructures were realized using laser lithography on oxide film followed by electrochemical dissolution. High precision was obtainable and new kinds of cavities were created,

some of them with high aspect ratios and others with 'amphora like' shapes.

### **REFERENCES:**

<sup>1</sup>H. Park and K. Park, *Pharmaceutical research*, **13**, 1770, (1996). <sup>2</sup>Y Ferri, O Piotrowski, P-F Chauvy, C Madore and D Landolt, *J. Micromech. Microeng.*, in press (2001). <sup>3</sup>P.F. Chauvy, P. Hoffmann, D. Landolt, *Electrochem. Solid State Lett.*, 4 (5), C31 (2001)

**ACKNOWLEDGEMENTS:** The authors thank P. Hoffmann (IOA/IMT/EPFL) for help with the laser installation. Financial support from the Swiss National fund is gratefully acknowledged.

# SINGLE PARTICLE FLUORESCENCE DETECTION – HIGH RESOLUTION MICROSCOPY, TEMPORAL BEHAVIOUR. TOWARDS CHIRALITY

R. Eckert, C. Minelli, M. Liley, and H. Heinzelmann\*

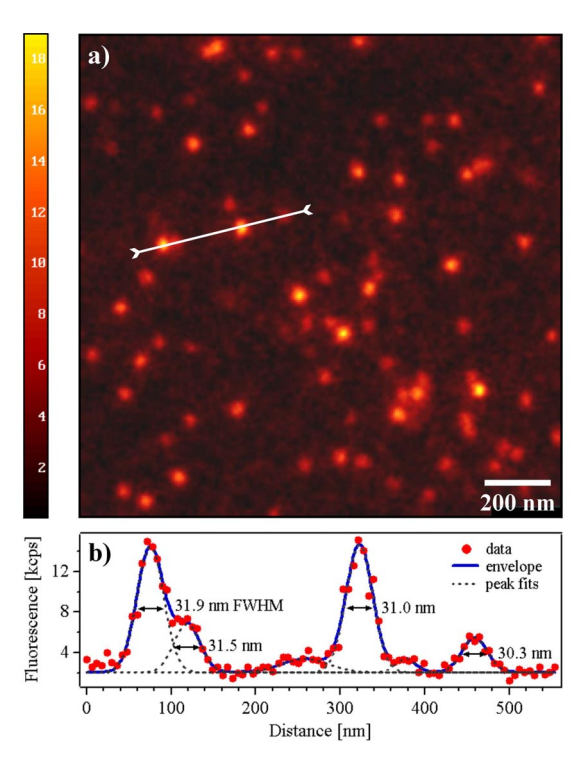
Nanoscale Technology & Biochemical Sensing Centre Suisse d'Electronique et de Microtechnique (CSEM) SA rue Jaquet-Droz 1, CH-2000 Neuchâtel, Switzerland

**INTRODUCTION:** Optical detection individual fluorophores has gained much attention due to its potential for using these molecules as probes highly sensitive for their environment. The recent development of highresolution and high-sensitivity optical techniques, such as scanning near-field optical microscopy (SNOM), confocal laser scanning microscopy (CLSM) as well as low temperature spectroscopy has made possible significant progress. Single fluorescent particles can now be routinely studied by individually addressing them in space or in the absorption frequency domain.

**RESULTS:** In this contribution we present recent progress made in scanning near-field optical microscopy (SNOM) using microfabricated cantilevered probes [1,2]. Both metal nanopatterns as well as single fluorescent molecules were imaged with a high lateral resolution approaching 30 nm (Fig.1). Since single fluorophores represent ideal point objects, the FWHM values of intensity traces recorded in constant height imaging (i.e. avoiding topography artefacts) are a good measure for the spatial resolution obtained. While some open issues concerning the imaging mechanism need to be solved, these data underline the importance of microfabricated probes for SNOM imaging.

In many areas of research and development high resolution microscopy is a very important technique. Nevertheless it turns out that confocal laser scanning microscopy (CLSM) is better suited in most experiments to quantitatively study the properties of individual fluorescent particles. Typically, the particles can be diluted in solution and separated on a substrate in such a way that CLSM's spatial resolution is sufficient to individually address them in the laser focus. We present data on the orientational and temporal behaviour of individual fluorophores, by using polarized excitation and time-sensitive detection. First experiments using fluorescence-detected circular dichroism (FDCD) on optically active single chiral molecules point towards the distinction of enantiomers in a non-racemic mixture. We will discuss sources for errors and uncertainties. Despite numerous open questions, this technique appears promising for detecting the chirality of single molecules.

Fig. 1: single fluorophores imaged by near-field optical microscopy with 32nm resolution.



**ACKNOWLEDGEMENTS:** This work was partially funded by the SPP MINAST and the Swiss National Science Foundation.

#### **REFERENCES:**

- [1] Microfabricated probes were developed in a collaboration in the framework of the Swiss Priority Program MINAST, and fabricated by G. Schürmann et al., IMT, U Neuchâtel.
- [2] R. Eckert et al., "Near-field fluorescence imaging with 32nm resolution based on microfabricated cantilevered probes", Appl. Phys. Lett. <u>77</u> 3695 (2000).

# NANOHANDLING AND MANIPULATION OF BIOLOGICAL SPECIMEN BY ATOMIC-FORCE MICROSCOPY

R.W. Stark <sup>1,2</sup>, G.Schitter<sup>1</sup>, J. Rubio <sup>2</sup>, S. Thalhammer<sup>2</sup>, A. Stemmer<sup>1</sup> and W.M. Heckl <sup>2</sup> Nanotechnology Group, Swiss Federal Institute of Technology ETH-Zurich, Switzerland <sup>2</sup> Institute for Crystallography and Applied Mineralology, University of Munich, Germany

**INTRODUCTION:** Micromanipulation techniques are valuable tools for the extraction and local structuring of smallest amounts of biological material<sup>1,2</sup>. Modern applications in biological research require high-resolution methods allowing the manipulation of biological samples with a precision beyond the resolution limit of light microscopy. For this purpose the atomic force microscope (AFM) is an appropriate tool. In order to enable precise sample manipulation an intuitive user interface is required together with as-fast-aspossible<sup>3</sup> nano-positioning capabilities of the instrument.

**METHODS:** A simple but intuitive human machine interface was realized by coupling a standard force feedback joystick to an AFM with integrated UV micro laser beam unit. Human metaphase chromosomes were dissected with the aid of this direct force feedback during sample manipulation. For mechanical AFM manipulation the loading force was increased, UV micro laser beam dissection was performed with a pulse repetition rate of 60 Hz and a pulse energy of  $0.7~\mu J$  at the sample with a scan speed of  $0.3~\mu m/s$ .

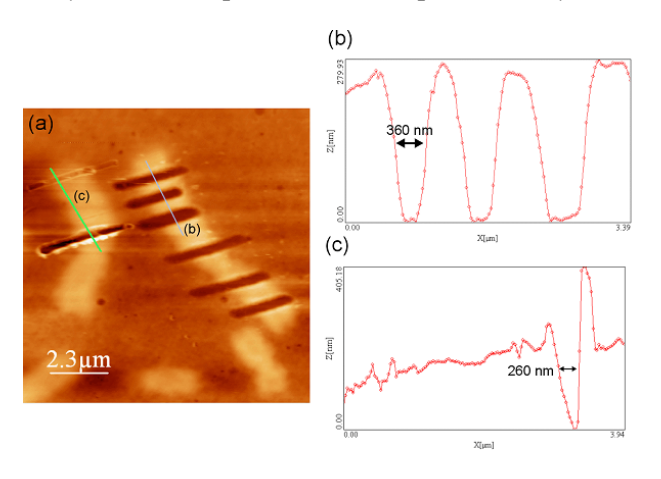


Fig. 1:(a) Topographic AFM images of human metaphase chromosomes dissected by AFM and UV-laser micro dissection. Cross section through (b) laser and (c) AFM cut chromosomes.

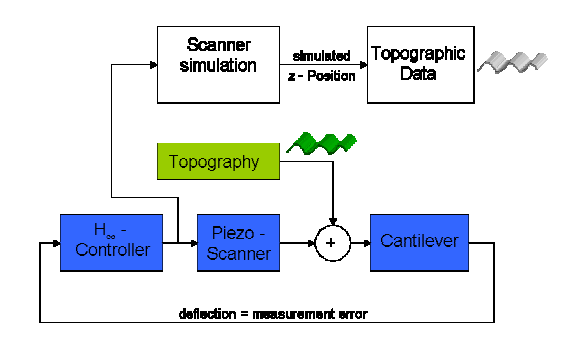


Fig. 2: Scheme of the control circuit for high-speed scanning AFM.

**RESULTS & DISCUSSION:** In the topographic AFM image (Fig. 1 a) the different cuts can be distinguished and analysed. The chromosome marked (b) was dissected with the UV-laser. A minimum cut width (full width at half maximum cut depth) of 360 nm could be achieved.

Different cut depths could be realized by AFM. At a loading force of 10  $\mu N$  of the tip onto the sample, a minute scratch with a cut depth of 20 nm and a cut width of 50 nm could be realized. At the side of the cuts biological material was deposited by the ploughing tip.

**CONCLUSIONS:** A high-speed mode that is realized by applying modern model-based control methods to the AFM will be implemented into a manipulation instrument (Fig. 2). The combination of both technical features will simplify and speed up nanostructuring of biological surfaces.

**REFERENCES:** <sup>1</sup> R. W. Stark, S. Thalhammer, J. Wienberg, et al., Appl. Phys. A: Mater. Sci. Proc. 66 (1-2), S579-84 (1998). <sup>2</sup> S. Thalhammer, R. W. Stark, K. Schütze et al., J. Biomed. Optics **2** (1), 115-119 (1997). <sup>3</sup> G. Schitter, P. Menold, H.F. Knapp, F. Allgöwer, A. Stemmer (2001), Rev. Sci. Instr. 72(8), pp 3320-3327.

**ACKNOWLEDGEMENTS:** Financial support (WMH) by Grant BMBF 13N7509/1 is gratefully acknowledged.

# FOCUSED ELECTRON BEAM DEPOSITION OF ONE-, TWO-, AND THREE-DIMENSIONAL NANOSTRUCTURES FOR BIOLOGICAL APPLICATIONS

P. Hoffmann, I. Utke, G. Jaenchen, F. Cicoira, and J. Rohner, <sup>1</sup>Swiss Federal Institute of Technology, Institute of Applied Optics, EPFL Lausanne, Switzerland

**INTRODUCTION:** We present a local deposition technique, which allows fabricating one-, two-, three-dimensional structures ofmicrometer down to nanometer size with focused electron beams (FEB). These structures or arrays of them can be functionalized with respect to electric, magnetic, optical, chemical properties by appropriate materials depositing inorganic) with selected shapes. Device prototypes can be flexibly fabricated with applications as biosensitive tips for all kinds of scanning probe microscopy (STM, AFM, MFM, ...), electrode single molecule capacitance measurements, potentiometry, cyclic voltammetry, ... to name a few. FEB can also be used for high resolution etching of organics and inorganic substrates making it possible to drill sub 100 nm holes, or shaping on the nanometer scale, without contamination as obtained by FIB machining.

**METHODS:** The deposition technique consists of supplying a selected volatile precursor (gas) to any substrate placed in the vacuum chamber of a electron microscope. The scanning interaction with the focused electron beam results in decomposition of the precursor molecules leaving a solid deposit with the desired properties. The lateral deposit shape is controlled by the electron beam movement and vertically by the beam exposure time. In this manner the substrate can be patterned with dot or electrode arrays, cross-line arrays, and 3D structures adjusted to the desired biologically interesting size and shape. The design is created with a standard electron beam lithography software. The choice of the substrate for FEB deposition is in general not limited, e.g. polymers, glasses, ceramics, semiconductors, and metals.

The focused electron beam induced etching method is much more limited to the substrate material, due to the fact, that electron induced synthesis of volatile products from gases and solids is much less known.

**RESULTS:** The diameter of FEB deposits depends almost proportional on the electron probe diameter. The resulting nanowires can be three-dimensionally arranged on a scale up to several

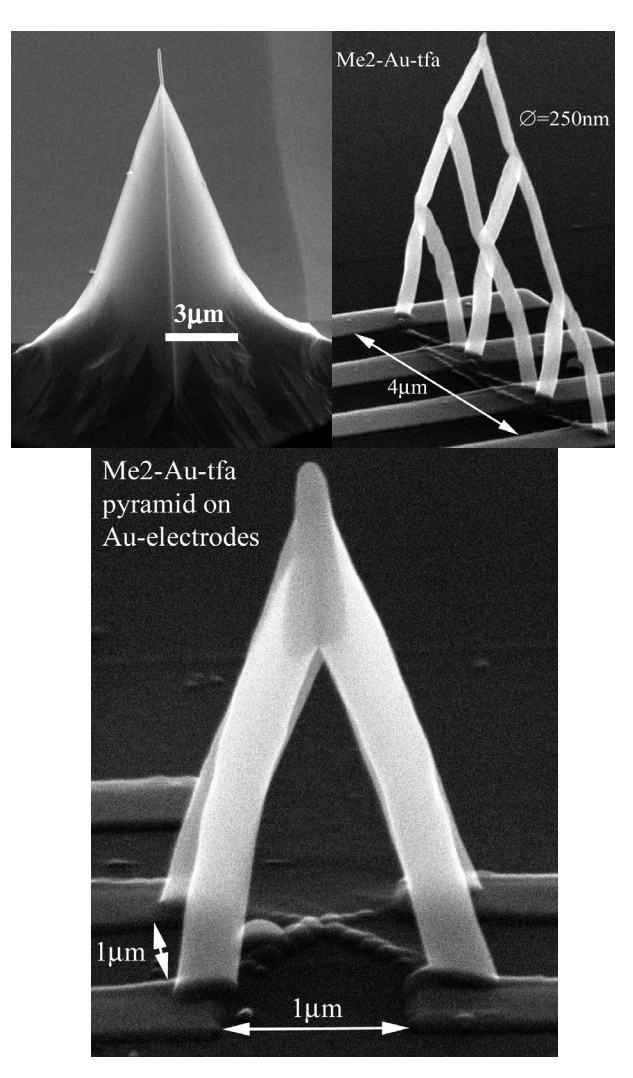


Fig. 1: Examples of FEB deposits: top left to right: magnetic nanocomposit deposit on commercial AFM tip, two dimensional deposit on gold electrodes on oxidized silicon substrate, bottom: 3-D pyramid of gold nanocomposit on gold electrodes.

tenth of micrometers in almost any texture/pattern by scanning the electron beam. The nano-structure of such nanowires consists of metallic nanoparticles of 2-8nm in diameter embedded in a stabilizing matrix of carbon. Examples are shown in Fig. 1. The left picture shows a one dimensional high aspect ratio magnetic deposit on a standard AFM cantilever, applied successfully for Magnetic Force Microscopy (MFM). Middle and right SEM pictures demonstrate the high flexibility of two

and three D constructions obtained with a gold containing precursor.

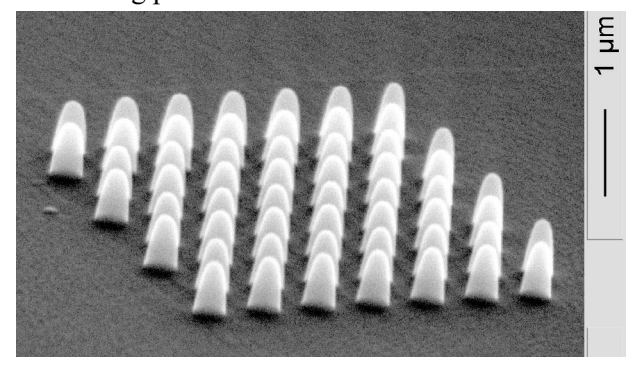
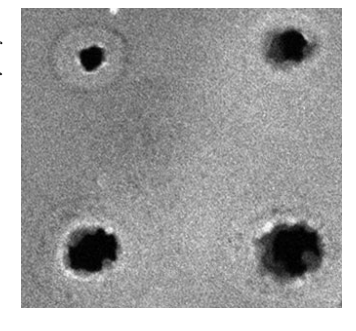


Fig. 2: Periodically arranged deposits of gold containing nanocomposit structures on oxidized silicon as substrate.

Pure Gold deposits can be obtained with a carbon free precursor<sup>1</sup>. Research for deposition of other pure materials is presently under investigation (C, Cu, Rh, ...). Focused electron beam induced etching of carbon is carried out with nontoxic reactive gases. The result is shown in figure 3. The obtainable aspect ratios in direct focused electron beam etching is presently under investigation. Applying selected electron activated gases will allow also the etching of other materials.

Fig. 3: Etched holes in thin carbon films of different diameters of 100 nm to 300 nm. The diameters can be controlled with high reproducibility by the focused electron beam conditions and the gas exposure.



DISCUSSION & CONCLUSIONS: The high flexibility of our focused electron beam induced deposition and etching processes is an outstanding enabling technology for the realization of test devices for scientists in research. As technology process specialists, we offer our technologies to research groups to supply the tools (hardware) for tackling challenging analytical questions. As an example we have chosen the local aminogroup functionalisation of one single electrode on a Scanning probe microscopy cantilever. In situ combination of FEB deposition (nanocomposit of gold in carbon) and selective carbon etching, followed by exposure to selected chemicals (e.g. amino-thiols) allows local chemical and/or biological functionalization of deposits. Programming the FEB machine allows to deposit, etch and expose to chemicals to realize individually biological active three dimensional electrode patterns. The process is compatible with 6 inch wafer technology, including millipede multicantilever approaches for example. Individual biologically active sites on individually addressable electrodes in the sub 100 nm range is therefore obtainable. To illustrate functionalization, the grafting of the final biologically active molecule is demonstrated in figure 4. For industrial use, the processes can partially be parallelized for sub 100 nm three D structuring and functinalization, offering one to two orders of magnitude higher resolution compared to light processing.

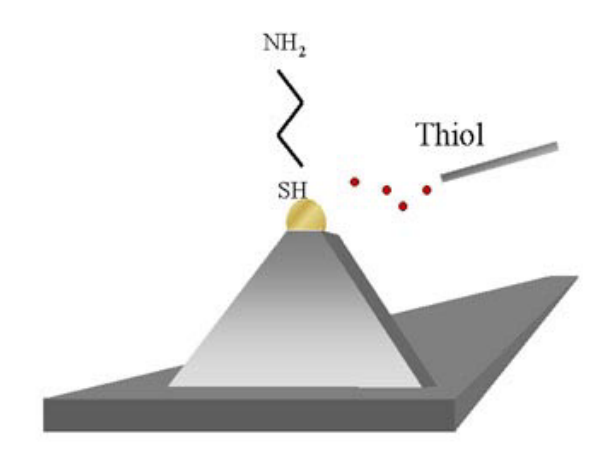


Fig. 4: Schematic drawing of one individual biologically functionalized gold electrode. After deposition of one electrically conducting structure on an electrode, in situ exposure to an appropriate chemical compound (e.g. an amino-thiol) the latter grafts selectively onto the gold<sup>2</sup>.

**REFERENCES:** <sup>1</sup> I. Utke, et al (2000) *Microelec Engin* **53**: 261-264. <sup>2</sup>J. Rohner, Semesterproject DMT/EPFL spring 2001.

ACKNOWLEDGEMENTS: The obtained results were carried out in close collaborations with research groups at EPFL, from IMO/DP: Prof. E. Kapon, Dr. B. Dwir, Dr. K. Leifer, from LMCH/DMX: Prof. Mathieu, N. Xanthopoulos, from CIME: Prof. Ph. Buffat, D. Laub. The precursors commercially not available were synthesized by P. Doppelt ESPCI, Paris. Industrial partners of this project are Nanosurf AG, Liestal and IBM Mainz (D). We thank the Swiss National Science Foundation (SNF), and the Commission for Technology and Innovation (CTI – TOP NANO 21) for financing the research.

### CONTORL OVER CYTOSKELETON OF ADHERENT CELLS BY GUIDANCE OF SUBCELLULAR COMPONENTS

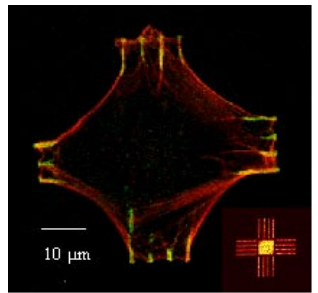
JW. Lussi <sup>1</sup>, R. Michel<sup>2</sup>, A. Goessl <sup>1</sup>, M. Textor<sup>2</sup> and JA. Hubbell <sup>1</sup> Biomed. Eng., ETH, Zurich, CH; <sup>2</sup>Surface Science (LSST), ETH, Zurich, CH

INTRODUCTION: Restricted cell size and shape achieved by adhesive/non-adhesive patterning have been shown to affect growth, differentiation and death of cells. In contrast to earlier studies we want to study not how the overall cell shape, but how spatial organization of the cell components responsible for contact formation (which also participate in signaling) affects cell physiology. Patterns with feature sizes down to 1 µm in width were chosen to target subcellular components with sizes in the same range (e.g. focal contacts). These patterns were specifically designed to study the effect of different geometries on cell attachment, focal adhesion formation and stress fiber orientation via guidance of subcellular components.

**METHODS:** 10x10 mm Si-or glass wafers exposing hydrophobic features in a non-fouling background were produced by a novel technique, termed SMAP, described elsewhere. Briefly, structures of TiO<sub>2</sub> in a matrix were created bv standard phototlithographic techniques on these substrates. Selective adsorption of dodecylphosphate to the TiO<sub>2</sub> rendered these structures hydrophobic, while the subsequent adsorption of poly(lysine)-graftpoly(ethylene glycol) to SiO<sub>2</sub> lead to the formation of a non-fouling background. Upon exposure to the medium, adhesion proteins present in serum, particularly fibronectin and vitronectin, strongly adsorb onto the hydrophobic areas and mediate cellsurface contact formation. These samples were then placed in 24-well plates and seeded with human foreskin fibroblasts (HFF) at a density of 5000 cells/cm<sup>2</sup> in serum containing medium. After an incubation for typically 15 hours the cells were fixed and immunostained for f-actin and the focal adhesion protein vinculin to visualize stress fibers and focal contact sites, respectively. Stained samples were imaged on a Zeiss 510 confocal laser scanning microscope.

RESULTS: The chemical contrast created by SMAP is well recognized by the cells who show clear discrimination between cell adhesive and non-adhesive areas. This contrast is maintained for at least 10 days. Experiments with oxide patterns not subjected to SMAP treatment showed no pattern recognition by the cells, and cells spread freely over the whole substrate. The topography present on SMAP substrates (10-20 nm) by itself has no visible effect. Chemical patterning is therefore needed for spatial cell organization.

Focal contacts represented by vinculin only form on the adhesive features, as can be seen in Figure 1. No adhesion plaques can be observed in the surrounding non-fouling areas. Stress fibers themselves originate in and terminate on these vinculin-rich areas. This shows that SMAP allows us to spatially control focal contact distribution. and therefore dictate cytoskeleton distribution. We have looked at different specific pattern geometries, two of which can be found as insets in Figure 1. We wanted to test whether it is possible to restrict focal contact formation such that these generally elongated structures could only be formed when oriented in a particular direction, either parallel to the main axes of the cell or perpendicular to them. And does it affect the distribution of stress fibers in the cell body?



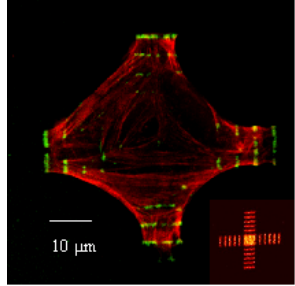


Fig. 1: Single cells, stained for f-actin (red) and vinculin (green), on two types of patterns (insets).

While no distinct correlation between stress fiber distribution and substrate pattern have been observed on the patterns it was found that stress fiber density along the periphery of the cell is higher on patterns with lines perpendicular to the main axes. We speculate that this could be a direct consequence of the fact that our patterns allow formation of larger focal contacts ( $>1\mu m^2$ ) only when elongated in the direction of the lines. We will test this further using pattern sizes down to 200 nm created by electron beam lithography.

CONCLUSIONS: We have shown that by using SMAP it is possible to control distribution of focal contacts and therefore to dictate where stress fibers can be formed. With the availability of nanometer patterns we will investigate whether also orientation of stress fibers can be controlled and study a possible effect of different pattern geometries on physiological functions of the cell.

**ACKNOWLEDGEMENTS:** This work is funded by TopNANO21/SNSF.

# DIVALENT BIODEGRADABLE MICROSPHERE VACCINES INCUDE PROTECTIVE IMMUNE RESPONSE AGAINST TETANUS AND DIPHTHERIA

Marisa Peyre<sup>1</sup>, Dorothea Sesardic<sup>1</sup>, Hans P. Merkle<sup>2</sup>, <u>Bruno Gander</u><sup>2</sup>, Pål Johansen<sup>2</sup> *Dept. of Bacteriology, Nat. Institute for Biological Standards & Controls, Hertfordshire EN6 3QG, UK.* 

<sup>2</sup> Institute of Pharmaceutical Sciences, ETH Zurich, Switzerland.

INTRODUCTION: Biodegradable microspheres (MS) represent a promising approach in the development of single-injection vaccine delivery system. MS made of poly(lactide) (PLA) or poly(lactide-co-glycolide) (PLGA) and loaded with tetanus or diphtheria toxoid have demonstrated strong immune stimulation with lasting antibodies in mice and guinea-pigs after a single inoculation, and a first human trial with a tetanus vaccine is presently envisaged. So far, most of the studies have used single microencapsulated antigen, whereas the feasibility of combining several antigens in a single microsphere formulation is unknown.

In this study, we have tested the immunological performance of divalent MS vaccines against tetanus and diphtheria in guinea pig. The animals were subcutaneously immunised once with diphtheria and tetanus toxoids contained in PLGA-MS. All formulations were strongly immmunogenic, irrespective of MS size and hydrophobicity. ELSIA antibodies, mainly of the IgG1 subtype, were quantitatively comparable with those induced after two immunisations with a licensed vaccine which contain the antigens adsorbed on aluminium hydroxide. The MSformulations provided increasing levels of antibodies during the 16 weeks of testing. The antibody responses were also weakly polarised in favour of tetanus. After a challenge with tetanus and diphtheria toxins, the MS mediated protective immunity comparable or better than did the licensed divalent vaccine. The protection efficacy did not correlate well with toxin neutralisation. which demonstrated superiority of the licensed vaccine when given twice. However, MS-aided neutralising antibodies against both diphtheria (2-4 IU/ml) and tetanus (5-18 IU/ml) toxins were orders of magnitude above protective level (0.01 IU/ml) when immunised with MS. These levels were similar to those obtained with a single injection of the licensed vaccine.

In conclusion, this study showed that a single administration of biodegradable MS vaccines provided protective immunity against diphtheria

and tetanus and that this immunisation approach may be feasible for multivalent vaccines. However, direct challenge and toxin neutralisation assays yielded contrasting information on the product quality of the vaccine, so methods for testing the efficacy of slow-release formulation might need to be revised.

**REFERENCES:** Men Y., Thomasin C., Merkle H.P., Gander B., and Corradin G., A single administration of tetanus toxoid in biodegradable microspheres elicits T cell and antibody responses similar or superior to those obtained with alum. Vaccine 13, 683-689 (1995)

Thomasin, C., Corradin, G., Men, Y., Merkle, H.P. and Gander, B., Tetanus toxoid and synthetic malaria antigen containing PLA/PLGA-microspheres: Importance of polymer degradation and antigen release for immune response. J. Controlled Release 41, 131-145 (1996)

Men, Y., Audran, R., Thomasin, C., Eberl, G., Demotz, S., Merkle, H.P., Gander, B. and Corradin, G., MHC class I- and class II-restricted processing and presentation of microencapsulated antigens. Vaccine 17, 1047-1056 (1999).

Johansen, P., Men, Y., Merkle, H.P. and Gander B., Revisiting PLA/PLGA microspheres: an analysis of their potential in parenteral vaccination. Europ. J. Pharm. Biopharm. 50, 129-146 (2000)

Johansen, P., Merkle H.P. and Gander B., Technological considerations related to the upscaling of protein microencapsulation by spraydrying. Eur. J. Pharm. Biopharm. 50,:1413-1417 (2000).

Johansen, P., Estevez, F., Zurbriggen, R., Merkle, H.P., Glück, R., Corradin, G. and Gander, B., Towards clinical testing of a single-administration tetanus vaccine based on PLA/PLGA microspheres. Vaccine 19, 1047-1054 (2000). *Arthritis* (eds B. Henderson, J. Edwards, and R. Pettipher) Academic Press, pp 163-204.